

https://dspace.org/

A permutation coding and OFDM-MFSK modulation scheme for power-line communication

Ndlovu, Mpendulo Mike Comfort

2015-03

http://hdl.handle.net/10539/18365

Downloaded from a DSpace repository. https://dspace.org/

A PERMUTATION CODING AND OFDM-MFSK MODULATION SCHEME FOR POWER-LINE COMMUNICATION

Mpendulo Mike Comfort Ndlovu

A dissertation submitted to the Faculty of Engineering and the Built Environment of the University of the Witwatersrand in fulfilment of the requirement for the degree of

Master of Science in Engineering

March 2015

Contents

Declaration v

Acknowledgements vi

Author's Publications vii

Abstract viii

List of Figures viii

List of Tables x

Acronyms xii

Symbols xiii

1 Introduction 1

1.1 Digital Communication System 2

1.2 Problem Statement 4

1.3 Research Output 4

1.4 Dissertation Outline 5

2 Literature Review 6

2.1 Power-line Communication 6

2.2 Channel Coding 9

2.2.1 Channel Capacity 9

2.2.2 Algebraic Codes 11

2.2.3 Probabilistic Codes 13

2.2.4 Concatenated Codes 15

2.2.5 Permutation Codes 16

2.2.6 Trellis-Coded Modulation 17

2.3 Chapter Summary 20

3 Modulation Schemes **21**
3.1 An Overview of Modulation in PLC . . . 21
3.2 Multiple Frequency Shift Keying . . . 21
3.2.1 Advantages . . . 22
3.2.2 Disadvantages . . . 23
3.3 Multiple Phase Shift Keying . . . 23
3.3.1 BPSK . . . 24
3.3.2 QPSK . . . 25
3.4 OFDM . . . 27
3.4.1 OFDM Design . . . 29
3.4.2 OFDM Impairments . . . 31
3.4.3 Implementation Parameters . . . 38
3.5 OFDM-MFSK . . . 39
3.6 Other OFDM-based Schemes . . . 40
3.7 Chapter Summary . . . 41

4 Research Methodology **42**
4.1 Data Generation . . . 42
4.2 Noise Addition . . . 42
4.3 Error Control Coding . . . 44
4.3.1 Reed-Solomon Encoder . . . 44
4.3.2 Convolutional Encoder . . . 46
4.3.3 Interleaver . . . 47
4.3.4 Viterbi Decoder . . . 50
4.3.5 Reed-Solomon Decoder . . . 51
4.4 Modulation Techniques . . . 53
4.5 Chapter Summary . . . 54

5 OFDM-MFSK Permutation Coding **55**
5.1 Understanding OFDM Permutation Coding . . . 55
5.2 Problem Understanding from IFFT/FFT Theory . . . 58
5.3 Subcarrier Encoding Schemes . . . 59
5.3.1 BPSK-based Permutation Sequence Encoding . . . 60
5.3.2 QPSK-based Permutation Sequence Encoding . . . 60
5.4 Decoding Techniques . . . 61
5.4.1 Minimum Distance Decoding . . . 62
5.4.2 Encoding Sequence-Dependent Decoding . . . 65
5.5 Chapter Summary . . . 67

6 Results and Analysis **68**
6.1 Noise Impact 68
6.1.1 DQPSK and 4FSK-based OFDM Schemes 69
6.1.2 DBPSK and 2FSK-based OFDM Schemes 71
6.2 CFO Impact 72
6.2.1 General Case 72
6.2.2 PLC case 75
6.3 Chapter Summary 78

7 Conclusion **82**
7.1 Carrier Frequency Offsets Mitigation 82
7.2 Bandwidth Considerations 83
7.3 Noise Mitigation 84
7.4 Comparison with Similar Work 84
7.5 Research Contribution 85
7.6 Future Work 85
7.7 Conclusion 86

Bibliography **87**

DECLARATION

I hereby declare that this dissertation is my own work. It is being submitted to the Faculty of Engineering and the Built Environment of the University of the Witwatersrand in fulfilment of the requirement for a Master of Science in Engineering. It has not been submitted to any other institution before.

.....
(Signature of Candidate)

on this ..... day of ..... year .....

ACKNOWLEDGEMENTS

This achievement is dedicated to my family: Mother; for her selfless efforts, and my siblings; Sandile, Nonduduzo and Sikhumbuzo, for their support.

To God, our source and peerless teacher, for the gift of right thinking.

To my supervisor Dr. Ling Cheng, for his prompt responses to my 911 calls, and for entrusting me with the grisly console of Error Control Coding. I often felt like a lobotomized amoeba intellectually jousting with Einstein.

To Dr. Jaco Versfeld, for his expertise in Reed-Solomon codes and modulation.

To the Centre of Excellence for Telecommunications Access and Services (CeTAS), for the generous scholarship. A special vote of thanks to Prof Rex van Olst.

To my future spouse I might have seen in sporadic visions, for inspired hope.

I am indebted to Z. Mtsetfwa, for diligently proof-reading this dissertation, and to A. Familua for technical critique.

Once more into the fray

Into the last good fight I'll ever know

Live and die on this day

Live and die on this day

Thank You | Graciàs | Siyabonga

A Dios sea la Gloria

AUTHOR'S PUBLICATIONS

1. M. Ndlovu and L. Cheng. "A Permutation Coding and OFDM-MFSK Modulation Scheme for Power-line Communication." Presented at: SATNAC 2013, Stellenbosch, South Africa, Sep. 1 - 4, 2013, pp. 429-430. (*Published*).

2. M. Ndlovu and L. Cheng. "An OFDM Inter-Subcarrier Permutation Coding Scheme for Powerline Communication." To be presented at: IEEE ISPLC 2014, Glasgow, Scotland, Mar 30 - Apr 2, 2014. (*Published*).

ABSTRACT

Power-line communication offers a networking communication over existing power lines and finds important applications in smart grid, home and business automation and automatic meter reading. However, the power-line channel is one of the harshest known communication channels currently in use and it requires robust forward error correction techniques. Powerful decoding algorithms tend to be complex and increase latency while robust modulation schemes offer lower data rates and reduced spectral efficiency. The presented research is a frequency domain error-correcting scheme that extends the existing narrowband power-line communication forward error correction concatenated scheme of Reed-Solomon and Convolutional codes in the OFDM framework. It introduces a combination of M-ary phase shift keying as an OFDM subcarrier modulation scheme and a permutation sequence encoding between subcarriers to combat narrowband interference and carrier frequency offsets by introducing frequency diversity. The scheme offers improved BER performance over OFDM and OFDM-MFSK in high narrowband disturbance and impulse noise probability channels and improves the performance of OFDM in the presence of carrier frequency offsets.

List of Figures

1.1 Digital Communication System 2

2.1 A simple (n, k) block code 12
2.2 Convolutional encoding 15
2.3 Concatenated scheme 16
2.4 8-PSK TCM constellation partitioning 19

3.1 2FSK modulation 22
3.2 BPSK encoding 24
3.3 BPSK modulation 25
3.4 QPSK encoding 26
3.5 Gray-coded QPSK constellation 27
3.6 OFDM frequency-time representation 28
3.7 Two orthogonal subcarriers 34
3.8 Two non-orthogonal subcarriers 35
3.9 Many orthogonal subcarriers 35
3.10 Many non-orthogonal subcarriers 36
3.11 OFDM-4FSK 40

4.1 Testbed architectural design 43
4.2 [133, 171] convolutional encoder 48
4.3 Burst error corrupting consecutive OFDM symbols 49
4.4 Frequency fade corrupting adjacent frequencies for a large number of OFDM symbols 50
4.5 Differential encoding 54

5.1 OFDM subcarriers 56
5.2 PE OFDM using [3 1 2] codeword 57
5.3 M = 2 and M = 4 codewords 59
5.4 3-permutation sequence decoding scenarios 63
5.5 Minimum distance decoding algorithm 65
5.6 Encoding-sequence decoding algorithm 66

6.1 DQPSK-based schemes at varying Γ 70
6.2 DQPSK-based schemes at $4f_{sc}$, $P_{nbi} = \frac{1}{256}$, $P_{imp} = \frac{1}{64}$ 71
6.3 DQPSK-based schemes at $4f_{sc}$, $P_{nbi} = \frac{1}{1/64}$, $P_{imp} = \frac{1}{256}$ 72
6.4 OFDM-2FSK and DBPSK-based Schemes at varying noise bandwidth 73
6.5 Performance of DBPSK modulated ODFM 75
6.6 Performance of DQPSK modulated ODFM 76
6.7 Performance of 8-DPSK modulated ODFM 77
6.8 $M = 2$ PE DQPSK subcarrier-modulated OFDM 78
6.9 $M = 4$ PE OFDM with DQPSK modulated subcarriers 79
6.10 OFDM-4FSK and DQPSK-based schemes at varying CFO . . . 80
6.11 OFDM-4FSK and DQPSK-based schemes at varying CFO . . . 80
6.12 OFDM-4FSK and DQPSK-based schemes at a of CFO 0.02 . . . 81

List of Tables

3.1 4FSK mapping 22
3.2 QPSK mapping 27
3.3 OFDM parameters 39

4.1 Convolutional code parameters 47

5.1 Permutation coding mapping 56
5.2 4-permutation codebook 61

ACRONYMS

ARQ	-	Automatic Repeat reQuest
AWGN	-	Additive White Gaussian Noise
BER	-	Bit Error Rate
BCJR	-	Bahl, Cocke, Jelinek and Raviv
BPSK	-	Binary Phase Shift keying
CFO	-	Carrier Frequency Offset
DAC	-	Digital to Analogue Conversion
DBPSK	-	Differential Binary Phase Shift Keying
DQPSK	-	Differential Quadrature Phase Shift Keying
ECC	-	Error Control Coding
FEC	-	Forward Error Correction
FFT	-	Fast Fourier Transform
FSK	-	Frequency Shift Keying
ICI	-	Inter-Carrier Interference
IDFT	-	Inverse Discrete Fourier Tranform
IFFT	-	Inverse Fast Fourier Transform
ISI	-	Inter-Symbol Interference
I-Q	-	In phase - Quadrature axis of a complex plane digital signal
LDPC	-	Low-Density Parity-Check
LTE	-	Long Term Evolution
MAP	-	Maximum Posteriori Probability
MFSK	-	Multiple Frequency Shift Keying
MPSK	-	Multiple Phase Shift Keying
NBI	-	Narrowband Interference
OFDM	-	Othorgonal Frequency Division Multiplexing
PAPR	-	Peak to Average Power Ratio
PLC	-	Power Line Communication
PE OFDM	-	Permutation-Encoded OFDM
PSK	-	Phase Shift Keying
QAM	-	Quadrature Amplitude Modulation
QPSK	-	Quadrature Phase Shift Keying
RS	-	Reed-Solomon
SNR	-	Signal-to-Noise Ratio
TCM	-	Trellis-Coded Modulation

SYMBOLS

α	-	Reed-Solomon minimum degree polynomial
β	-	E_b/N_0 value at 10^{-3} bit error rate
Δf	-	OFDM carrier frequency offset in Hertz
ϵ_s	-	PSK constellation power
η	-	Spectral efficiency
f_{sc}	-	OFDM subcarrier frequency
λ	-	Poisson distribution parameter
μ	-	Reed-Solomon error-location calculation iteration number
P_{imp}	-	Impulse noise probability at any time instance
P_{nbi}	-	Narrowband interference probability on any frequency
Γ	-	Narrowband noise bandwidth
π	-	Half revolution radian angle
ψ	-	Carrier frequency offset
Ψ	-	Carrier frequency offset vector
σ	-	Reed-Solomon error locator polynomial
θ	-	Modulated symbol phase
ζ	-	Permutation code performance index

1 INTRODUCTION

In recent times there has been a great demand for internet access across the world because of the almost limitless services that it provides. Since the mid 1990s, the internet has revolutionized culture, commerce, social lives, education and many other aspects of our lives. Social networking, Voice over Internet Protocol (VoIP), instant messaging, electronic mail, and the world wide web are some of the services that have been brought about by the internet. The internet's takeover of global communication and services has significantly soared in recent decades. While it only communicated 1% of the information in two-way telecommunications networks in 1993, the contribution had increased to 51% in 2000, and more than 97% of all telecommunicated information by 2007 [1].

Because of the escalating demand for information services, there has been an ever-increasing need for the development of infrastructure to support the transmission of data. Presently, the fibre optic cable is the most used infrastructure for sending data from Internet Service Providers (ISPs) to consumers. However, it is expensive and it takes a significant amount of time to lay out. Moreover, it is not feasible for remote settlements and for most rural areas as the demand is significantly small compared to expenses incurred in setting up the infrastructure and maintaining it.

As a result of the challenges posed by the costs of developing infrastructure for communication, power lines were identified as a good alternative. A communication signal can be impressed on an existing middle and low voltage power line to carry information. The advantage of using the power line is that it is by far the most established and most connected physical connection between urban areas and remote settlements.

But the power line was not designed to carry information. As a consequence of which there are several challenges encountered when sending a signal over it. The propagation of signals over power-line introduces attenuation, which increases with both the frequency at which the signal is transmitted and the

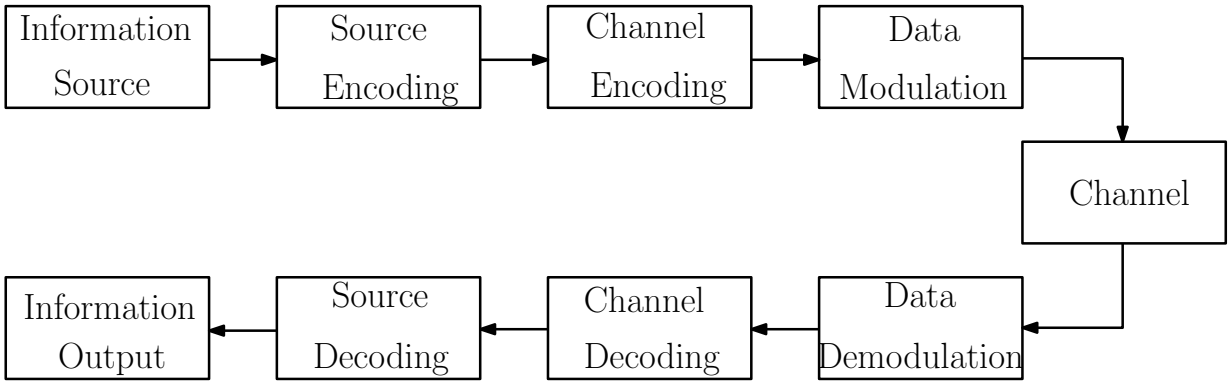

Figure 1.1: Digital Communication System

length of the line. This attenuation is a function of the power-line characteristic impedance and the propagation constant of the power line [2]. Impedance mismatch over the length of power line accentuates the problem further as it causes reflections of the signal. The frequency dependency of the signal attenuation is one of the reasons narrow-band power-line communication uses lower frequencies of normally less than 500 kHz over long distances of signal transmission. On the other hand, broadband power-line communication uses a much higher frequency of 1-30 MHz over shorter distances for last mile applications at much higher data rates over low voltage lines.

1.1 Digital Communication System

The digital communication system is shown in Figure 1.1. The information source in a typical communication system outputs information that can be continuous or discrete. The source usually has a transducer that converts the information to a time-varying electrical or optical representation.

Source encoding involves encryption and data compression. In the case of an analogue transmitter, source encoding includes the sampling and quantization of time-continuous signals and then compression of the information. Channel encoding comprises the addition of redundancy to the digital signal to enable error detection and correction. Different types of encoding exist and these will be discussed in detail in subsequent sections.

The essence of modulation involves the use of Digital to Analogue Conversion (DAC) of a transmitted signal and can be achieved by varying a specific

attribute of the carrier signal on which the transmitted signal is impressed. Some of the attributes that can be varied are amplitude, frequency and phase amongst others. Modulation is performed to alleviate interference, noise, channel assignment and to enable multiplexing of several input signals.

The channel can be a coaxial cable, optical fiber, a free-space optical link, a power line cable and much more. However, a channel is not perfect. Some of the limitations of a communication channel include time-varying noise, frequency disturbances, cross-talk and attenuation. Because of some of these limitations, channel encoding is a necessity. The rest of the blocks involve inversing the processes carried out before the information is transmitted over the channel.

Channel noise is the major interest of the power line in this research. The channel experiences background noise in the form of Additive White Gaussian Noise (AWGN), impulse noise and narrow-band interferences. The presence of noise requires powerful error correction techniques to recover information corrupted during transmission. A wide range of Forward Error Correction (FEC) schemes has been studied over the years. These include low-density parity-check (LDPC) codes, Reed-Solomon (RS) codes, Turbo codes, Convolutional codes, permutation codes and concatenated schemes that combine more than one FEC scheme to provide robustness. Each scheme has applications where it is most convenient to use. RS algebraic block codes have been widely used in PLC because they are good for correcting multiple-burst bit errors and erasures. An algebraic code is usually combined with a probabilistic code in a concatenated scheme.

These techniques tend to reduce the data rate and introduce latency. In order to improve balance between a good data rate and the integrity of the data being transmitted, Orthogonal Frequency Division Multiplexing (OFDM) is used as a modulation scheme. Instead of transmitting data using one subcarrier, OFDM uses a large number of orthogonal parallel subcarriers that can be modulated using a conventional M-PSK or M-QAM modulation scheme. The advantage of OFDM is that it splits the signal into several frequencies that are orthogonal to each other and then send the signal et all the frequencies simultaneously. This improves the bit-rate. The downside of this scheme is that when orthogonality is lost, Inter-Carrier Interference (ICI) is introduced.

The loss of orthogonality in power-line communication is normally caused by timing jitter, fading and Carrier Frequency Offsets (CFO). These problems imply a need for further research into mitigating ICI. A combination of two modulation schemes is often used to make the system more robust. To improve the performance of the communication system, OFDM is often combined with Multiple Frequency Shift Keying (MFSK) to produce a scheme called OFDM-MFSK whereby MFSK is employed to modulate the subcarriers of OFDM.

1.2 Problem Statement

The conventional OFDM scheme used in PLC is adversely affected by frequency disturbances, impulse noise and carrier frequency offsets which degrade its performance. OFDM-MFSK was recently developed to mitigate the impact of these problems on the communication system, but has poor bandwidth efficiency. It can only transmit $\log_2 M$ information bits for every M frequencies used. The research question therefore is *how can the bandwidth usage of OFDM-MFSK be improved without compromising its ability to combat frequency disturbances, impulse noise and carrier frequency offsets?*

1.3 Research Output

I propose a new transmission channel condition-adapted type of OFDM-MFSK scheme that incorporates permutation coding. This is called Permutation Encoded OFDM (PE OFDM). This novel frequency-domain encoding scheme uses a permutation sequence coding of inter-subcarrier spacings in OFDM to add a shielding layer to combat the effect of carrier frequency offsets in OFDM. By ensuring that no two symbol-carrying subcarriers are adjacent to each other, inter-carrier interference is minimized. Also, because the scheme sends more information bits per number of OFDM subcarriers, it achieves a better bandwidth efficiency than the conventional OFDM-MFSK scheme. Moreover, the scheme intelligently decodes information using a pseudo-random sequence that is known to both the encoder and the decoder, and therefore ignores any frequency disturbances at unused subcarriers. This improves the system's robustness against narrow-band noise. The proposed technique has superior error rate performance than OFDM and OFDM-MFSK in the presence of narrow-band interference, impulse noise and carrier frequency offset.

1.4 Dissertation Outline

The remaining part of the document is outlined in this chronology. Chapter 2 is the literature review. Here the power-line communication architecture is presented and the evolution of error control coding schemes studied. Different types of algebraic and probabilistic codes used in PLC are studied. These can also be classified as block codes and convolutional codes respectively. Both their construction and applications are discussed. The different types of FEC concatenation schemes used in PLC are explored. Chapter 3 presents the test-bed architectural design - the different subsystems forming it, how they function and their role in the entire system. Chapter 4 is on OFDM, which forms the principal medium of the proposed encoding scheme. It discusses the principles of an OFDM signal, the design considerations as well as the impairments and limitations of the OFDM system. Chapter 5 then delves into the permutation encoding scheme. It discusses the scheme design and the aspects considered in its design. It also explains how the scheme functions and how it improves the performance of OFDM in the presence of noise disturbances and other channel impairments, mainly carrier frequency offsets. The results are presented and analyzed Chapter 6. The outcome-based analysis is compared against the requirements of the research aim. Chapter 7 is the last chapter which concludes the dissertation and a qualitative assessment of the work is made and alternative solutions and possible developments are suggested.

2 LITERATURE REVIEW

2.1 Power-line Communication

Power-line communication (PLC) is a technology that leverages existing power-lines to relay data signals [3]. This is achieved by impressing a modulated signal at a certain carrier frequency on an energy line to make use of the existing framework and hence avoid the costs of laying new cables. PLC can be classified as either broadband or narrow-band technology. Narrow-band power-line communication (NB-PLC) is used for frequencies of up to 500 kHz while broadband PLC works for frequencies ranging between of 1 - 30 MHz. PLC has applications in smart grid and last mile communication and data transfer technologies. NB-PLC over distribution networks is gaining the attention of researchers, as a communication medium in future power grids [4].

In 1922, the first carrier frequency systems began to operate over high voltage lines in the frequency range of 15 - 500 kHz for telemetry applications [5, 6]. In the 1930s, ripple carrier signalling was introduced on the medium voltage and low voltage distribution systems [7]. Nowadays PLC can be used for remote monitoring, control systems, sensor control, data acquisition, voice-over-power-line and multimedia applications. The most popular applications being smart grid and automatic meter reading [5]. Because the noise in the channel is a summation of different types of noise that result in different error types, various combinations of error correction schemes for mitigating various corresponding noise type effects have been proposed [8–10].

A narrow-band PLC system is vulnerable to background noise, narrow-band interference (NBI) and impulsive noise. Background disturbance takes on the form of AWGN resulting from the sum of different low power noise harmonics present in the system.

Narrow-band interference exists for a permanent long period at one frequency while impulse noise dominates all frequencies at one time instance and background noise occurs from time to time and from frequency to frequency [11].

Narrow-band interference consists of semi-permanent amplitude modulated sinusoidal signals existing in a range of frequencies caused by ingress of radio broadcasting stations, while impulsive noise is generated by electrical appliances connected to the PLC network and is time-variant. Impulsive noise may be AC half cycle synchronous due to rectifier diodes in power supplies or asynchronous due to switched-mode power supplies and AC/DC power converters. They may also either be periodic or aperiodic [12, 13]. Consequently, such impulsive events induce both random and burst errors at the receiver [14].

While the traditional coding and modulation paradigms were usually designed with the AWGN assumption in mind, the power-line channels, however, are mainly characterized by non-Gaussian and non-stationary interferences [15,16]. This serious mismatch between traditional signal transmission technologies and power-line channel characteristics motivates the development of robust modems that are more effective to cope with non-Gaussian interferences encountered in power-line channels [17].

Aside from the hostile channel impairments, the allowable transmission power is limited by statutory electromagnetic compatibility (EMC) emission constraints. To facilitate protection for the transmitted data over the noisy power-line channel at low signal-to noise (SNR) values, provision should be made for FEC at the receiver. Therefore, in order to exploit the full potential of PLC systems while the SNR margin is lowered to comply with the EMC requirements, protection against impulsive disturbances has become very crucial [10].

There have been a number of coding schemes that have been used to combat PLC errors. Most of these utilize either RS codes, or convolution codes or both. Some schemes have tried to improve performance by adding interleaving to randomize the data and this helps in spreading burst errors so that the probability to decode the data is increased. RS encoding is a block coding scheme that is known to be effective in correcting burst errors that usually occur due to impulsive noise [12]. Convolutional codes, on the other hand, are a kind of probabilistic coding that are used to correct random errors and they use the Viterbi decoding algorithm for decoding. While algebraic coding finds codes that maximize the minimum distance, probabilistic coding finds codes that optimize the performance as a function of coding and decoding complexity [13].

Given the complementary effectiveness of RS codes and convolutional codes, it is logical to combine them so that both burst errors and random errors can be combated. The combination of these schemes was first introduced by Dave Forney in 1966, which he referred to as concatenated codes [18]. Concatenated codes are formed by two linear block codes that are cascaded serially, where a block code like RS or BCH code becomes the outer code followed by a trellis code used as an inner code, with convolutional code being an example. The concatenation of RS encoding with convolutional encoding is a logically well attempted approach to simultaneously solving bursty and random errors. However, some communication standards proposed eliminating RS encoding to bring down the complexity of the system, replacing it with an interleaving scheme which converts the bursty errors into random errors which can then be decoded with Viterbi decoding. One such scheme is the PRIME standard [9].

On the other hand, it has also been shown that a combination of RS encoding and interleaving may be insufficient to correct all the burst errors in a power line channel. Chuah [10] analysed the performance of a scheme that combined RS encoding with a symbol interleaver and showed that in the presence of impulse noise, the RS decoder suffers drastic performance degradation even when a powerful symbol interleaver is used. This is attributed to the fact that while the interleaver converts burst errors into random errors, the count of residual burst errors at the interleaver may still be more than the error correcting capability of the RS code [19].

Error correction schemes that have incorporated concatenated codes with interleaving have since then been suggested and investigated. Daneshgaran et al. [20] investigated the interleaver design for serially concatenated convolutional codes. They brought forward a theoretical framework for a cost function-based interleaver optimization which is similar to the asymptotic Bit Error Rate (BER) of the block code. In addition, they implemented a systematic iterative technique for the construction of these interleavers. Likewise, Cao [21] investigated the performance of a concatenated coding scheme that combines an RS code and a convolutional code with a multi-dimensional trellis coding modulation.

Having taken much previous research into consideration and the developments

that had been made, the G3-PLC specification [22] proposed a new error correction scheme that was specifically developed for PLC in narrowband channels. Their scheme used a combination of RS encoding and convolutional encoding that have been well established already, but added a repetition encoding scheme that introduced considerable redundancy in the data which cascaded with a two-dimensional time and frequency interleaving algorithm.

2.2 Channel Coding

Because of the harsh nature of the PLC channel which degrades the quality of the signal sent over it, it is necessary to apply corrective measures that restore the integrity of the information sent. Error control coding, and specifically forward error correction is the used technique in PLC schemes to mitigate the effects of different types of noise disturbances affecting information transmission. Error correction coding is a technique whereby errors that are introduced into digital data, while it is transmitted through an unreliable communication channel are corrected based on received data. On the other hand, error detection coding is a technique to detect errors introduced in the channel. Collectively, error correction and error detection is referred to as Error Control Coding (ECC). ECC may be generalized into two types, namely Automatic Repeat Request (ARQ) and FEC. Power-line communication utilizes FEC. In this technique the sender encodes data using an error-correcting code prior to transmission. Redundancy is added to the information and is used by the receiver to reconstruct the original data that was sent.

2.2.1 Channel Capacity

The concept of channel capacity is important to know as it helps one understand the limitations of a channel and of the codes used when transmitting information in the channel. Channel capacity is synonymous with channel coding. Although the theory of channel capacity is not treated to detail in this dissertation, the concept is introduced. It should be noted that while spectral efficiency, or bandwidth efficiency (which relates to the information rate over a given bandwidth) is used to compare the data throughput of different modulation schemes at the physical layer, channel capacity relates to the bit rate that can be achieved in a channel with negligible error rate. Channel capacity therefore relates to the limitations posed by error correcting schemes and modulation rate adaptation to achieve a certain transmission rate without errors. Because spectral efficiency calculation requires sending information over

a physical channel and calculating the throughput and then divide it by the bandwidth of the system, the determination of spectral efficiency is outside the scope of this research as this work is only simulation-based.

The AWGN channel is the simplest estimation model of a channel that is commonly in use. If a coding scheme sends R bits per second (b/s) over an AWGN channel of bandwidth W Hz, the spectral efficiency in (b/s)/Hz is

$$\eta = \frac{R}{W}. \tag{2.1}$$

The field of channel coding theory was introduced in 1948 by Claude Shannon [23]. Since the introduction of this theory, researchers have been working on developing codes that approach channel capacity, also known as the Shannon limit. Shannon showed mathematically that for an AWGN channel with a signal-to-noise ratio SNR and bandwidth W Hz the reliable rate of transmission in b/s has an upper bound of

$$R < W \log_2(1 + SNR). \tag{2.2}$$

The SNR can be also defined as the average signal power to the average noise power. From equation 2.1 and equation 2.2, Shannon's hypothesis shows that the spectral efficiency has an upper bound in (b/s)/Hz of

$$\eta < \log_2(1 + SNR). \tag{2.3}$$

Equation 2.3 can be rearranged to obtain the lower bound of the SNR that is required for a reliable transmission and is given by

$$SNR > 2^{\eta} - 1. \tag{2.4}$$

Equations 2.2, 2.3 and 2.4 are a representation of the Shannon's limit on rate, spectral efficiency and signal-to-noise ratio respectively. The development of different schemes which are largely classified as algebraic or probabilistic had the aim to achieve this limit for AWGN channels. A parameter widely used in describing the characteristic of a signal is the energy per bit to noise power spectral density given by

$$E_b/N_0 = \frac{SNR}{\eta}. \tag{2.5}$$

Therefore for a specific spectral efficiency the energy per bit to noise power

spectral density has a lower bound of

$$E_b/N_0 > \frac{2^\eta - 1}{\eta}. \tag{2.6}$$

In equation 2.6, it can be seen that Shannon's lower bound on the energy per bit as a function of the spectral efficiency decreases with η. Taking limits on the equation one obtains that

$$\lim_{E_b/N_0 \to 0} \frac{2^\eta - 1}{\eta} = \ln 2. \tag{2.7}$$

Therefore the lower bound of the Shannon limit on AWGN channels is about -1.59 dB.

2.2.2 Algebraic Codes

Algebraic coding theory is a branch of coding theory concerned with the (n, k, d) block codes over the binary field F_2 where by a binary linear (n, k, d) block code comprises 2^k binary codeword n-tuples whose property is such that a modulo-2 component-wise sum of any two codewords produces another codeword [24]. In this representation, d denotes the minimum Hamming distance between any two distinct codewords, n is the code length and k is the code dimension. The Hamming distance is the minimum number of positions in which any two codewords differ. The algebraic coding theory generalizes to linear block codes over non-binary fields F_q.

Block codes are error-correcting codes that encode data in blocks. An (n, k, d) block code C over an alphabet of q symbols is a set of q^k n-vector codewords. A block code C over a field F_q of q symbols of length n and q^k codewords is a $q-ary$ linear (n, k, d) code if and only if its q^k codewords form a k-dimensional vector subspace of all the n-tuples over the finite field GF(p^q). This field is known as the Galois field. The number n is the code length and k is the code dimension. The code rate is defined as $R = k/n$. A simple (n, k, d) block code is shown in Figure 2.1. The codeword length is n, where the symbol length is k and the rest is parity information [25].
For a block code to be effective in error correction, there must be a one-to-one correspondence between the message m and its codeword c. But for a given code C, there may be multiple ways of mapping the messages to codewords. Linearity is the imposed requirement to ensure that the list of the block codes is not exhaustive. The usefulness of the linearity property is that the sum of

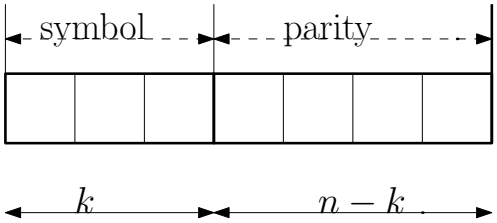

Figure 2.1: A simple (n, k) block code

any two codewords is also codeword. Hamming codes and Bose-Chaudhuri-Hocquengham (BCH) codes are the commonly used block codes in FEC [25].

Algebraic coding theory's primary objective is to maximize the minimum distance d for any given (n, k, d) code. This maximises the error-correcting capability of the code because the distance between any two possible codewords is increased meaning that the certainty of decoding correctly is maximised. For a code with a minimum distance d, the maximum number of errors that can be corrected t is

$$t = \frac{d-1}{2} \tag{2.8}$$

One of the first block codes is the Hamming code that was presented by Hamming in 1953 [26]. These codes are not suitable for practical applications but are useful to demonstrate encoding and decoding block codes [27]. Cyclic codes are an important type of codes of which BCH codes are part of. They are invariant under n-tuple cyclic shifts of the codeword and were first studied by in 1957 by Prange [28]. The advantage of cyclic codes is that they are simple and base their encoding and decoding around performing register cyclic shifts.

Binary BCH codes are the primary class of binary algebraic block codes. But they have found application in practice except as cyclic redundancy check (CRC) codes for error detection in Automatic-Repeat-Request (ARQ) systems [24]. The most important and popular subclass of non-binary BCH codes is the class of Reed-Solomon (RS) codes. Even though RS codes form a sub-class of BCH codes, they were constructed independently using a totally different approach by Reed and Solomon in 1960 [29], the same year that BCH codes were discovered.

The challenge with non-binary BCH codes like RS codes is that they pose a

difficulty in sending them over binary channels. As a result, the 2^m-ary RS has to be represented as binary m-tuples. A single binary bit error results in an entire 2^m-ary symbol to be incorrect and this phenomenon makes RS codes to be less effective than binary BCH codes in correcting binary errors. However, in this arrangement, RS codes are effective as burst-error-correcting codes since the m-bit burst is only one symbol meaning that the burst results in as single symbol error which can be easily corrected. It can be mathematically proven that RS codes are optimal binary burst-error-correcting codes [30].

The fact that RS codes are effective in correcting both random and burst errors makes them suitable for use in data storage systems and deep-space telecommunications systems where imperfections can cause bursty errors. Concatenation of these codes as outer codes with simple binary codes as inner codes provides high data reliability with reduced decoding complexity [31]. Because of these attributes, RS codes are among the most used codes today.

The paradigm of algebraic coding relied on the structure of finite-field algebra to design error correcting methods for hard-decision linear block codes. The aim was to develop codes with a guaranteed minimum distance and then making use of the algebraic structure of these codes to design distance-limited error-correcting algorithms whose complexity increases as a small power of the minimum distance [24]. In [24], it is shown that for the Shannon limit to be attained for block codes, the decoder must minimize the Euclidean and Hamming distances and the decoder must select the best of 2^k codewords. This requirement is also stated in [24].

Since typical block codes are not only hard-decision decoded but also use an exhaustive decoding algorithm which requires the order of 2^k computations, as the codes become large, the decoding complexity increases significantly making it very difficult for block codes to decode optimally and hence the reason why algebraic codes fail to meet the Shannon limit.

2.2.3 Probabilistic Codes

Probabilistic codes are derived from Shannon's probabilistic coding approach. While algebraic coding theory is aimed at finding codes that maximize the minimum distance, probabilistic coding focuses on finding classes of codes with an optimized performance with respect to coding and decoding complex-

ity. Probabilistic coding generally uses soft-decision decoding whether at the information input stage or at intermediary stages. Codes that fall into this category include convolutional codes, concatenated codes, product codes and trellis-coded modulation and the corresponding decoding of block codes.

Convolutional codes were first introduced by Elias [32] in 1955 as an alternative to block codes. Wozencraft and Reiffen [33] afterwards came up with sequential decoding as a decoding method for convolutional codes with large memory orders. Massey [34] proposed a simpler decoding method in 1963 that he referred to as threshold decoding. This advancement led to the rise of several practical applications of convolutional codes like digital transmission over the telephone, radio channels and satellite. It was in 1967 that Viterbi [35] proposed a maximum likelihood soft decision decoding algorithm that was easy to implement for short constraint length convolutional codes.

Viterbi's decoding algorithm together with soft decision sequential decoding innovated the use of convolutional codes in deep-space and satellite communication systems in the 1970s. Bahl, Cocke, Jelinek and Raviv (BCJR) [36] then introduced a Maximum Posteriori Probability (MAP) decoding algorithm in 1974. Ungerboeck and Csajka [37] introduced trellis-coded modulation using short constraint length convolutional codes in 1976. These codes had a rate of $R = k/(k+1)$ along with soft-decision Viterbi decoding. This scheme was to become the foundation for high-speed digital transmission over band-limited telephone channels.

Convolutional codes are often used in preference to block codes because they exhibit better performance than block codes of comparable encoding/decoding complexity. Also, they are among the earliest codes with effective soft decision decoding algorithms. The advantage of soft decision decoding is that it offers about 3 dB improvement on hard decision algorithms [25]. While block codes are made up of discrete blocks of k symbols, and $n-k$ parity bits, where n is the entire codeword length, convolutional codes are continuous codes in that they are encoded as a continuous stream of symbols using a window of length m that slides along the code to produce an encoded message only formed of parity bits. The size of this window is called the constraint length or the memory order. It is what determines the minimum distance and error correcting capabilities of convolutional codes.

A notable difference between convolutional codes and block codes is that the convolutional encoder has memory and its output at any time depends not only on the current input(s) but also on several previous inputs. A k-input, n-output, m-order convolutional encoder has a rate $R = k/n$ and an input memory of m. This means the encoder state has m bits, and information remains in the encoder for an additional m time units after data was fed into it [31]. The encoding of convolution codes is illustrated in Figure 2.2. The outputs p_1 and p_2 are obtained by convoluting the data in the memory window with the generator polynomials $g_1(x)$ and $g_2(x)$. The current input is shown as $x(n)$ and the immediate previous input is given by $x(n-1)$ while the input from two previous time units is $x(n-2)$. In this example, there is only one input and therefore the number of used shift registers is only one with a window length of three.

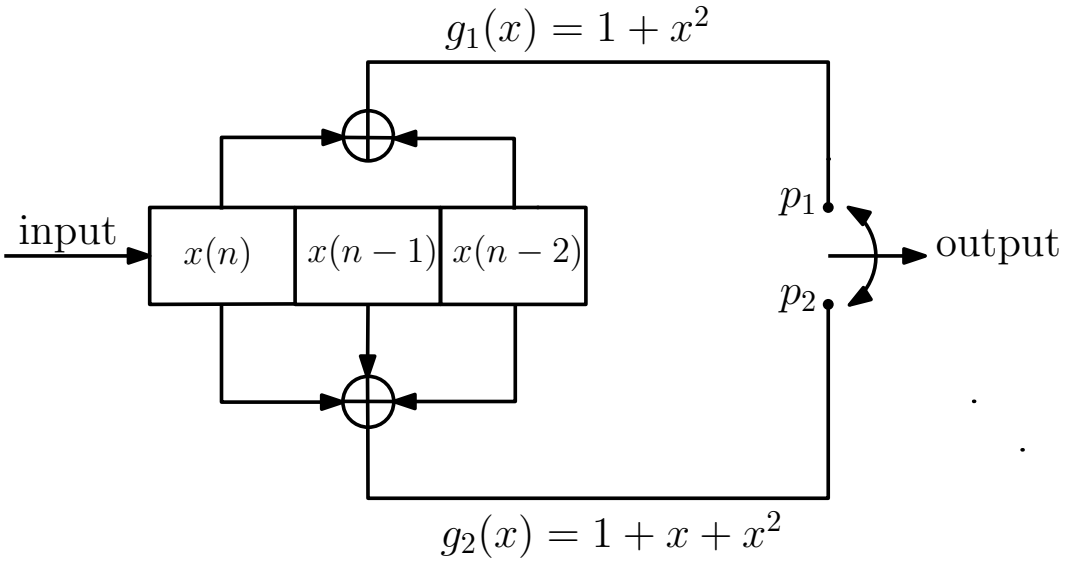

Figure 2.2: Convolutional encoding

2.2.4 Concatenated Codes

Concatenated codes were introduced by Forney in 1966 [18]. Concatenation involves cascading two linear block codes serially . The outer code is usually a non-binary code like RS codes over a finite field F_q and the inner code is normally a binary code. Although the individual codes may be short, the resulting code is longer and more robust. The occurrence of an error in the inner codeword can be easily corrected. However, if a couple of errors exist in the

inner codeword in such a way that the inner code is not capable to correct it, the error burst translates to one symbol in the outer code which again can be corrected.

Concatenated codes are not limited to only block codes. An outer block code can be concatenated with an inner convolutional code. The advantage of a convolutional code is that it uses soft decision decoding, which is usually achieved by the Viterbi decoding algorithm. On the other hand, block codes can employ the algebraic Berlekamp-Massey algorithm. Because convolutional codes are probabilistic and provide a closer performance to the Shannon limit than block codes, they have become popular in concatenation schemes.

Figure 2.3 shows a typical concatenated scheme. The outer encoder is a non-binary $GF(q)$ block code encoder where $q > 2$. An example is a Reed-Solomon encoder. The inner encoder can be either a binary $GF(2)$ encoder or a convolutional encoder depending on the application. The information is then sent over the channel. On the other end of the channel, the chronology is reversed and the binary decoder inner decoder comes before the non-binary coder outer decoder.

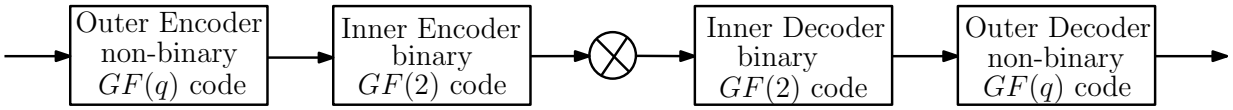

Figure 2.3: Concatenated scheme

2.2.5 Permutation Codes

A permutation code set C is made up of codewords that each have a symbol in the alphabet once and only once per codeword. Permutation decoding was first introduced by F.J MacWilliams [38]. Permutation codes are constructed in such a way that they have a specific minimum distance and they may both be cyclic and non-cyclic. Although permutation codes may not be very efficient in correcting disturbances or burst errors of several codewords, they do combat impulse noise and narrow-band interference existing in narrowband power-line channels [39]. The choice of permutation codes is based on the fact that they are capable of handling impulse and narrowband noise as well as frequency and time diversity as outlined in [40].

It can be stated without proof that for a permutation code with M unique symbols in every codeword and minimum Hamming distance d_{min}, the cardinality has an upper bound of

$$| C | \leq \frac{M!}{(d_{min} - 1)!} \tag{2.9}$$

However, the proof of this equation can be found in [40]. As the size of M increases, it becomes more difficult to obtain codewords of a good minimum distance with respect to the length of the codeword. This is one challenge experienced with using permutation codes. Special highly mathematical approaches become a necessity for larger codes, especially if the minimum distance desired is $M-1$. Such approaches include simulated annealing and genetic algorithms. Another challenge is that there is no established decoding procedure for these codes, which makes the decoding algorithm not only complex to write but also expensive to perform.

A notable advantage of permutation codes is their compatibility with M-FSK. Each symbol in a codeword can be mapped onto a specific frequency. This can be achieved in OFDM as well, where each Fast Fourier Transform (FFT) bin has N groups of M subcarriers whereby M-FSK is the modulation scheme used in the subcarriers.

2.2.6 Trellis-Coded Modulation

Trellis-coded modulation (TCM) is a coding-modulation technique based on the concept of *mapping by set partitioning* developed by Ungerboeck [41]. It is a scheme for band-limited channels that introduces encoding redundancy by expanding the signal constellation without increasing the bandwidth rather than increasing the bandwidth at a fixed signal constellation. The scheme uses minimum Euclidean distance as the design criterion instead of the Hamming distance. Ungerboeck showed that a coding gain of 3 to 4 dB could be achieved with 4 to 8-state trellis codes without incurring an expansion in bandwidth.

Trellis-coded modulation has been used in integer bit loading for power-line communication to jointly study the transmission rate and bit error rate as performance parameters. Biagi et al. [42] studied this scheme because of the advantage of its property to combine modulation and coding, in consideration

of power allocation as an optimization in which both transmission rate and bit error rate are related to the optimal design of TCM. A soft-decision code like trellis-coded modulation is often concatenated with an RS code, with a byte-interleaver between them.

Mapping by set partitioning can be combined with both block codes and convolutional codes although because of the optimal decoding of the Viterbi soft-decision algorithm convolutional codes are usually the preferred choice [43]. The principle in partitioning is to find subsets of the constellation that are similar in terms of spatial location and maximally separated. The goals is achieved by splitting the constellation into two congruent subsets with maximally separated points and then iteratively performing splitting using the same rule until a single constellation point is obtained.

Figure 2.4 shows the TCM partitioning of an 8-PSK constellation. Gray coding is applied to improve the decoding process. The minimum Euclidean distance of this 8-PSK constellation with a power ϵ_s is

$$d_0 = \sqrt{\epsilon_s(2 - \sqrt{2})}. \tag{2.10}$$

The second inner partition of two congruent subsets has an increased constellation minimum Euclidean distance of

$$d_1 = \sqrt{2\epsilon_s}. \tag{2.11}$$

The third inner partition has an even bigger Euclidean distance of

$$d_2 = 2\sqrt{\epsilon_s}. \tag{2.12}$$

TCM has an application in high speed telephone modems because of its ability of doubling the data rate by doubling the constellation size without increasing the bandwidth requirements. It is possible to use the scheme for transmitting information on power lines because it preserves bandwidth while increasing the rate at which information is sent. However, it is more suited to be used to reinforce the robustness of the transmission rather than to increase its speed because of the harsh nature of the channel. The treatment of the scheme in this literature is not only because it has been used before in power-line communication, but also because the scheme can be concatenated with block codes like Reed-Solomon codes, providing an alternative to the presented scheme. In

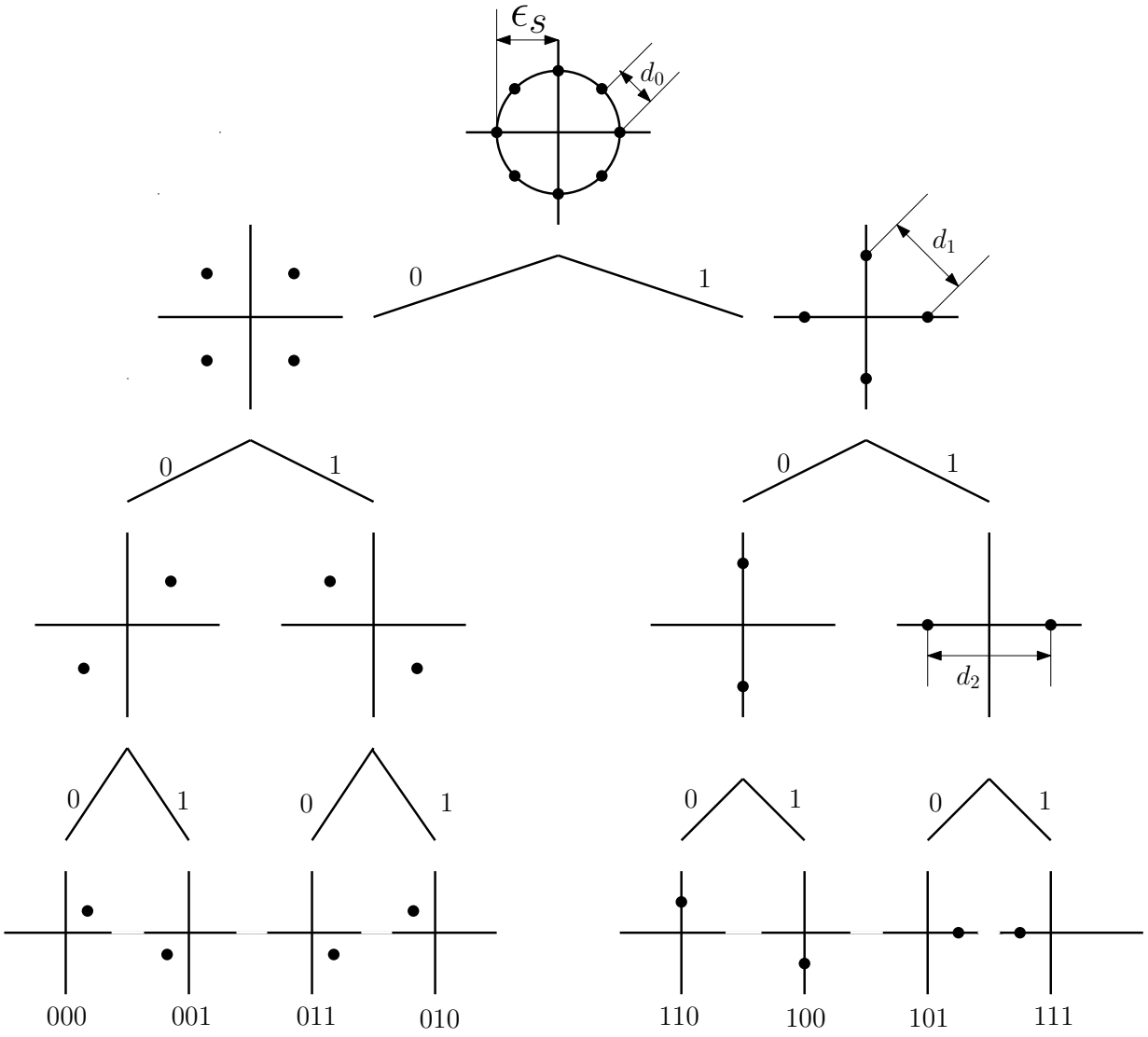

Figure 2.4: 8-PSK TCM constellation partitioning

addition, Trellis codes are designed based on Euclidean distance rather than Hamming codes, which provides a basis for understanding other schemes developed recently utilizing the minimum Euclidean distance of QPSK, which are discussed in this research.

2.3 Chapter Summary

The literature review is targeted at introducing the reader to the field of the research. The research is on power-line communication and has areas of interest in channel coding and modulation techiniques in light of the noise disturbances that exist in the channel that threaten the aim of increasing the transmission rate without incurring a significant error rate. The foundation of block codes and convolutional codes has been laid out as a tool for error correction. The design principles of concatenated codes has also been highlighted as an important aspect for understanding the choice of error correction codes in the concatenated scheme employed.

3 MODULATION SCHEMES

3.1 An Overview of Modulation in PLC

There are two main schemes used independently as a modulating carrier in power-line communication. These are MFSK and OFDM. MFSK has the advantage of being robust against impulse noise. But it has a low data rate compared to OFDM, and it does not perform well in handling burst errors. OFDM on the other hand has the advantage of a high data rate, immunity to delay spread if the symbol separation is kept longer than the delay. OFDM-MFSK was proposed in recent solutions as a reinforcement of OFDM to increase the scheme's resistance towards noise. M-ary PSK is normally used in conjunction with OFDM as a subcarrier modulation scheme. Permutation codes are sometimes used as a forward error correction scheme, often concatenated with another scheme. However, a simple predetermined permutation sequence has been used in this work that does not involve the usual error and erasure decoding. These different modulation techniques are first explored before the proposed technique is treated because they all play a role in the proposed technique.

3.2 Multiple Frequency Shift Keying

MFSK can be used independently as a modulation scheme in PLC. Frequency Shift Keying (FSK) is a frequency modulation scheme that conveys data by varying the frequency of a carrier wave while keeping the amplitude and phase of the modulated wave constant. In MFSK, the instantaneous carrier frequency is switched between M frequencies according to the baseband digital data. Table 3.1 shows the relationship between binary information and the corresponding modulating frequency if 4FSK is the used modulation scheme. Each two bit binary codeword is mapped onto a unique frequency that is impressed on the carrier signal. Frequency changes can slightly alter the measured frequency at the demodulator, but a good choice of frequencies makes it easier to decode the information. To further illustrate FSK, the relationship between a digital signal and the mapping to an analogue frequency-varying signal, Figure 3.1 shows how a digital signal is transformed from a binary sequence of

ones and zeros to a modulated 2FSK signal whereby the higher frequency corresponds to a digital one and the lower frequency corresponds to a digital zero.

Table 3.1: 4FSK mapping

Binary data	**4FSK frequency**
00	f_0
01	f_1
10	f_2
11	f_3

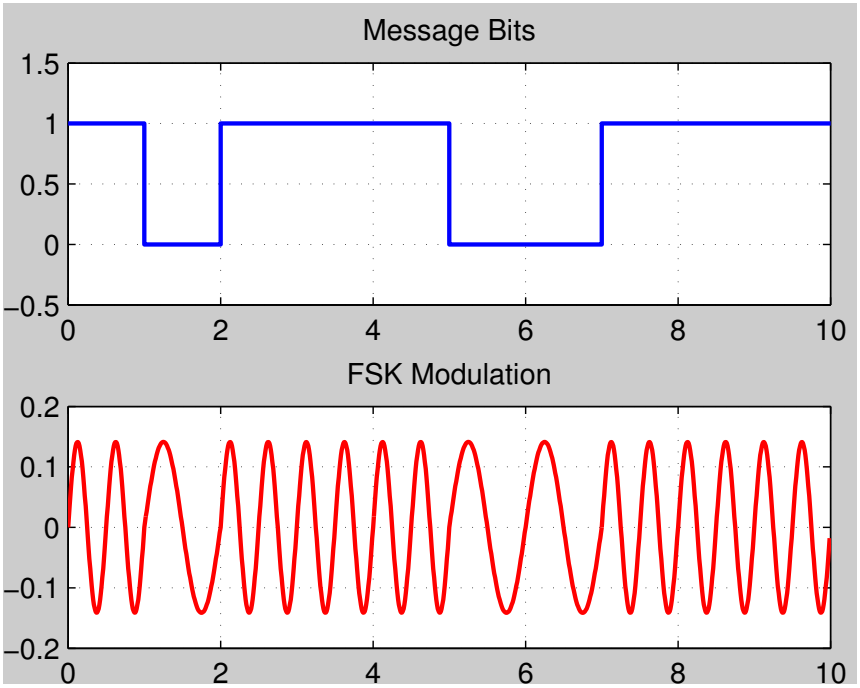

Figure 3.1: 2FSK modulation

Although more and more systems are now using digital modulation formats, the reason for the extended use of MFSK in power-line communication is because of a number reasons that make it suitable for the harsh power-line channel. Likewise, there are reasons why its use has declined over the years. Some of these are discussed subsequently.

3.2.1 Advantages

• *Resilient to noise:* Most noise is amplitude based, but phase shifts are also common. However, both amplitude variations and slight phase offsets do

not considerably affect FSK systems. This is because information in FSK is conveyed by varying the frequency at a constant amplitude. Therefore, any changes in amplitude do not upset the functioning of the system. By running the signal through a limiter such that only frequency variations are detected, the impact of noise is diminished.

• *Does not require linear amplifiers:* Because only frequency changes are sufficient to demodulate information, transmitter amplifiers do not need to be linear. In addition to the fact that FSK is easy to implement, the use of non-linear filters increases the efficiency of the system as linear amplifiers are inefficient.

• *Constant power requirements:* Because the scheme uses a constant amplitude, the power requirement is also constant.

3.2.2 Disadvantages

• *Spectrally inefficient:* FSK is not a very spectrally efficient modulation scheme. This is because for every M frequencies used, only $\log_2 M$ bits are transmitted. As a result, other schemes like M-ary Phase Shift Keying and Quadrature Amplitude Modulation are preferred in most data transmission systems because of their ability to increase the data rate without incurring a loss in spectral efficiency.

• *Slow speed:* Because of the $\log_2 M$ bits limitation for every M frequencies, it means that M-ary FSK is limited to low speeds to maintain bandwidth limitations. An increase in speed requires increased spectrum allocation, but an increase in speed means the symbol rate also increases. The increase in symbol rate accentuates inter-symbol interference, which is undesirable.

• *Sidebands extensions:* One of the setbacks of frequency modulated transmissions is the the sidebands extend beyond the desired bandwidth, and as a result, filters have to be used to limit the bandwidth. But these cause signal distortion.

3.3 Multiple Phase Shift Keying

PSK involves the modulation of information by varying the signal phase while maintaining its frequency to relay information.

3.3.1 BPSK

Binary phase shift keying is the simplest form of phase shift keying, which is also the most robust. In this scheme, each digital information bit is mapped to one of two phases. These phases are 0 and π radians. Equation 3.1 describes BPSK modulation. The signals representing binary 0 and binary 1 are out of phase by π radians.

$$s_1(t) = Acos(2\pi f_c t), \quad 0 \leq t \leq T, \quad for \quad 1 \tag{3.1a}$$

$$s_2(t) = Acos(2\pi f_c t + \pi), \quad 0 \leq t \leq T, \quad for \quad 0. \tag{3.1b}$$

BPSK maps each binary bit into a single modulated symbol and it has only two possible symbols π radians apart. This method offers the best performance in terms of demodulation accuracy because a symbol corrupted by channel noise has to suffer a phase shift of over +/- $\pi/2$ radians to be incorrectly decoded. Although the data rate is low at one bit per symbol, the integrity of the information is maximised. The theoretical bit error rate for BPSK in AWGN is

$$P_b = \frac{1}{2}\text{erfc}\left(\sqrt{\frac{E_b}{N_0}}\right). \tag{3.2}$$

The BPSK modulation scheme is shown in Figure 3.2. It maps a binary zero to -1 and a binary one to 1, where 1 has a phase of 0 radians and -1 a phase of π radians.

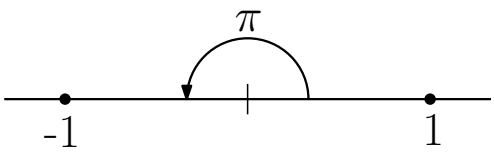

Figure 3.2: BPSK encoding

One of the main problems with phase shift keying is that the receiver cannot know the precise phase of the transmitted signal. Synchronizing the oscillator clocks would still not solve the problem because only the path length is what would determine the precise phase of the received signal. To overcome this problem, differential PSK is used to encode the data onto a carrier. As a result, M-ary PSK is normally used in OFDM as a subcarrier modulation

scheme in differential mode.

The advantage of differential mode is that it eliminates the necessity for coherent detection, which is sensitive to small changes in phase. In M-ary PSK, the phase is varied between M phases corresponding to the number of symbols in the I-Q constellation diagram. Figure 3.3 shows how binary information is modulated using PSK. Using the simple case of BPSK, there are two distinct phases used to modulate information. MPSK uses M symbols that are out of phase by $2\pi/M$ (where $M = 2$ for BPSK).

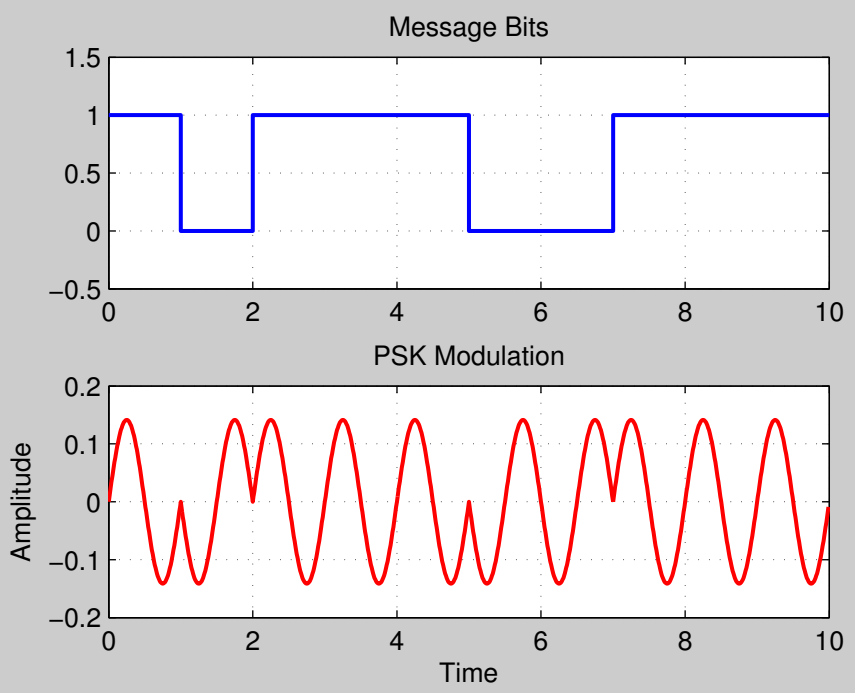

Figure 3.3: BPSK modulation

3.3.2 QPSK

The motivation behind the use of M-ary PSK is to improve the bandwidth efficiency of the PSK scheme. The number of bits represented per symbol is given by $n = \log_2 M$. This increases the spectral efficiency n times. The counteracting factor to this advantage is that BER degradation increases with an increase in the value of M. M-ary PSK is defined by

$$s_i(t) = Acos(2\pi f_c t + \theta_i), \quad \theta \leq t \leq T, \quad i = 1, 2, ..., M, \tag{3.3}$$

where

$$\theta_i = \frac{(2i-1)\pi}{M}.$$

QPSK is a good trade-off between data rate and robustness in power line communication. This technique maps two binary bits into one I-Q symbol whereby the symbols are $\pi/2$ radians apart. The points of the constellation diagram are chosen to give a uniform angular separation in a circle to maximise the phase separation between two adjacent constellation points. This maximises the immunity of the system to noise and ensures that the symbols are transmitted with equal energy.

Gray coding is used to improve the performance of the scheme. This technique involves ensuring that any two adjacent symbols differ by only one binary symbol to increase the probability of correctly decoding a symbol. This technique is shown in Figure 3.4. The unit symbols obtained QPSK are $0.707 + j0.707$, $-0.707+j0.707$, $-0.707-j0.707$ and $0.707-j0.707$ corresponding to a discrete-time binary-valued input singnal represented by the bit sets of 00, 01, 11 and 10 respectively.

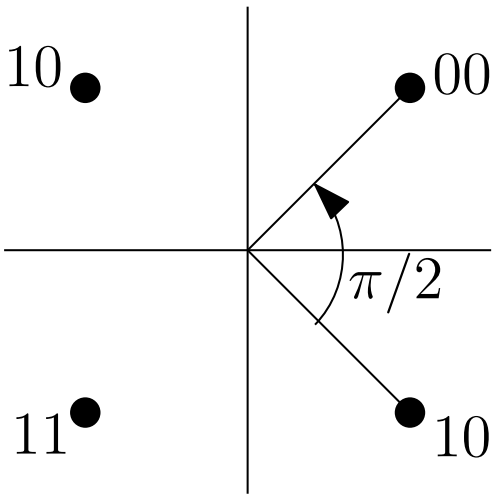

Figure 3.4: QPSK encoding

Assuming a Gray-encoded QPSK constellation point set, Figure 3.5 shows how the points are arranged in the I-Q axes. QPSK maps each two bit word to a symbol. Table 3.2 shows how a two bit binary codeword maps onto one of the four QPSK symbols. The magnitudes of the constellation point vectors from the origin are equal and the symbol phases are $\pi/2$ apart.

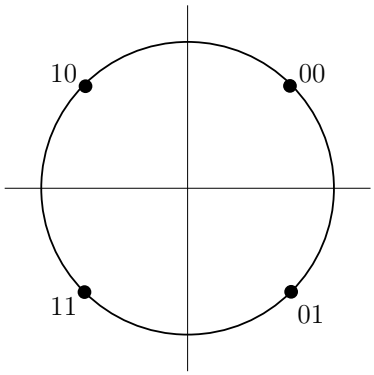

Figure 3.5: Gray-coded QPSK constellation

Table 3.2: QPSK mapping

Binary data	**QPSK symbols**
00	0.707 + i0.707
01	-0.707 + i0.707
10	-0.707 - i0.707
11	0.707 - i0.707

One of the advantages of M-ary PSK over M-ary FSK is that it is possible to increase the data rate in PSK without increasing the bandwidth. Combining M-ary PSK with a high data rate multi-carrier scheme like OFDM the throughput can be significantly increased. The setback with using PSK is that it is sensitive to phase changes as the number of symbols in the constellation increases.

3.4 OFDM

Orthogonal Frequency Division Multiplexing (OFDM) is a multicarrier digital modulation scheme in which a signal is split into several narrowband channels at orthogonal frequencies which maximizes spectral efficiency. While in general overlapping adjacent channels interfere with one another, in OFDM the channels are orthogonal to each other and therefore do not interfere. Because of this advantage, OFDM is widely used in power-line communication not only because of its high data rate but also because of its ability to be manipulated in several ways to combat noise in the power line channel. The OFDM signal is generated from an Inverse Discrete Fourier Transform (IDFT) and it is given by

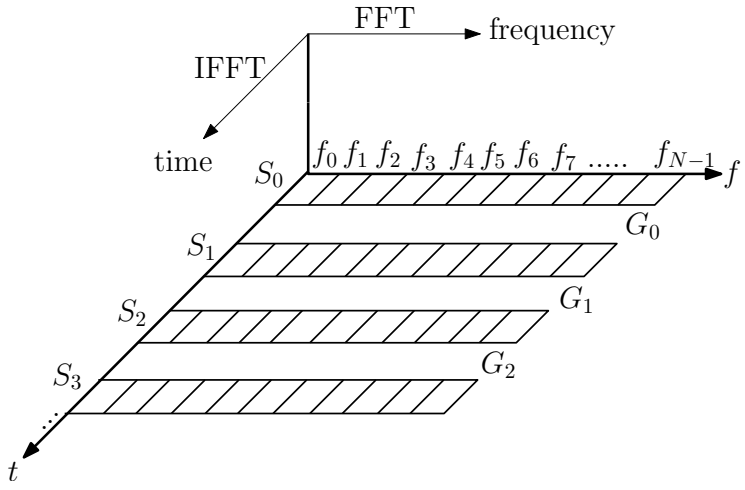

Figure 3.6: OFDM frequency-time representation

$$x(n) = \sum_{k=0}^{N-1} X(k) e^{j2\pi kn/N} \tag{3.4}$$

Where N is the number of data subcarriers. A frequency-time representation of OFDM is shown in Figure 3.6. It can be seen that there are N subcarriers in an FFT window at one time instance with centre frequencies denoted by $f_0, f_1, ..., f_{N-1}$ that collectively form an OFDM symbol. The frequency difference between two adjacent subcarrier centre frequencies, or simply the subcarrier frequency f_{sc} is equal to the subcarrier bandwidth and $N \times f_{sc}$ is the system bandwidth. The OFDM symbols denoted by $S_0, S_1, S_2, S_3...$ can be seen from the time domain to be separated by guard intervals $G_0, G_1, G_2...$ which are time quantities.

Because of the scheme's ability to overcome delay spread and impulse noise among other issues, while at the same time offering improved data rate over traditional modulation schemes, OFDM has found many applications including in power-line communication and in Long Term Evolution (LTE), which is a fourth generation (4G) mobile telecommunications standard. Despite the advantages, OFDM is susceptible to many undesirable phenomena that affect not only its performance but the quality of the information being transmitted as well. This chapter is therefore dedicated to understanding OFDM and studying these phenomena, their causes and mitigation techniques as well as the design problems experienced in designing an OFDM system. The research approach implemented in overcoming some of these problems is then presented in the next chapter.

3.4.1 OFDM Design

The design of OFDM involves making trade-offs with several conflicting requirements depending on the specific application. Some of the parameters that are part of requirements are:

- Bit rate
- Bit error rate
- Bandwidth
- Delay spread of the transmission channel

Depending on the targeted outcome, the specific requirements involving these parameters can be achieved by precisely adjusting a couple of parameters. As already indicated, these requirements are affected by several other parameters that produce conflicting results.

Cyclic Prefix

The cyclic prefix is an extension of the symbol either by preceding the symbol with its periodic extension taken from the back of the symbol or by appending a portion of the symbol from the front at the back of the symbol. This is done to mitigate Inter-Symbol Interference (ISI). The cyclic prefix C_p affects the SNR and the energy per bit as it consumes power because it carries redundant information. A very long cyclic prefix therefore degrades the signal to noise ratio. As a common standard, the cyclic prefix is set to be 0.25 times the symbol length.

Guard Time

The guard interval or guard time t_g is the time duration that is allowed between successive OFDM symbols to reduce ISI caused by interference between two adjacent symbols. The value of the guard time is chosen based on the multipath delay spread of the channel, which is a known quantity. In PLC, this is not a very big issue as it may be in the wireless channel whereby the sender or the receiver or both may be mobile. To have a reliable communication with respect to this quantity, it is necessary to have the guard time bigger than the delay spread. As a rule of thumb, the guard time is set to be at least twice the root mean square of the delay spread. As the constellation size of the subcarrier modulation scheme increases, the sensitivity of OFDM to ISI and

ICI also increases. That means that 64 Quadrature Amplitude Modulation (QAM) is more sensitive than 16 QAM, and requires a longer guard time.

Symbol Duration

As already explained in Section 3.4.1, the guard time affects the SNR. To minimize the impact the symbol duration has on the SNR, the symbol duration must be significantly larger than the guard time. The challenge is that for the symbol period

$$T_s = \frac{1}{f_{sc}}, \tag{3.5}$$

where f_{sc} is the channel spacing (subcarrier frequency), an increase in the symbol duration corresponds to a decrease to the subcarrier frequency, meaning the system becomes more prone to jitter, fading and CFO. The total symbol duration is given by

$$T_t = T_s + t_g. \tag{3.6}$$

Number of Subcarriers

The number of subcarriers is a very important parameter in OFDM design. If the desired subcarrier frequency spacing is fixed, then the bandwidth B is the deciding factor on the number of subcarriers N in a symbol, since the relationship between the subcarrier spacing and the bandwidth is

$$N = \frac{B}{f_{sc}}. \tag{3.7}$$

If the number of subcarriers is the fixed parameter, then the subcarrier spacing can be calculated from the bandwidth. However, as explained in Section 3.4.1, the subcarrier spacing affects the sensitivity of the OFDM system, especially if higher constellation size modulation schemes are used. In addition, the number of required subcarriers has implications on the FFT window size, and since the window size can only be a length of 2^k where k is a positive integer, it is possible to have many unused frequencies which lowers the spectral efficiency of the system.

3.4.2 OFDM Impairments

OFDM suffers from a number of impairments, including peak to average power ratio (PAPR) and carrier frequency offset. This research has a focus on improving the usage of bandwidth of current power-line communication schemes in use without exacerbating the impact of carrier frequency offsets.

Peak to Average Power Ratio

PAPR is caused by constructive and destructive interference in subcarriers which causes saturation in power amplifiers. It is treated mathematically by Muller and Huber [44], and is also addressed by the use of block coding by Jones, Wilkinson and Barton in [45]. Li and Ritcey also proposed a solution involving m-sequences in [46], while Eetvelt, Wade and Tomlinson [47] used a selective scrambling technique.

There are two more commonly used approaches to the problem. The first is peak windowing proposed by Pauli and Kuchenbeeker [48] and generalised by Van Nee and Wild in [49]. The second approach is clipping and filtering. This method is treated at depth by O'Neill and Lopes [50], Li and Cimini [51] and also by Wulich and Goldfeld in [52].

Carrier Frequency Offsets

OFDM has overlapping spectra and rectangular impulse responses. As a result, each OFDM sub-channel (subcarrier) has a sinc-shaped frequency response. Therefore, time variations of the channel over an OFDM symbol duration destroys the orthogonality of subcarriers, as a result of which there is power leakage among subcarriers. This is known as inter-carrier interference, which causes degradation in the system performance [53].

The OFDM orthogonality attribute enables the scheme to effectively optimize bandwidth. Each subcarrier overlaps with its immediate adjacent subcarriers in such a way that it does not interfere with them. Consider an OFDM signal that is represented by the equation

$$s(t) = \sum_{k=0}^{N-1} X(k) e^{j2\pi f_k t}. \tag{3.8}$$

Orthogonality is observed if

$$\int_0^T g_1(t)g_2^*(t)dt = \int_0^T e^{j2\pi f_p t}e^{-j2\pi f_q t} = 0, \quad p \neq q, \tag{3.9}$$

where $f_k = \frac{k}{T}$, and f_p and f_q are centre frequencies of adjacent subcarriers. Orthogonality is lost if Equation 3.9 is not equal to zero. This happens when the system has a carrier frequency offset. A carrier frequency offset in simple terms is a measure of the loss orthogonality. One of the most common causes of this phenomenon in stationary architectures where the Doppler shift does not occur is the mismatch in the sampling frequencies between the transmitter and receiver oscillators. The relationship between the received signal $r(n)$ and the sent signal $x(n)$ is

$$r(n) = x(n)e^{j2\pi n\Delta f/F_s}, \tag{3.10}$$

where Δf is the frequency offset in Hz and F_s is the sampling frequency. This can be expressed in Euler form as

$$r(n) = A(n)e^{j\theta(n)}e^{j2\pi n\Delta f/F_s} \tag{3.11a}$$

$$= A(n)e^{j(\theta(n)+2\pi n\Delta f/F_s)}, \tag{3.11b}$$

where $A(n)$ and $\theta(n)$ are the magnitude and phase of the modulated symbol $x(n)$ respectively. From Equation 3.11b, it can be seen that the CFO introduces a phase offset whose effect on the signal is dependent on the time instant n of the modulated symbol $x(n)$.

In practice, CFO is caused by the Doppler effect for mobile systems and/or instability and mismatch of the local oscillators at the transmitter and receiver. In the presence of CFO, the modulated symbols of the DFT are given by

$$R(k) = X\left(k - \frac{\Delta f}{f_{sc}}\right). \tag{3.12}$$

Equation 3.12 shows that the frequency offset results in a change in the sampling instants of the modulated signal. This not only means that the subcarrier is not sampled at its peak amplitude but it also means that the subcarrier is sampled at a time instant where the adjacent subcarrier is not zero and hence the orthogonality of the subacarriers is lost. This is the cause of ICI.

To express the continuous time representation of the sent signal $x(t)$, the Sam-

pling theorem is invoked. This is expressed as [54]

$$x(t) = \sum_{k=-\infty}^{\infty} X(k) \frac{sin[\pi(2Wt - k)]}{\pi(2Wt - k)}, \tag{3.13}$$

where W is the baseband bandwidth of the signal, which is the subcarrier bandwidth. Therefore, the received signal $R(m)$ can be expressed as

$$R(m) = X\left(m - \frac{\Delta f}{f_{sc}}\right) = \sum_{k=-\infty}^{\infty} X(k) \frac{sin\left[\pi\left(\frac{2W}{F_s}\left(m - \frac{\Delta f}{f_{sc}}\right) - k\right)\right]}{\pi\left(\frac{2W}{F_s}\left(m - \frac{\Delta f}{f_{sc}}\right) - k\right)}. \tag{3.14}$$

Using the Nyquist theorem, the assumption $F_s = 2W$ is made, and Equation 3.14 can be simplified to

$$R(m) = X\left(m - \frac{\Delta f}{f_{sc}}\right) = \sum_{k=-\infty}^{\infty} X(k) \frac{sin\left[\pi\left(m - \frac{\Delta f}{f_{sc}} - k\right)\right]}{\pi\left(m - \frac{\Delta f}{f_{sc}} - k\right)}. \tag{3.15}$$

Equation 3.15 shows that every received I-Q symbol is the sum of all the transmitted I-Q symbols, with a scaling that is dependent on m, k and the ratio $\frac{\Delta f}{f_{sc}}$. Because all the subcarriers interfere with the current subcarrier due to the loss of orthogonality, it is for this reason that the effect of carrier frequency offset in OFDM systems is termed inter-carrier offset. Carrier frequency offset is a major limitation in OFDM because the scheme is sensitive to frequency errors caused by frequency differences at the transmitter and receiver of local oscillators. The two main detrimental effects caused by the frequency offset are:

- Signal amplitude reduction due to offset sampling.
- Inter-carrier interference due to loss of orthogonality.

ICI mitigation techniques are generally divided into three categories. These are:

1. Frequency domain equalization. Ahn and Lee [55] treat the subject using training signals.
2. Time domain windowing using windowing functions [56].
3. ICI self-cancellation [57].

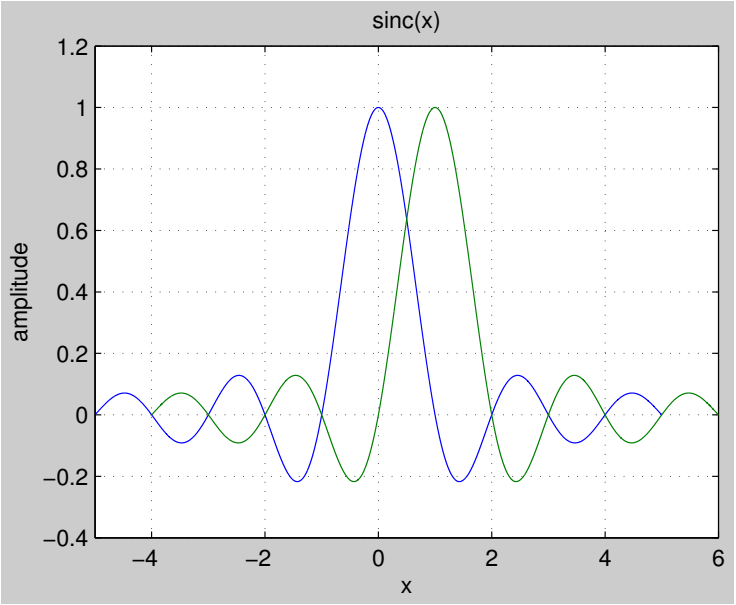

Figure 3.7: Two orthogonal subcarriers

It has already been established that the presence of CFO destroys the orthogonality of subcarriers. Figure 3.7 illustrates two orthogonal subcarriers. From the figure, a zero crossing of one subcarrier corresponds to the peak of the adjacent subcarrier. The sum of the two subcarriers at this point is equal to the value of the non-zero subcarrier. Mathematically, the dot product of two subcarriers is zero. On the other hand, Figure 3.8 displays two subcarriers that are not orthogonal. In this case, when one subcarrier is at maximum amplitude the other subcarrier is at minimum negative amplitude. The subcarriers therefore interfere destructively. Such a phenomenon is referred to as inter-carrier interference.

Figures 3.9 and 3.10 show how several subcarriers are oriented when orthogonal and when they are not orthogonal respectively. The latter is the undesirable effect of CFO.
The carrier frequency offset is simulated by using the equation

$$r(n) = x(n)e^{j2\pi\psi n/N}, \tag{3.16}$$

where $0 \leq n < N$ and ψ is the normalized CFO scalar quantity (the phase shift per symbol interval due to a carrier frequency offset Δf), N is the size of the Fast Fourier Transform (FFT) window and $x(n)$ and $r(n)$ are the transmitted and received signal instances respectively. The normalized CFO scalar quantity

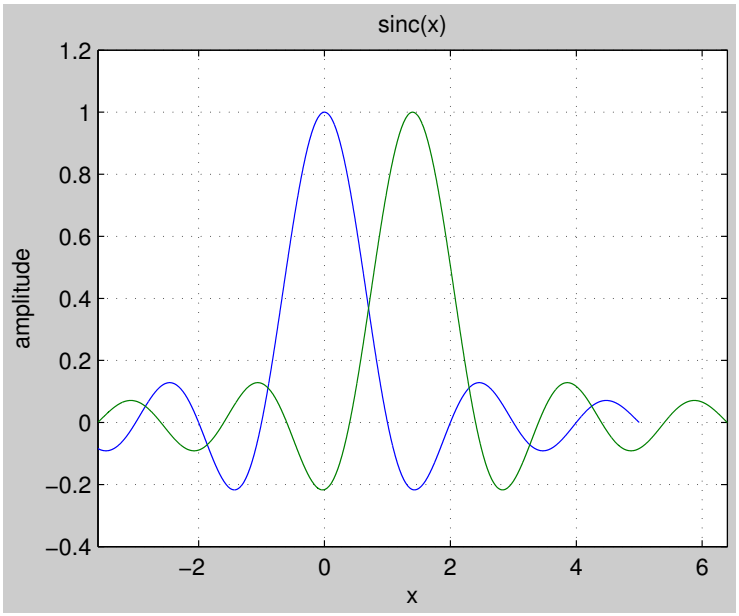

Figure 3.8: Two non-orthogonal subcarriers

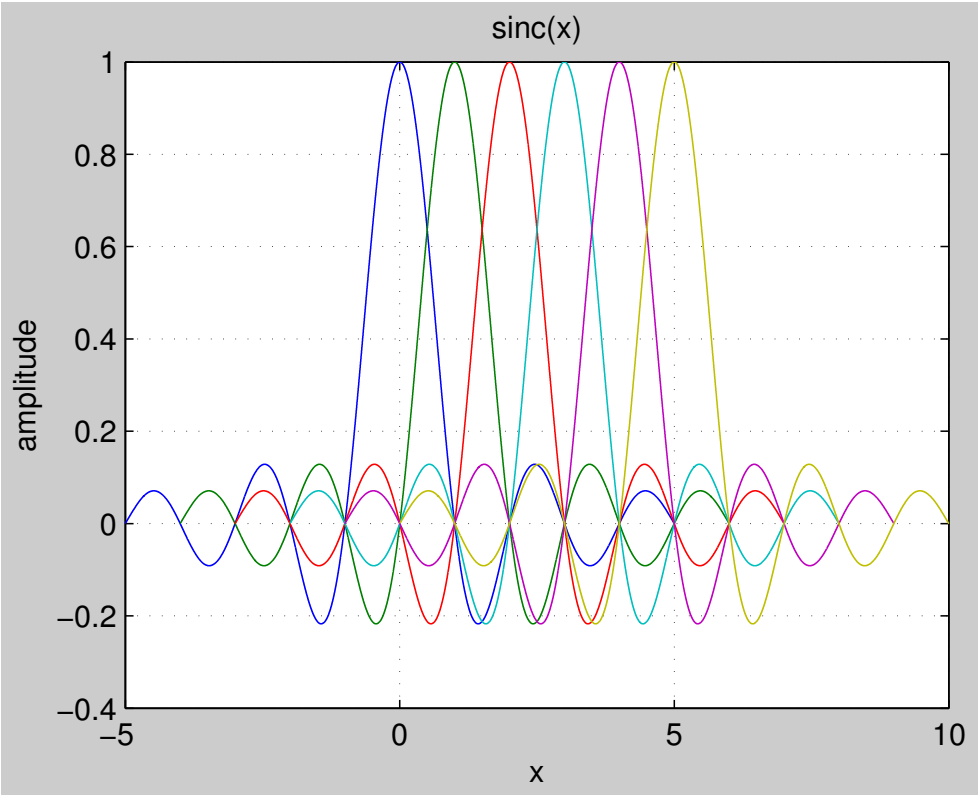

Figure 3.9: Many orthogonal subcarriers

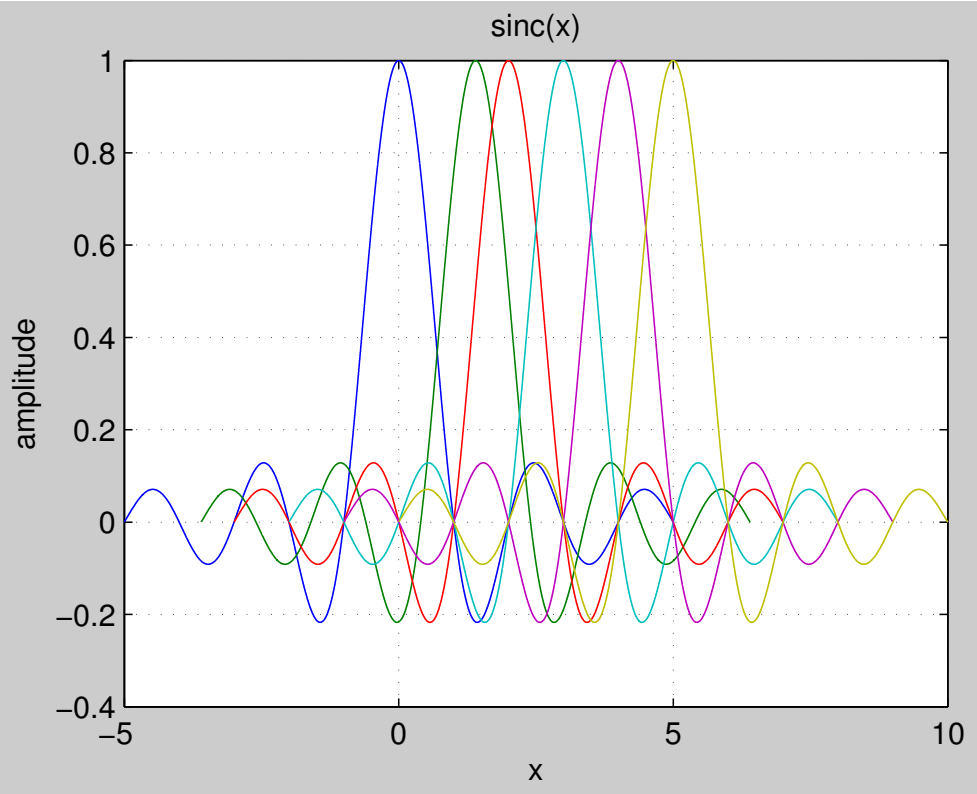

Figure 3.10: Many non-orthogonal subcarriers

ψ is given by [58, 59]

$$\psi = \frac{\Delta f}{f_{sc}} = \Delta f T_s, \tag{3.17}$$

where Δf is the carrier frequency offset in Hz, f_{sc} is the subcarrier frequency spacing and T_s is the symbol interval (OFDM symbol duration including the cyclic prefix). It follows that if $\Delta f = 0$, the CFO is zero. This is the condition when orthogonality is preserved. If $\psi \neq 0$, then the received signal has a phase shift.

The normalized frequency offset of Equation 3.17 can be divided into an integer part l and a fractional part ψ_f such that $\frac{-1}{2} \leq \psi_f \leq \frac{1}{2}$. The normalized CFO therefore can be expressed as

$$\psi = l + \psi_f. \tag{3.18}$$

The integer frequency offset l results in a cyclic shift of the subcarriers while the fractional part reduces the SNR of the signal and increases the symbol error rate [60]. The comprehensive effect of carrier frequency offsets can there-

fore be summarised as follows:

• The desired signal $X(k)$ is received at the $(k+1)$-th subcarrier instead of the k-th subcarrier.

• The magnitude of $X(k)$ is attenuated by the magnitude of the DFT of the CFO factor, given by $\left|\frac{sin(\pi\psi)}{Nsin(\pi\psi/N)}\right|$.

• The phase of the desired signal is shifted by $e^{j2\pi\psi_f}$.

• The signal is subjected to inter-carrier interference.

The typical frequency accuracy of most commercial crystal oscillators is 3 - 13 ppm [61]. In G3-PLC where a sampling frequency of 0.4 MHz is used and a subcarrier frequency spacing of 1.5625 kHz employed for an FFT size of 256, this accuracy translates to a frequency offset range of 1.2 - 5.2 Hz. This frequency offset corresponds to a maximum of 0.33 % of the subcarrier frequency spacing. In practice, an inter carrier interference resulting from a sampling frequency offset of about 2 % of the subcarrier frequency spacing, is negligible [22], meaning that the typical carrier frequency offsets caused by oscillator frequency drift are not likely to cause detrimental effect on the inter carrier interference. However, with increasing demand for higher data rates, power-line communication will use higher sampling frequencies, which will not only increase the offset frequencies but also the sensitivity of the system to frequency offsets. This research therefore takes into account such future developments in power-line communication.

Impulse Noise

Impulse noise is a powerful time localized burst caused by switching mode transients generated by switch mode power supplies. It can occur over a large frequency band and it is visible in the time domain. Impulse noise corrupts information over several OFDM subcarriers. Because impulse noise is a time domain noise, it is added to the signal after the IFFT in simulation environments. Both the amplitude and width of impulse noise are known to follow a Gaussian distribution with a zero mean and non-zero variance. However, arrival of impulse noise follows a Poisson distribution, which is a discrete probability distribution for the count of events that take place randomly in a given

time interval. The probability of observing k events in a given time interval is given by

$$P(k, \lambda) = e^{-\lambda} \frac{\lambda^k}{k!} \tag{3.19}$$

Where λ is a Poisson parameter of distribution giving the number of events occurring in a given time period. Impulse noise typically lasts no longer than 0.1 ms and it has a Poisson distribution with an impulse arrival rate of $0 \leq \lambda \leq 5 \times 10^{-3}$ s [62]. The OFDM symbol duration T is typically 4 μs after the addition of a guard interval. It follows that the probability of the arrival of k impulse events in an OFDM symbol duration T is

$$P(k, T, \lambda) = e^{-\lambda} \frac{(\lambda T)^k}{k!} \tag{3.20}$$

Narrowband Noise

Narrowband disturbances are frequency-limited but time-ubiquitous disturbances that arise from an ingress of radio and TV broadcasts at frequencies near the modulating frequency. It goes without saying that narrowband disturbances occur in the frequency domain and therefore they are simulated by the addition of noise to the signal after the I-Q symbols have been loaded onto the OFDM subcarriers before the IFFT is applied.

3.4.3 Implementation Parameters

The G3-PLC uses the frequency range of 35.9 kHz to 90.6 kHz of the CENELEC-A band[1]. A sampling frequency F_s of 0.4 MHz is used at the transmitter and receiver which provides sufficient margin above the Nyquist frequency for signal filtering. The maximum number of carriers used is 128, and since not all carriers are used this corresponds to an IFFT size N of 256. The subcarrier spacing as a result is given by

$$f_{sc} = F_s/N = 0.4 \times 10^6/256 = 1.5625 \quad \text{kHz}$$

Table 3.3 summarizes the system parameters.

[1]The CENELEC-A band is one of the frequency bands that G3-PLC may use in Europe. It has a range of 35 kHz to 91 kHz.

Table 3.3: OFDM parameters

Parameter	Quantity
F_s	0.4 MHz
f_{sc}	1.5625 kHz
N	256

3.5 OFDM-MFSK

OFDM-MFSK is an application of MFSK in OFDM that has been exploited because of the strengths of MFSK in noisy channels. The scheme combines OFDM and MFSK to come up with a scheme exhibiting the strengths of both OFDM and MSFK.

Wetz et al. [63] presented a scheme for fast fading channels combining OFDM-MFSK and DPSK using non-coherent detection. In the scheme, M-ary FSK is combined with OFDM by dividing OFDM symbol subcarriers into groups of M and employing MFSK to each one of them. The value one is assigned to the transmitted subcarrier while the rest of the $M-1$ subcarriers are set to zero energy.

Figure 3.11 shows the arrangement of subcarriers in a OFDM-4FSK scheme with a frequency spacing of Δf. The red arrows depict frequencies of transmission while green arrows show unused frequencies and each frequency corresponds to a two-bit word. Increasing the value of M increases the power efficiency of the modulating scheme. The more the value increases, the more the efficiency approaches the Shannon bound. However, the spectral efficiency diminishes towards zero as M increases because only $\log_2 M$ bits can be transmitted for every M frequencies. This poor spectral efficiency of MFSK is a major drawback of MFSK and MFSK-based OFDM schemes.

M-ary PSK has the advantage of the capability to increase the corresponding value of M without incurring a drop in the spectral efficiency. Hence, OFDM based on MPSK is adopted in this work. Another notable advantage of M-ary PSK over M-ary FSK is that because of its ability to convert any number of bits to one symbol, it is possible to increase the bit rate without increasing the symbol rate, and consequently, without increasing the inter-symbol interference, because ISI worsens with an increase in the symbol rate.

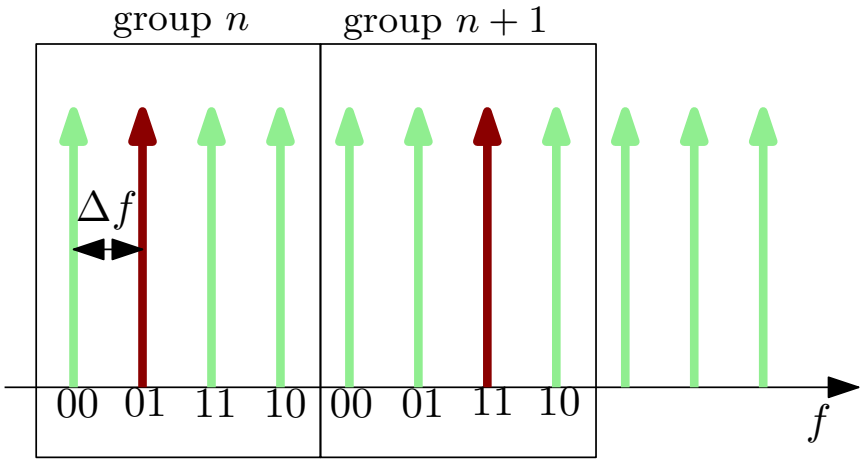

Figure 3.11: OFDM-4FSK

3.6 Other OFDM-based Schemes

Papilaya et al [64] modified the conventional QPSK-OFDM and OFDM-MFSK schemes to come up with new schemes with improved bit error rate performances in comparison to either conventional scheme. In their definition, QPSK-OFDM is an OFDM scheme whereby the subcarriers are modulated using QPSK. On the other hand, OFDM-MFSK is as defined in Section 3.5.

In their modified OFDM-MFSK scheme, instead of sending a one in the selected subcarrier and setting the rest of the subcarriers in the group to zero, a QPSK symbol is loaded to the selected subcarrier. This way, two bits are used to select the subcarrier and another two bits are used in the QPSK symbol. This improves the number of bits per subcarrier from 0.5 in the conventional OFDM-MFSK to 1 in the modified scheme, because a total of four bits are used in a group of four subcarriers.

On the other hand, in their adapted QPSK-OFDM, the real and imaginary parts of a QPSK symbol S are independently assigned to different subcarriers in the group. This implies that a QPSK symbol is spread over more than one subcarrier. The rest of the subcarriers in the group carry components of a QPSK symbol S' in such a way that the Euclidean distance between S and S' is maximized. This consequently improves decoding.

They claim that their modified QPSK-OFDM scheme yielded no net loss in SNR requirements and demonstrated superior bit error rate performance in the presence of frequency disturbances and frequency selective fading noise,

although the resultant data rate is half that of conventional QPSK-OFDM. Their encoding involves using an (n, k) RS code and a permutation code. In their work, they combined the quality of OFDM-MFSK of performing well in fast fading channels with the strength of the conventional QPSK-OFDM scheme of performing well in AWGN and impulse noise conditions as the FFT size increases.

One of the major differences between their research work and the presented work is that in one of their solutions, they used OFDM-MFSK whereby they substitute sending a one with sending a QPSK symbol in the subcarrier carrying information while in this work OFDM subcarriers are arranged by using a permutation sequence instead of grouping them using MFSK. In their modified QPSK-OFDM solution, they transmitted information in all the $M-1$ subcarriers by assigning real and imaginary parts to separate subcarriers to maximise the Euclidean distance. On the contrary, the presented work assignes the whole QPSK symbol to one subcarrier, and the other subcarriers do not share any information.

3.7 Chapter Summary

The modulation schemes used in this work, BPSK, QPSK and OFDM are discussed in detail in this chapter. The generation of OFDM is explained in detail and the design parameters that are considered when designing an OFDM system, the property of OFDM they affect and the trade-offs involved are also discussed. The nature of the OFDM signal is also studied together with the conditions that are responsible for corrupting the signal, including frequency carrier offsets, peak to average power ratio and noise disturbances. OFDM-MFSK and similar OFDM-based schemes proposed by other researchers are also discussed and compared.

4 RESEARCH METHODOLOGY

The testbed design of the approach employed in this work is shown in Figure 4.1. The whole architecture and experimental work and results is simulation-based using MATLAB R2012a. It comprises two systems, one at the sender end and another at the receiver side with a power-line channel in-between as a medium of information transmission. The design of both the error correction subsystems and the carrier modulation is based on the nature of the channel. It represents a trade-off between robustness and the data rate, have strong dependencies on the error correction schemes and modulation techniques employed.

4.1 Data Generation

The data is generated by using MATLAB's pseudorandom integers generating function that outputs integers from a uniform discrete distribution. The function

$$D = randi([X \quad Y], M, N)$$

returns an M-by-N matrix containing pseudorandom integer values drawn from the discrete uniform distribution on X:Y. In this work whereby binary data is used, $X = 0$ and $Y = 1$. The value of M is set to 1 and N is the length of the information vector. The information is then encoded as detailed in Section 4.3. The modulation techniques used include BSPK, QPSK and OFDM, and these are discussed in the previous chapter. OFDM-MFSK permutation encoding is treated in detail in Chapter 5.

4.2 Noise Addition

Because AWGN is a normal distribution profile noise in the time domain, it is added to the signal after performing the IFFT. The mean of AWGN is zero and variance is one. Narrowband noise is also referred to as frequency disturbances because it affects the signal in the frequency domain. It is consequently introduced to the system in the frequency domain before the IFFT. Carrier frequency offsets likewise are added at this stage. Narrowband interference has

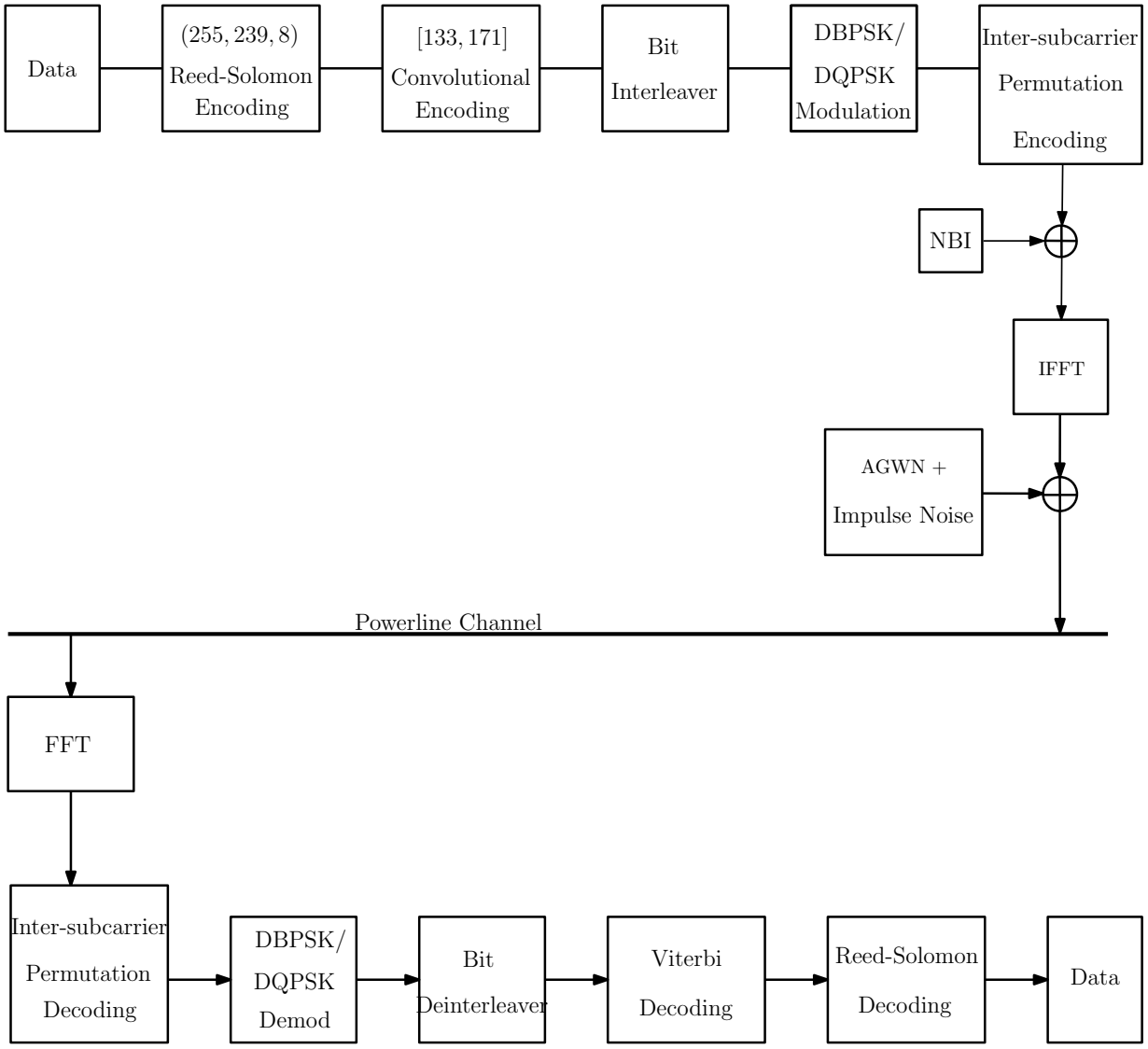

Figure 4.1: Testbed architectural design

a bandwidth and this attribute affects how severe the interference can affect the system. In this work, the bandwidth of narrowband interference is varied to study how it affects the ability of each scheme to combat frequency disturbances. An assumption made is that the probability of a frequency disturber being experienced in the system equates to the probability of the disturber coinciding with a subcarrier frequency. This subcarrier may or may not be carrying a modulated symbol. Impulse noise is an instantaneous time domain noise, and just like AGWN, this noise is added after the IFFT is performed.

4.3 Error Control Coding

A concatenated scheme is used as the forward error correction architecture of this work. The configuration and general design rule for concatenated codes is detailed in Chapter 2 and also in more detail in Section 2.2.4.

4.3.1 Reed-Solomon Encoder

Finite Field Algebra

Before the RS encoder could be discussed, it is important to understand finite field algebra as RS encoding and decoding significantly rely on it. A finite field is a field with a finite number of elements. It is also known as the Galois Field (GF), named after the discoverer. Let p be a prime number. Let the set of integers $\{0, 1, 2, ..., p-1\}$ be a commutative group under modulo-p addition whose non-zero elements are commutative under multiplication, and that the multiplication of these elements is distributive over addition. This set of integers is denoted as GF(p) and is called a prime field. For $p = 2$, a binary field GF(2) is obtained. For any positive integer m, this field can be extended to form a finite field of p^m elements given by GF(p^m) = {0, 1, 2, ..., $p^m - 1$}.

In GF(q), q can either be a prime number or a power of p. A non-zero element in the field is referred to as being *primitive* if its order is q - 1. Therefore, all the non-zero elements in GF(q) are generated by the powers of the primitive element. A polynomial $\mathbf{p}$(X) over GF(p) is *irreducible* over the field if $\mathbf{p}$(X) is not divisible by any polynomial of degree less than m but greater than zero. An irreducible polynomial $\mathbf{p}(X)$ of degree m is primitive if the smallest positive integer n for which $\mathbf{p}(X)$ divides X^{n+1} is $n = 2^m - 1$. Therefore, not every irreducible polynomial is primitive. It is hereby stated without proof that

Lemma 4.3.1. *Any irreducible polynomial over GF(2) of degree m divides $X^{2^m-1} + 1$*

Construction of Galois Field

Let us define the element α such that the set F = {0, 1, α, α^2,...,α^j...} contains 2^m elements and is closed under multiplication and division, since every nonzero field integer has a reciprocal modulo p. Let $\mathbf{p}(X)$ be a primitive polynomial of degree m over GF(2). Assume that the element α is a root of $\mathbf{p}(X)$,

i.e $\mathbf{p}(\alpha) = 0$. Recalling that $\mathbf{p}(X)$ divides $X^{2^m-1} + 1$ from lemma 4.3.1, and replacing X by α,

$$\alpha^{2^m-1} + 1 = q(\alpha)p(\alpha).$$

Since α is a root of $\mathbf{p}(X)$, $\mathbf{p}(X) = 0$. Therefore,

$$\alpha^{2^m-1} + 1 = 0.$$

The equation yields $\alpha^{2^m-1} = 1$ by adding 1 on both sides of the equal sign using modulo-2 addition. From this result, it follows that F is a finite field of elements

$$F = \{0, 1, \alpha, \alpha^2, ..., \alpha^{2^m-2}\}.$$

Let α be the primitive element in GF(q). The generator polynomial of an RS code capable of correcting a maximum of t errors with symbols from the field GF(q) has α, α^2,..., α^{2t} as its roots. Consider α^i as an element of the field, the minimal polynomial is given by

$$\Phi_i(X) = X - \alpha^i.$$

The generator polynomial is therefore given by

$$\mathbf{g}(X) = (X - \alpha)(X - \alpha^2)...(X - \alpha^{2t}). \tag{4.1}$$

RS codes are a non-binary class of BCH codes. On the other hand, BCH codes are a type of cyclic codes. Therefore, RS codes are non-binary cylic codes. Therefore, using the procedure used for encoding cyclic codes applies to RS codes well. The encoding can be accomplished in three steps:

1. Multiply the message polynomial $\mathbf{u}(X)$ by X^{n-k} where

$$\mathbf{u}(X) = u_0 + u_1X + ... + u_{k-1}X^{k-1}. \tag{4.2}$$

2. Divide $X^{n-k}\mathbf{u}(X)$ by the generator polynomial $\mathbf{g}(X)$ to obtain the remainder $\mathbf{b}(X)$.

$$\mathbf{b}(X) = X^{n-k}\mathbf{u}(X) \pmod{\mathbf{g}(X)} \tag{4.3}$$

where

$$\mathbf{g}(X) = g_0 + g_1X + ... + g_{n-k}X^{n-k}.$$

3. Multiply the message polynomial by the generator polynomial to obtain the codeword $\mathbf{c}(\mathrm{X}) = \mathbf{u}(X)\mathbf{g}(X)$,

$$\mathbf{c}(X) = \mathbf{b}(X) + X^{n-k}\mathbf{u}(X). \tag{4.4}$$

A systematic ($n = 255$, $k = 239$, $t = 8$) RS encoder defined by $GF(2^8)$ encodes input data. The parameter n is the length of the block code after encoding, k is the length of the code without the parity information and t is the maximum number of errors the code is capable to correct. The RS symbol length is fixed at 8 bits. Since the generated information is binary, a window of length 8 is used to break down the information stream into blocks that are converted into integer symbols to be used by the RS encoder. After encoding, the data is converted back into binary after which it is sent to the convolutional encoder. The choice of an RS(255, 239, 8) code over an RS(255, 247, 4) is that because narrow-band power-line communication is a highly noise-prone communication technology, a more robust, better error-correcting code with a slightly higher latency is preferred of over a better code rate code with less error-correcting ability.

The output of the RS encoder is Galois Field (GF) symbols. However, the convolutional encoder is designed to take binary input. Therefore the information is converted to integer symbols and eventually binary before being sent to the convolutional encoder.

4.3.2 Convolutional Encoder

A convolutional code is specified by the parameters (n, k, K). The parameter k is the number of inputs of the encoder, while n is the number of outputs and K is the constraint length or window length. The coding rate $R_c = k/n$ determines the number of data output bits per coded input bit. The performance of a convolutional code depends on the constraint length and the code rate. The longer the constraint length the more powerful the code and the better is the coding gain. However, the decoder complexity and the decoding delay both increase with an increase in K. A smaller coding rate corresponds to a more powerful code because of the high redundancy of the encoded information. On the downside, it has less bandwidth efficiency.

Table 4.1: Convolutional code parameters

Parameter	Value
k	1
n	2
K	7
g_1	[1 1 1 1 0 0 1]
g_2	[1 0 1 1 0 1 1]

Generally, an input sequence $\mathbf{u}^{(i)}$, for $i = 0, 1, 2, ..., k-1$ enters a shift register of length K bit by bit until k different sets of shift register sequences are obtained. Each output sequence $\mathbf{v}^{(j)}$, for $j = 0, 1, 2, ..., n-1$ is generated by using the calculation

$$\mathbf{v}^{(j)} = \mathbf{u}^{(1)} * \mathbf{g}_1^{(j)} + ... + \mathbf{u}^{(i)} * \mathbf{g}_i^{(j)} + ... + \mathbf{u}^{(k)} * \mathbf{g}_k^{(j)}$$

where the sign "*" symbolizes the convolution operation and $\mathbf{g}_i^{(j)}$ is the generator sequence of the output $\mathbf{v}^{(j)}$ that is associated with the input sequence $\mathbf{u}^{(i)}$. Convolution can also be performed by polynomial multiplication which is done by shift registers. The coefficients of the polynomial multiplication $\mathbf{u}^{(i)}(D).\mathbf{g}_i^{(j)}(D)$ are the components in the vector $\mathbf{u}^{(i)} * \mathbf{g}_i^{(j)}$. The polynomial multiplication codeword is given by

$$\mathbf{v}(D) = \mathbf{v}^{(0)}(D^n) + D\mathbf{v}^{(1)}(D^n) + ... + D^{n-1}\mathbf{v}^{(n-1)}(D^n)$$

In the testbed, the data is encoded with a half rate $K = 7$ convolutional encoder. The encoder uses the set of generator matrices: $g_1 = [1\ 1\ 1\ 1\ 0\ 0\ 1]$ and $g_2 = [1\ 0\ 1\ 1\ 0\ 1\ 1]$. The comprehensive list of parameters for the encoder is found in Table 4.1. Figure 4.2 shows the convolutional encoder employed. In octal representation, the encoder is called a [133,171] encoder. The input sequence $\mathbf{u} = (u_0, u_1, u_2, ...)$ is fed into a six-memory state shift register one bit at a time. After convolution with the two encoder generator polynomials, the output sequences $\mathbf{v}^{(0)} = (v_0^{(0)}, v_1^{(0)}, v_2^{(0)})$ and $\mathbf{v}^{(1)} = (v_0^{(1)}, v_1^{(1)}, v_2^{(1)})$ are obtained. The final output stream which is the parity information is simply a bit concatenation of the two outputs one bit at a time.

4.3.3 Interleaver

The use of the interleaver is to protect against burst errors that corrupt a few consecutive OFDM symbols and a frequency deep fade that corrupts adjacent

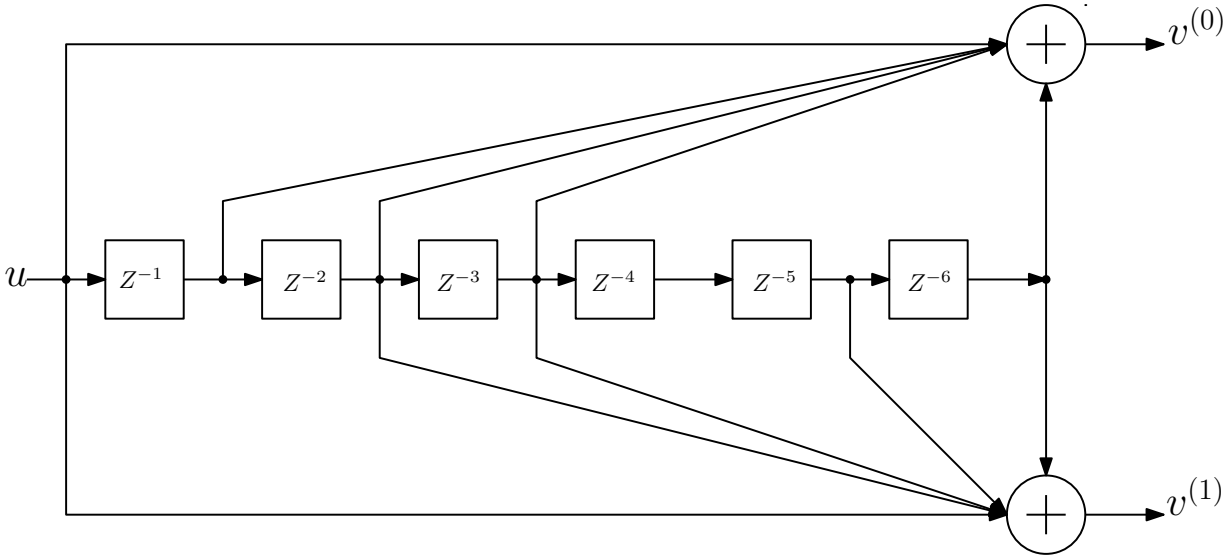

Figure 4.2: [133, 171] convolutional encoder

frequencies for a large number of OFDM symbols [22]. To achieve this, interleaving is performed in two steps. In the first step, each column is shifted circularly several times to spread a corrupted OFDM symbol over a few symbols. Then, each row is shifted circularly to prevent deep frequency fading from disrupting the entire column. The number of times a circular shift is performed is chosen based on the number of subcarriers in each OFDM symbol and the number of OFDM symbols in each interleaving block.

The size of the interleaving block depends on whether Differential BPSK (DBPSK) or Differential QPSK (DQPSK) is used to encode the subcarriers. When DBPSK is used, each interleaving block comprises 16 OFDM symbols where each symbol has a length of 256. In the case of DQPSK, the interleaving block is composed of 8 OFDM symbols. The difference in the interleaver sizes is because DBPSK produces twice as many I-Q symbols as DQPSK. The algorithm used for the interleaver is adapted from the G3-PLC specification [22]. The index positions of the interleaved bits (I, J) is given by

$$J = (j \times n_j + i \times n_i) \quad mod \quad n \tag{4.5a}$$

$$I = (i \times m_i + J \times m_j) \quad mod \quad m, \tag{4.5b}$$

where I and J are the row and column positions respectively. The index (i, j) is

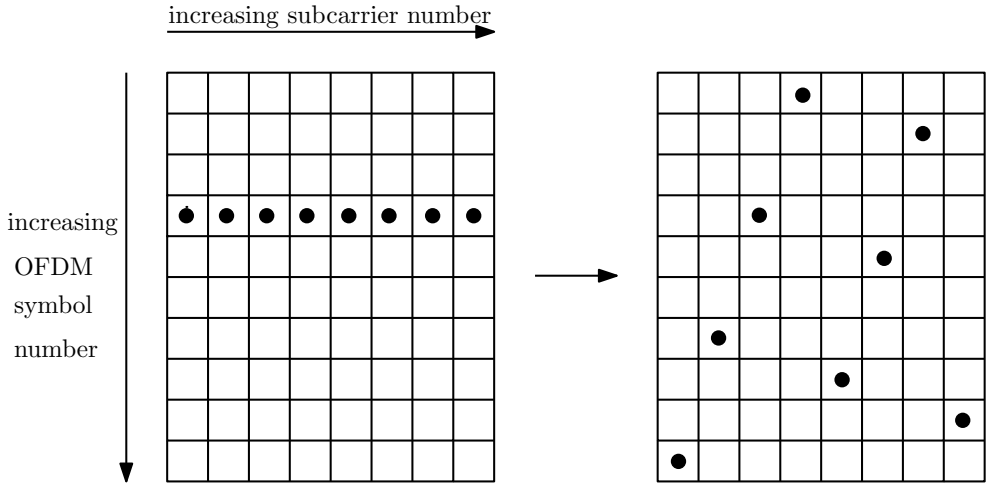

Figure 4.3: Burst error corrupting consecutive OFDM symbols

the original bit position. An interleaver table is generated by (I, J) positions which is used to perform interleaving. The parameters n_i, n_j, m_i and m_j are constants determined based on the number of subcarriers in each OFDM symbol (m) and the number of OFDM symbols in each interleaving block (n). A good interleaving pattern is obtained only if the greatest common divisor (GCD) for (m_v, m) and (n_v, n) is 1 for all values of v. Here the subscript v represents a running variable for both i and j. This can be represented in the form of an equation as

$$GCD(m_i, m) = GCD(m_j, m) = GCD(n_i, n) = GCD(n_j, n) = 1. \qquad (4.6)$$

An example of a good interleaving pattern obtained from following these rules is shown in Figure 4.3. A burst error is shown before interleaving and after interleaving. It can be observed that after interleaving no two corrupted bits are adjacent, whether horizontally or vertically. As a result, FEC can easily correct the bit errors. Numbering from zero, the set of (i, j) positions affected by the burst error on the left block in the figure is given by C_{burst} = (3, :) in MATLAB notation, which denotes all columns in row number 3. The corresponding set of positions obtained after interleaving, giving the block on the right in the figure is given by

$$C_{int} = \begin{bmatrix} 6 & 1 & 0 & 9 & 4 & 3 & 8 & 7 \\ 1 & 6 & 3 & 0 & 5 & 2 & 7 & 4 \end{bmatrix}$$

where the first row represents row positions and the second row has column

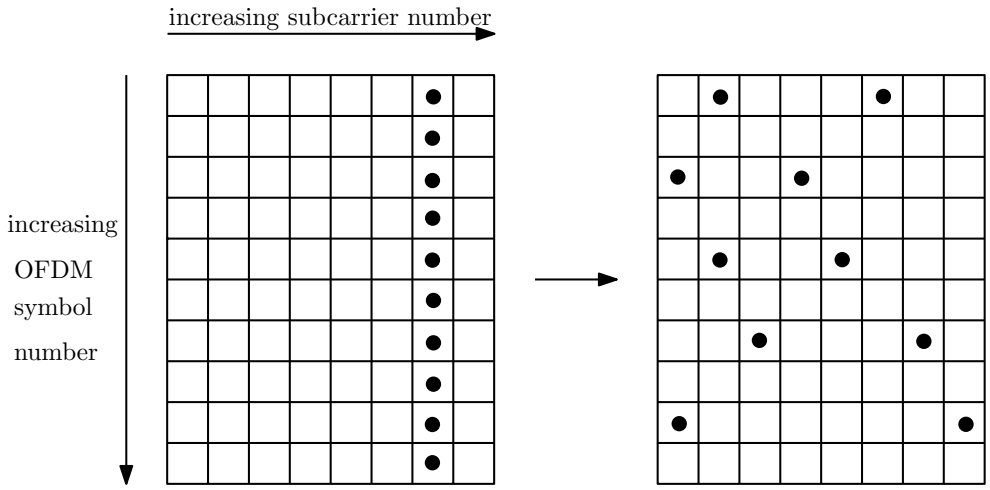

Figure 4.4: Frequency fade corrupting adjacent frequencies for a large number of OFDM symbols

positions. In a similar example, Figure 4.4 shows a vertical burst error affecting all n bits in a column before interleaving and the same after interleaving. Once again, the bit errors are dispersed in such a way that error correction is possible. The burst error positions is given by $C_{burst} = (:, 6)$, which denotes all rows in column number 6. After interleaving, the new positions are

$$C_{int} = \begin{bmatrix} 2 & 0 & 4 & 8 & 6 & 0 & 8 & 2 & 6 & 4 \\ 6 & 1 & 4 & 7 & 2 & 5 & 0 & 3 & 6 & 1 \end{bmatrix}$$

The bit de-interleaver reverses the row and column shifts to obtain the original order of the information. To achieve this, the interleaver table containing the new bit positions with respect to the original ones is used. This table is generated before interleaving is done and is common to both the interleaver and de-interleaver.

4.3.4 Viterbi Decoder

Viterbi decoding is used to decode convolutional codes. It can be a hard decision or soft decision decoding algorithm that makes use of a trellis structure. For practical communication design, the process of generating highly accurate data using soft decision is costly in practical circuits and it is highly computational and therefore not often used. The hard decision method is therefore adopted in this work. The Viterbi decoder is a maximum likelihood sequence estimator, that estimates the most likely encoder state using the sequence of transmitted codewords. It works well under noisy and fading channels but has a shortcoming of causing burst errors when it loses track of the sequence.

If the decoder decodes a received codeword r as c the maximum likelihood decoder maximizes the quantity denoted by $P(r|c)$ such that the conditional probability that r was received given that c was sent is maximized. If the received codeword r and the sent codeword c differ in d bit positions, implying a Hamming distance of d, then the conditional probability is given by a Binomial probability expression. If p is the probability of correctly decoding a codeword and N is the codeword length, then the conditional probability quantity is given by

$$P(r|c) = p^d(1-p)^{N-d} \tag{4.7}$$

Expressing equation 4.7 as a *log-likelihood* equation,

$$\log P(r|c) = d\log p + (N-d)\log(1-p) \tag{4.8a}$$

$$= d\log\frac{p}{1-p} + N\log(1-p) \tag{4.8b}$$

It can be seen from Equation 4.8b that minimizing the log-likelihood is all about minimizing the Hamming distance d, as the second term of the equation is a constant. The obvious approach of traversing through a list of possible transmit sequences and comparing the Hamming distances is a very expensive operation because a sequence of N bits contains 2^N possible digits, which can become very large. The Viterbi decoder uses a trellis that is more efficient to decode the codewords. The Hamming distance again plays an important role as the path metric in the process.

4.3.5 Reed-Solomon Decoder

The decoding of t-error correcting non-binary BCH codes involves the same three procedures used in decoding binary BCH codes, with an addition of one extra step involving computation of error values. These steps are summarised as follows:

1. Computation of the syndrome $(S_1, S_2, ..., S_{2t})$
2. Determination of the error-locator polynomial σ(X)
3. Calculation of the error-value evaluator

4. Evaluation of the error-location numbers and error values

Syndrome Calculation

Suppose that the codeword $\mathbf{v}(X) = v_0 + v_1X + v_2X^2 + ... + v_{n-1}X^{n-1}$ is transmitted, but as a result of transmission errors the following vector is received: $\mathbf{r}(X) = r_0 + r_1X + r_2X^2 + ... + r_{n-1}X^{n-1}$.

Let the error pattern be given by e(X). Then, the three quantities are related by the equation

$$\mathbf{r}(X) = v(X) + e(X) \tag{4.9}$$

The $2t$-tuple syndrome is

$$S = (S_1, S_2, ..., S_{2t}) = \bar{r}\mathbf{H}^T \tag{4.10}$$

Where **H** is the parity check matrix.

Error-Location Polynomial

The determination of the error-locator polynomial $\sigma(X)$ uses Berlekamp's iterative algorithm [65]. The first step involves calculating the minimum degree polynomials $\alpha^{(1)}(X)$, $\alpha^{(2)}(X)$,...$\alpha^{(2t)}(X)$. The error locator polynomial is then given by the last iteration, that is,

$$\sigma(X) = \sigma^{(2t)}(X). \tag{4.11}$$

However, it is not always necessary to do all $2t$ iterations if the number of errors are less than t. In that case, the error locator polynomial $\sigma(X) = \sigma^{(\mu)}(X)$ is given by the $\mu_{(th)}$ iteration polynomial. The comprehensive procedure of this step is well documented in literature and can be found in [31] and therefore is not discussed in detail.

Error-value Evaluation & Error Correction

After the error-locator polynomial has been determined, the error location numbers are simply the inverses of the roots of the error-locator polynomial. Suppose that the roots of $\sigma(X)$ are α^2, α^9 and α^{11}, the error location numbers are the inverses of these and are given by α^{13}, α^6 and α^4. The error pattern is obtained from error location values and in this case is therefore

$$\mathbf{e}(X) = X^4 + X^6 + X^{13}.$$

Decoding is accomplished by adding (modulo-2) $\mathbf{e}(X)$ to the received vector $\mathbf{r}(X)$. That is,

$$\mathbf{v}(X) = e(X) + r(X). \tag{4.12}$$

4.4 Modulation Techniques

This section focuses on the different modulation schemes used, with the exception of OFDM which is treated at depth in Chapter 5. Differential phase modulation is used because it uses non-coherent detection at the receiver which has the advantage of requiring less phase information than coherent detection and it also requires no phase tracking algorithms at the receiver. Instead, carrier phases of adjacent symbols are used as a reference for phase detection of the current symbol.

In this work, differential encoding is achieved by performing a bitwise XOR operation between the data being sent and a copy of the data that has been bit-shifted by one bit. Assuming that the bit to be transmitted is x_i and the differential encoding output bit is y_i, then the relationship between the input bit and the output bit is given by

$$y_i = x_i \oplus x_{i-1}, \tag{4.13}$$

where x_{i-1} is the next bit to be encoded in the input sequence preceding x_i. The last output bit is obtained by performing the bitwise between the last x_i value with a reference bit that can either be 0 or 1. This can alternatively be done at the beginning of the operation. During decoding, the corresponding operation is

$$x_i = y_i \oplus y_{i-1} \tag{4.14}$$

shifted by any number of shifts except either zero or a number equivalent to the length of the data. This technique is illustrated in Figure 4.5. Differential encoding makes the receiver design significantly simpler since no tracking circuitry is required at the receiver for coherently detecting the phase of each carrier. Instead, the phases of carriers in the adjacent symbol are taken as reference for detecting the phases of the carriers in the current symbol.

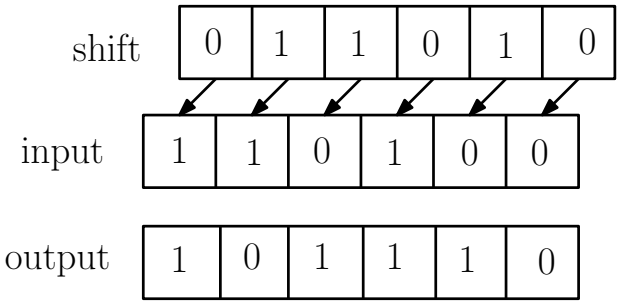

Figure 4.5: Differential encoding

Both BPSK and QPSK are investigated as OFDM subcarrier modulation schemes in this work because they are the most robust M-PSK modulation schemes. An indepth treatment of these schemes is given in the previous chapter. The study of CFO on these two schemes sheds light on which scheme performs better for a given CFO and a desired data rate.

4.5 Chapter Summary

In this chapter, the design of the entire system is presented. The chronology of processes during transmission of data is explained and the different blocks, subsystems and their functionalities are treated at length.

The data is first encoded using a forward error correction scheme involving a concatenation of Reed-Solomon encoding followed by Convolutional encoding with the aim of introducing redundancy for error detection and correction at the decoder. The data is then interleaved to break burst error blocks and spread errors in order to reduce the number of errors per symbol and effectively improve error correction. After the error bursts have been dispersed the data is then modulated with the appropriate modulation scheme. This is normally either DBPSK or DQPSK. OFDM modulation follows whereby the DBPQK/DQPSK-modulated symbols are loaded on the Inverse Fourier Transform (IFFT) block to form OFDM subcarriers. Noise is added and subcarrier spacing encoding is carried out by applying a known permutation sequence before the data is sent over the channel. At the receiver, the reverse processes are carried out to obtain the data that is sent at the sender.

5 OFDM-MFSK PERMUTATION CODING

5.1 Understanding OFDM Permutation Coding

Firstly, it should be noted that permutation sequence encoding developed in this research is not the standard permutation coding used as a forward error correction scheme. Therefore the concept of minimum distance and the scenarios of erasures in decoding does not apply. It follows that there is no need to map the subchannels to permutation symbols. Instead, permutation sequence encoding involves using a permutation sequence to separate information-carrying subcarriers in OFDM. However, because of similarities between the two schemes, the concept of permutation coding is first introduced before the technique developed is explained.

Suppose binary information is to be encoded using permutation coding. A permutation codeword size is chosen based on the desired ability to decode (minimum distance) and on the bandwidth limitations. The bigger the minimum distance (translates to the length of the codeword in general terms), the better the decoding ability of the permutation code but the longer the codeword the more bandwidth it uses and the greater the extent of latency introduced.

Suppose a codeword length of three with a minimum distance of two is adopted to encode each of the four possible pairs of binary bits. There are six possible codewords satisfying the criteria but since there are only four different possible binary bit pairs, only four codewords can be used. Table 5.1 shows the two bit words to be encoded and the corresponding permutation codewords after mapping.

Decoding a codeword is only possible if at least two symbols of the three-symbol codeword received have not been altered. Suppose that the received codeword is [2 3 3]. This can be decoded correctly to [2 1 3] and procedurally to the binary word 10 because the first and the last symbols of the codeword have not been altered. However, supposing that the received codeword instead

Table 5.1: Permutation coding mapping

Binary data	Codewords
00	1 2 3
01	1 3 2
10	2 1 3
11	3 1 2

is [3 2 1], then the codeword cannot be decoded because there is no codeword which has at least two matching symbols in respective positions between the received codeword and the list of possible codewords of Table 5.1.

Having explained permutation coding, the adapted application of the permutation coding technique referred to as permutation sequence encoding is now presented. Suppose that an OFDM scheme is implemented whereby all subcarriers are used to carry symbols. Assume any of the modulation schemes: BPSK, QPSK, or 8PSK could have been used to modulate the subcarrier information. If a snapshot of a portion of an IFFT window is taken at a random time it would look like the illustration in Figure 5.1.

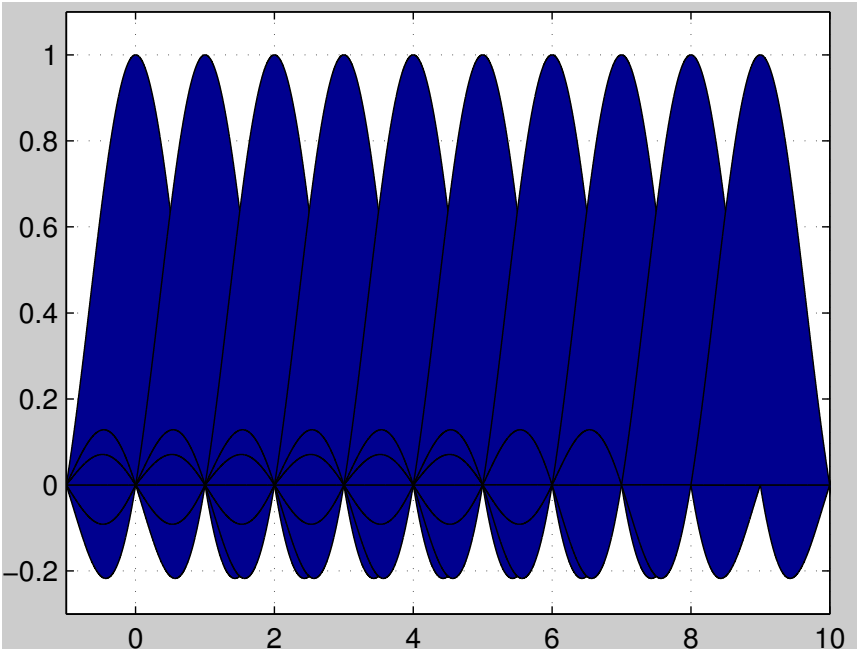

Figure 5.1: OFDM subcarriers

Now if permutation sequence encoding is applied to OFDM to obtain PE OFDM, the subcarriers carrying information are spaced according to the code-

word symbols. Suppose that the permutation codeword [3 1 2] is to be used. This would mean that between the first and the second symbol-carrying subcarriers there are three unused frequencies. Likewise, between the second and the third subcarriers, there is one unused frequency, and finally between the third and the last subcarrier there are two unused frequencies. This technique is illustrated in Figure 5.2. The darker regions represent the used subcarriers while the lighter regions correspond to the unused frequencies.

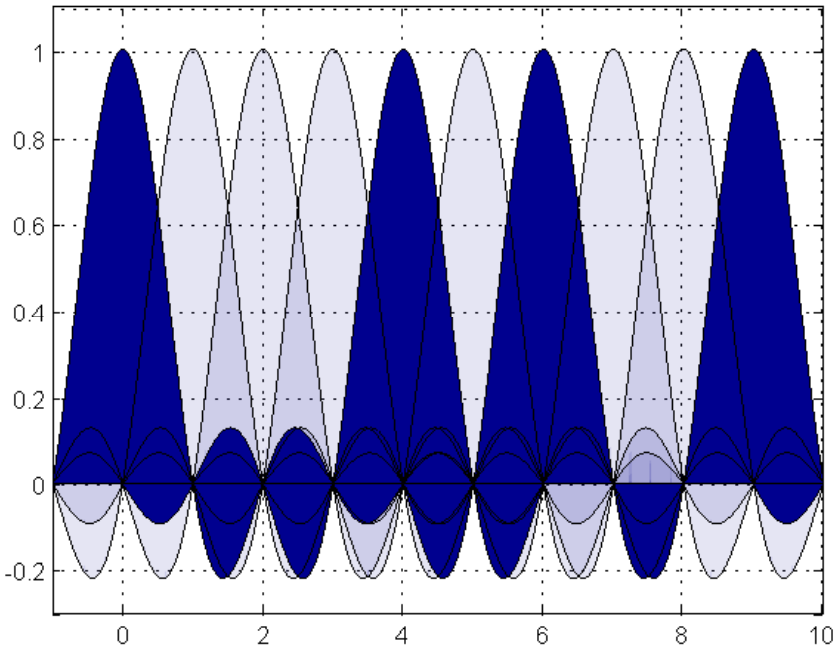

Figure 5.2: PE OFDM using [3 1 2] codeword

Before the coding technique employed is treated at depth, it is important to understand how the different OFDM impairments affect OFDM both from a macroscopic and a microscopic level. Macroscopic here refers to how a corrupted symbol-carrying subcarrier affects the performance of OFDM and microscopic refers to the treatment of the problem as viewed from an IFFT/FFT perspective. The macroscopic treatment has been covered significantly in previous chapters and has a straight forward measure, which is the bit error rate of the scheme. The microscopic treatment of the problem is therefore addressed here.

5.2 Problem Understanding from IFFT/FFT Theory

OFDM uses a linear transform at the transmitter and its inverse at the receiver. This transform and its inverse are known as the IFFT and the FFT respectively. Since the signal passes through both transforms, it is not affected while on the other hand impulse noise which is added in the time domain after the IFFT passes through one transform, that is the FFT, is affected. The energy of the impulses as a result is dispersed over the OFDM symbol duration (it should be recalled from Section 3.4.2 that both the amplitude and width of impulse noise follow a Gaussian distribution). Consequently, the error floor typical in uncoded OFDM is reduced. The addition of a cyclic prefix increases the length over which the dispersion occurs and is therefore another factor that contributes in diminishing the effect of impulsive noise in an OFDM symbol. However, the relationship is not proportional as one has to consider the power spectral density of the impulse.

The use of a permutation coded OFDM means that the new OFDM symbol contains even less information than the standard OFDM symbol. This means that the impulse noise energy is distributed over even a smaller component of the signal. This explains why using fewer subcarriers per symbol combats impulse noise by reducing its undesired effect on the transmitted signal. The applied time-frequency block interleaving decreases the correlation of received noise at the decoder which helps in providing diversity.

Narrowband interference is a serious problem in PLC communication because it can appear at one or more frequencies and remains there all the time. That means that information sent on those specific frequencies is corrupted, if not entirely unrecoverable. What makes frequency disturbances problematic is that they exist before the IFFT and hence go through both OFDM transforms. This means that narrowband interference is immune to the effect of the transforms.

One of the main methods to mitigate the impact of frequency disturbances is to avoid sending information at those frequencies that are affected. However, it is not possible to determine these frequencies, hence the need for good schemes that hop transmission frequencies. The presented scheme uses a simple permutation that keeps changing the frequencies at which information is sent and in the process improving the probability of avoiding some of the frequencies at

which interferences occur.

5.3 Subcarrier Encoding Schemes

The principle of subcarrier permutation sequence encoding is using a permutation codebook containing codewords that are used to encode OFDM subcarrier spacing. Two different values of M are used to describe different OFDM permutation sequence encoding systems; namely $M = 2$ for BPSK and $M = 4$ for QPSK. In this notation, *M does not represent the size of the subcarrier group but rather the size of the codeword used.* For instance, the $M = 2$ codeword comprises a total of five subcarriers, three of which carry BPSK symbols, while the $M = 4$ codeword comprises fifteen subcarriers, with only five subcarriers loaded with QPSK symbols. The two codeword sizes are illustrated in Figure 5.3. In this illustration, the subcarriers loaded with modulated symbols are show with dots while the unused subcarriers are blank. The value for M does not affect the IFFT size because although the number of subcarriers forming a subcarrier group varies with each value for M, any surplus subcarriers insufficient to form another subcarrier group are simply assigned zero power.

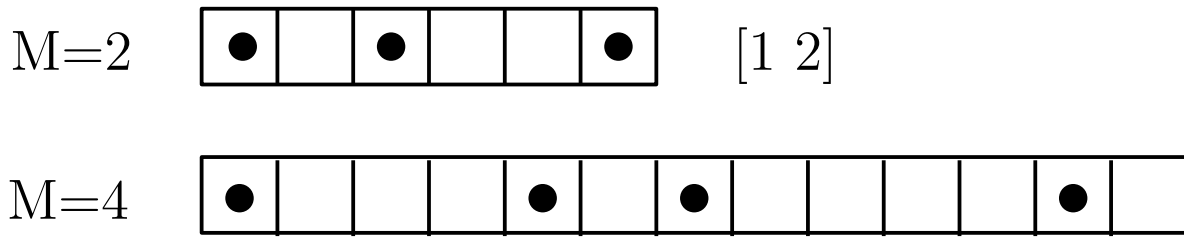

Figure 5.3: M = 2 and M = 4 codewords

5.3.1 BPSK-based Permutation Sequence Encoding

In this scheme, an $M = 2$ permutation sequence is used for encoding. The codebook consists of only two codewords, namely [1 2] and [2 1]. Encoding involves alternating these two codewords as the subcarrier spacing sequence in the order in which they are arranged in the codebook. For instance, if [1 2] is used first as the spacing between the first two subcarriers, that is, subcarriers numbered k_0, k_2 and k_4 are assigned 1 and the rest of the subcarriers are left as nulls. In other words, the first subcarrier in the FFT (k_0) is assigned the value 1, then sub subcarrier k_1 is a null. Subcarrier k_2 is also assigned the value 1, followed by subcarriers k_3 and k_4 left as nulls, and finally subcarrier k_5 is also assigned the value 1, completing the subcarrier group (refer to Figure 5.3). After this codeword has been applied, the next codeword in the codebook [2 1] is used afterwards. In this case subcarriers k_0, k_3 and k_5 are assigned 1 while the rest of the subcarriers in-between them are assigned zero. The sequence will then repeat until the end of an OFDM symbol. In the next symbol, the sequence is reversed, meaning the order becomes [2 1], [1 2]. The reason for reversal is that the occurrence of narrowband disturbances at specific frequencies will always affect the decoding the same way if the same sequence is used, and alternating the sequence is to provide frequency diversity. In an FFT window of 256 subcarriers, there are 42 $M = 2$ complete subcarrier groups, with a total of 126 used subcarriers. This gives BPSK-based permutation sequence encoding a total bandwidth usage of $0.49B$, where B is the total system bandwidth used by 256 subcarrier bandwidths given by $B = 256f_{sc}$.

The usefulness of the application of this scheme is that since it ensures that no two information-carrying subcarriers are adjacent to each other at all times, the effect of carrier frequency shifts and inter carrier interference is reduced. Although it provides better frequency diversity than standard OFDM, it does not offer much shielding against narrowband frequency disturbances because exactly half of the subcarriers carry information in a codeword sequence, giving an equal probability for an narrowband disturber to hit either a null subcarrier or a subcarrier carrying information.

5.3.2 QPSK-based Permutation Sequence Encoding

Encoding using an $M = 4$ permutation sequence code is similar to that of Section 5.3.1 except that the codeword size is bigger, and codeword table is larger. The codebook for the $M = 4$ codebook is presented in Table 5.2. This scheme

uses a total of fifteen subcarrier frequencies per codeword, with five subcarriers carrying information. There is a total of 17 permutation codeword sequences in an IFFT window, resulting in a total of 85 information subcarriers out of 256 subcarriers. It follows that out of the entire bandwidth allocated, only $0.33B$ is utilized. The bandwidth usage efficiency decreases with an improvement in decoding capability because the more powerful scheme the larger is the permutation codeword size, and hence the longer is the permutation sequences. QPSK is more prone to ICI than BPSK because as it is shown in Equation 3.11b, ICI introduces a phase shift which will have more adverse effect on less angular separated constellation points in the I-Q diagram. Because QPSK has a smaller angular separation than BPSK, it requires a larger permutation codeword.

There is improved shielding against both narrowband interference and inter-carrier interference as there are fewer subcarriers carrying information per codeword sequence. The improved protection against ICI stems from the fact that the subcarriers are further apart compared to OFDM and BPSK-based permutation sequence encoding schemes with a smaller size codeword. The increased spacing causes less interference of one subcarrier on the next. It should be noted that CFO cannot be reduced on the system, but ICI which is an effect of CFO can be reduced. Coding therefore minimizes ICI and not CFO.

Table 5.2: 4-permutation codebook

Codewords		
1 2 3 4	1 4 2 3	1 3 4 2
2 3 1 4	2 4 3 1	2 1 4 3
3 4 1 2	3 1 2 4	3 2 4 1
4 3 2 1	4 1 3 2	4 2 1 3

5.4 Decoding Techniques

There are two methods that could potentially be used to decode subcarrier permutation-encoded OFDM. The first makes use of the permutation code minimum distance property. This is the standard well known permutation decoding method that involves decoding codewords retaining the condition of minimum distance, with erasure declared on codewords that no longer exhibit minimum distance. The second approach is permutation sequence decoding

which involves making use of the codewords arrangement in the codebook, which requires that the sequence of the codewords used during encoding be known at the receiver. The latter technique is the employed approach. The standard approach is discussed also for the sake of understanding how it is normally done and to be in a position to draw a comparison between this approach and the presented approach.

5.4.1 Minimum Distance Decoding

Minimum distance decoding makes use of the minimum distance of permutation codes. One of the advantages of permutation codes in forward error correction is that if the number of corrupted symbols S_c, is less than or equal to the difference between the order of the permutation code M, and its minimum distance d_{min}, the codeword can be decoded. In other words, the codeword can be decoded if the number of uncorrupted symbols S_u, is greater than or equal to the minimum distance. In equation form, the condition for successful decoding is

$$S_c \leq M - d_{min}, \tag{5.1}$$

or

$$S_u \geq d_{min}. \tag{5.2}$$

This decoding algorithm relies on nullset sequences. A null is an unused frequency. A nullset is the number of consecutive nulls. It follows that a nullset sequence is the arrangement of M nullsets. The total number of frequency slots S_t (both nulls and information carrying frequencies) is equal to

$$S_t = (M+1) + (M + M - 1 + M - 2 + ... + M - d_{min}) \tag{5.3}$$

It is not hard to understand how this number is reached because for every M nullsets forming a nullset sequence, there are $M + 1$ information subcarriers. The nullset sequence comprises a combination of nullsets of sizes from 1 up to M, satisfying the property of permutation codes illustrated in Lemma 5.4.1. The challenge is that it is difficult to determine which set of nulls is valid if a frequency disturbance exists in one of the nulls. Moreover, a separate permutation encoding algorithm is required to decode the codeword before the I-Q QPSK symbols can be obtained from the information-carrying subcarriers. This introduces further latency. Because of these challenges, this scheme is not

implemented in this research and is only left for future work with improvement.

Figure 5.5 is a flow diagram depicting the summary of the minimum distance-based decoding algorithm. Initially, the first M consecutive nulls are checked if they form a valid codeword. This is done by counting the number of nulls per null set for the first M null sets. If the null set sequence corresponds to a valid M-permutation codeword, then the information from the information-carrying subcarriers is read and demodulated and decoded using the M-ary PSK demodulation technique corresponding to the modulation scheme used in encoding the subcarrier symbols. The advantage of low order permutation codes is that to determine if a codeword is valid, no calculation has to be done, and there is no need to refer to the codeword table. It can be achieved by using the property of permutation codes:

Lemma 5.4.1. *A permutation code C is composed of codewords that have each symbol in the alphabet once and only once per codeword.*

There are four possible scenarios when attempting to decode a nullset sequence. These scenarios can be studied from Figure 5.4.

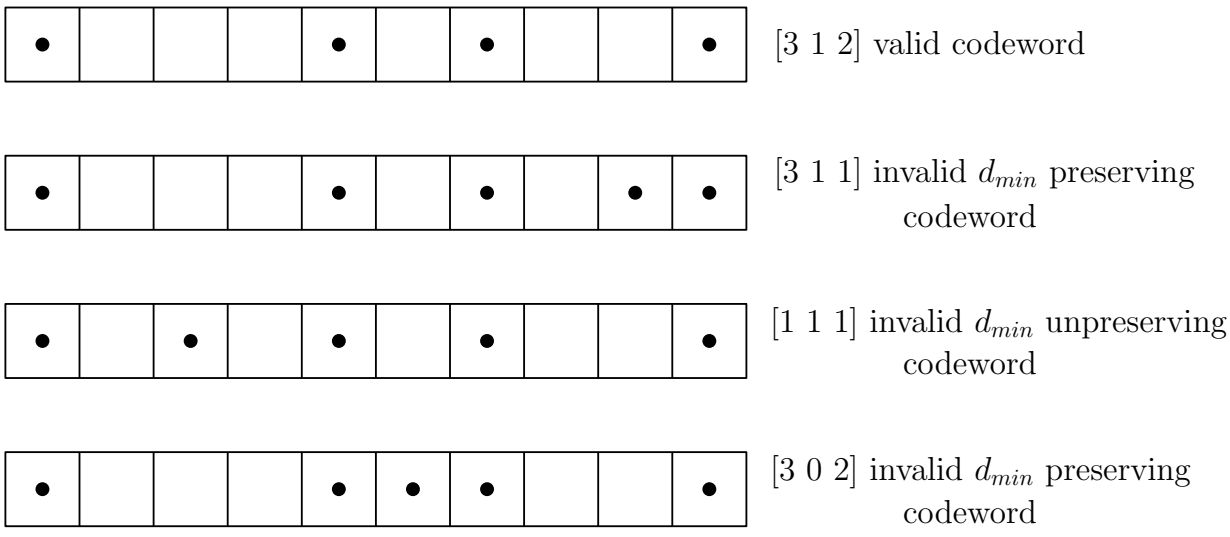

Figure 5.4: 3-permutation sequence decoding scenarios

1. Nullset sequence is a valid codeword.

When no symbol of the codeword appears more than twice the codeword is valid. The first permutation sequence diagram illustrates this condition

whereby a correct codeword of [3 1 2] is obtained and it is the easiest scenario to deal with.

2. Nullset sequence is an invalid d_{min} preserving codeword.

If the nullset sequence does not form a valid codeword, it implies that a frequency disturbance occurred. The second permutation sequence shows the same sequence affected by a frequency disturbance in the last null position (second last frequency). The nullset sequence as a codeword is read as [3 1 1]. Because the minimum distance is 2 and the first two symbols are intact, the codeword can be decoded correctly. In such a case, the algorithm traverses through the codebook until a codeword that matches the nullset permutation sequence in d_{min} symbol positions is found. The last permutation sequence diagram also illustrates the same scenario. Here, there are less than M nullsets, and whenever this condition arises it is because a frequency disturbance is positioned adjacent to a non-zero subcarrier. If two adjacent frequencies are non-zero, that is read as a 0. It does not affect decoding.

3. Nullset sequence is an invalid d_{min} non-preserving codeword decodable at second attempt.

The disturbance can be positioned in such a way that decoding is not possible even if the minimum distance condition is met. The third permutation sequence shows the same codeword with a frequency distance in the second null. The nullset sequence is now read as [1 1 1]. Only one symbol remains intact, which is less than the minimum distance, and as a result, the codeword cannot be decoded. For decoding to be possible in this condition, the algorithm has to start reading the sequence from the second nullset and perform decoding again, which makes the algorithm expensive. In this case, the permutation sequence is read as [1 1 2] and the last two symbols of the permutation sequence are correct, meeting the minimum distance of 2 condition for decoding to be possible.

4. Nullset sequence is an invalid d_{min} non-preserving undecodable codeword.

If there are more than M - d_{min} disturbances in different nullsets, then decoding is not possible. Erasure is declared and the information carried in the

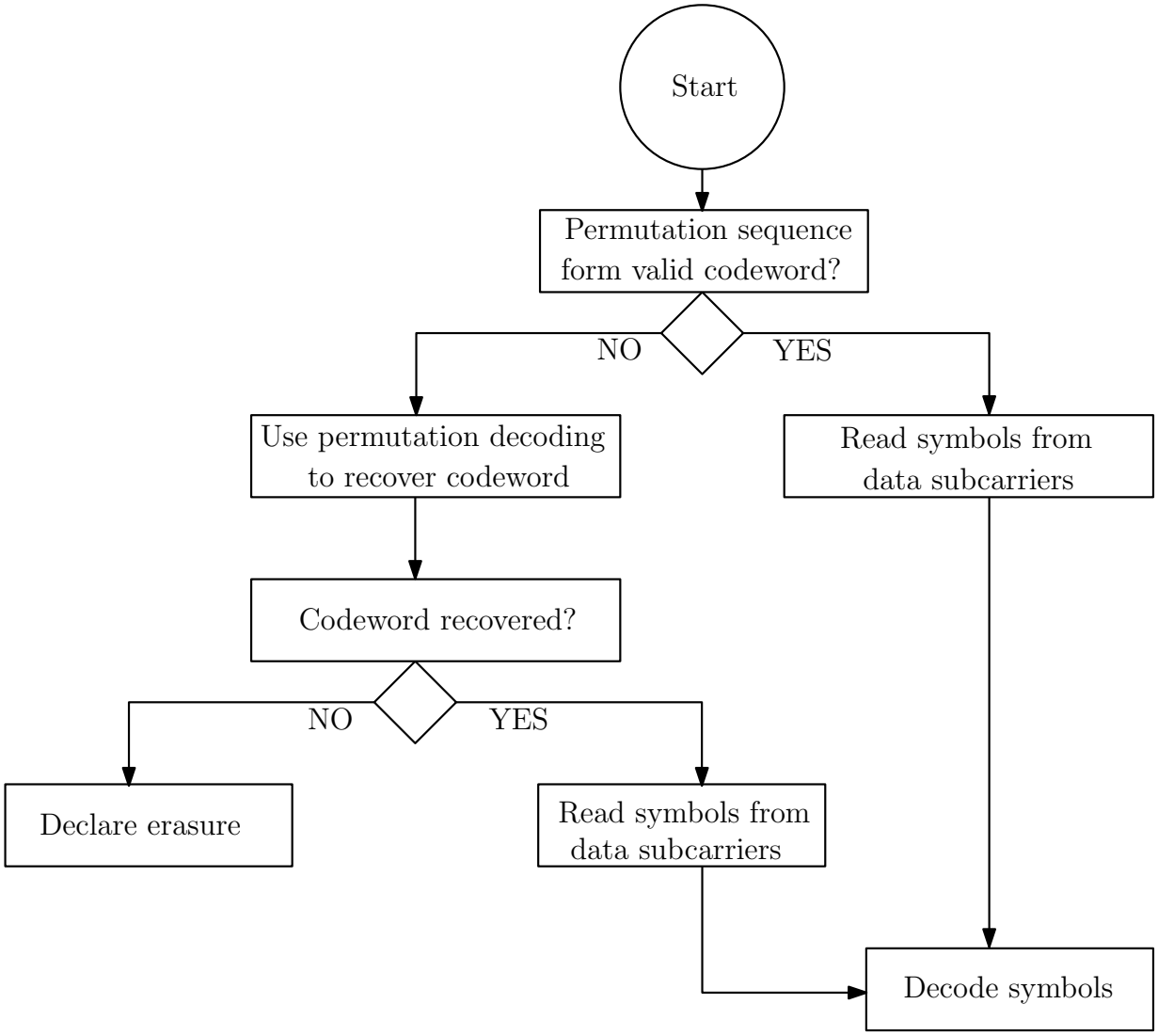

Figure 5.5: Minimum distance decoding algorithm

subcarriers is lost.

5.4.2 Encoding Sequence-Dependent Decoding

The encoding-sequence dependent decoding algorithm uses the predetermined encoding sequence of Section 5.3 to track the codewords used in encoding. After the position in the codebook of the encoding codeword has been determined, the codeword is retrieved and used to identify the $M + 1$ positions of subcarriers carrying information relative to the last subcarrier decoded. The I-Q symbols of the MPSK modulation scheme used are demodulated and decoded. The Figure 5.6 illustrates this technique. It can be seen that there are no *if statements* because every step is known and the outcome does not

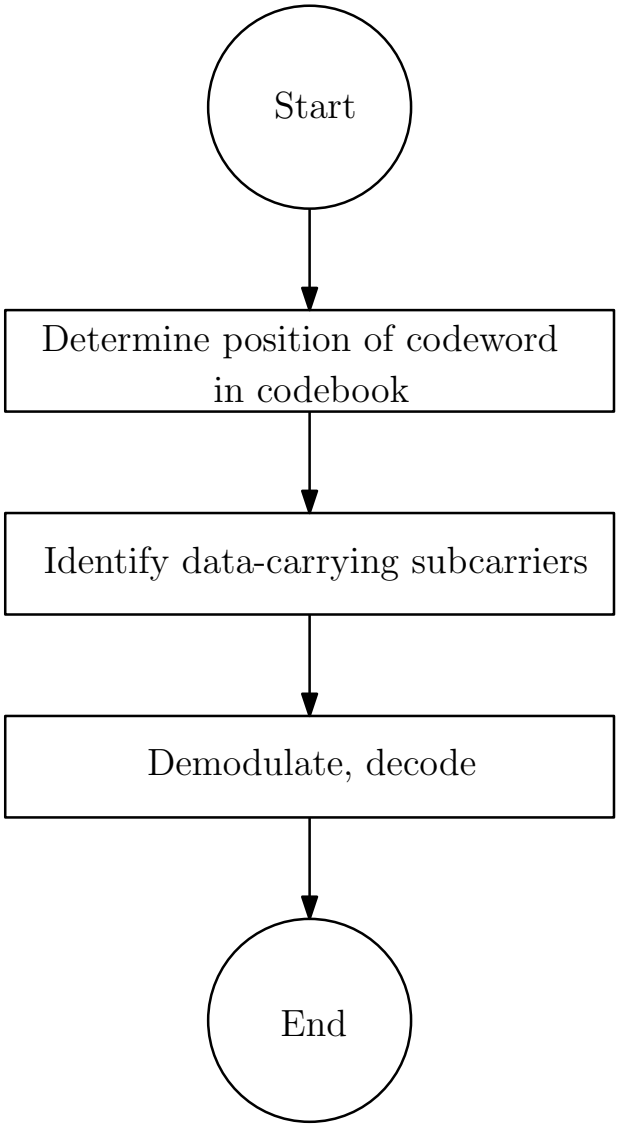

Figure 5.6: Encoding-sequence decoding algorithm

depend on any conditions. It follows that the cost of the algorithm is constant.

The beauty of this technique is that frequency disturbances in the null positions do not affect decoding as the content of the frequency positions where nulls are expected is ignored. The possible impedance to accurate decoding is the existence of narrowband interference on the subcarriers carrying modulated symbols, and given the fact that only 0.33 of the total number of subcarriers are carrying information, the probability of this incidence is reduced.

5.5 Chapter Summary

In this chapter, the permutation sequence encoding of OFDM is presented. The impact of narrowband disturbances on the system is analysed with respect to the codeword size. Permutation sequence encoding solutions are adapted to suit different subcarrier modulation schemes namely; BPSK and QPSK. These are $M = 2$ and $M = 4$ permutation sequence encoding respectively. The bandwidth usage implications are also considered. The different types of decoding techniques, that is, minimum distance decoding and encoding sequence dependent decoding are compared and analysed.

6 RESULTS AND ANALYSIS

The aim of the research is to develop a scheme that improves the performance of OFDM in the presence of carrier frequency offsets and narrowband interference while also improving the bandwidth usage of OFDM-MFSK. Because frequency offsets can be caused by a number of factors, most notably frequency mismatch between transmitter and receiver oscillators and Doppler effect in transmitters and/or receivers mounted on high speed modes of transport such as high speed trains, the application of the study is not limited to power-line communication.

There are three modulation schemes being investigated for error rate performance in varying conditions of narrowband disturbances and carrier frequency offsets. These schemes are OFDM, OFDM-MFSK and permutation sequence encoded OFDM (PC OFDM). Permutation sequence encoded OFDM comprises two techniques adapted to suit BPSK-modulated and QPSK-modulated OFDM subcarriers.

6.1 Noise Impact

Noise is a major issue in power-line communication. The major noise types affecting the channel significantly are impulse noise and narrowband disturbances. Because the research focuses on the frequency domain communication impairments impact mitigation, narrowband interference is the focus. This is reflected in the presentation of the results and the analysis.

Narrowband interference is a major problem because when a narrowband disturber falls on a subcarrier, decoding is affected, whether the subcarrier is carrying information or not. If the disturber coincides with an information subcarrier, the information may be lost entirely. In the case of OFDM-MFSK, even if a disturber falls on a subcarrier not carrying information, the decoding is significantly affected because further steps need to be taken to ascertain which of the subcarriers in a group of subcarriers is meant to convey information.

6.1.1 DQPSK and 4FSK-based OFDM Schemes

DQPSK is a widely scheme in OFDM for power-line communication. Although it may have a better data rate compared to DBPSK, it is more susceptible to noise. Figure 6.1 shows the BER performance of permutation sequence encoded OFDM (PC OFDM) with QPSK-modulated subcarriers and OFDM-4FSK under AWGN, impulse noise and varying frequency disturbance bandwidth. All results presented are obtained in the presence of all three noise types. Both the impulse noise and narrowband interference probability of occurrence is fixed at $\frac{1}{256}$. In this setup, the NBI bandwidth is varied from $2f_{sc}$ to $4f_{sc}$, where f_{sc} is the subcarrier bandwidth. This means that when a narrowband interference occurs, it affects two consecutive subcarriers in an IFFT window in the one scenario, and four consecutive subcarriers in the other scenario. This is to simulate frequency-limited burst disturbances, which are common in the power-line.

At a disturber bandwidth of $2f_{sc}$, OFDM-MFSK has a better BER performance than PC OFDM by 1 dB at 10^{-4} bit error rate, as can be read from the annotated points. However, at a disturber bandwidth of $4f_{sc}$ PC OFDM performs better by 0.5 dB at the same BER. This result shows that OFDM-MFSK performs well in low frequency disturber bandwidths but is not suited for large noise bursts. The ability for PC OFDM to perform well in a more stringent noise burst environment can be attributed to the frequency nulls between information subcarriers. On the other hand, noise bursts affect decoding in OFDM-MFSK as it relies on the unused $M-1$ subcarriers to correctly perform decoding. The bigger the number of the unused frequencies are affected by a frequency disturber, the more difficult it becomes to correctly decode a codeword.

Analyzing the noise bandwidth impact on both schemes, the behaviour can be easily explained. $M = 4$ PC OFDM has a permutation encoding sequence codeword of size 4, take [2 4 1 3] as an example. In this codeword instance, there are two null frequencies between the first and second information carriers, four null frequencies between the second and the third, one null between the third and the fourth, and three nulls between the fourth and the fifth subcarriers. A frequency disturber with a bandwidth of $4f_{sc}$ can fall on any of the nulls, affecting no information subcarrier or at most one if it falls on either the four or the three nulls, and affecting a maximum of two information

subcarriers if it falls on the one or two nulls part of the sequence. However, with OFDM-4FSK, the same noise bandwidth will always affect two subcarrier groups, except on the one instance when it exactly coincides with all four subcarriers of the same group. In either situation, decoding is significantly affected. With a disturber bandwidth of only two, OFDM-4FSK performs better as the advantage of sending ones instead of QPSK symbols becomes vital.

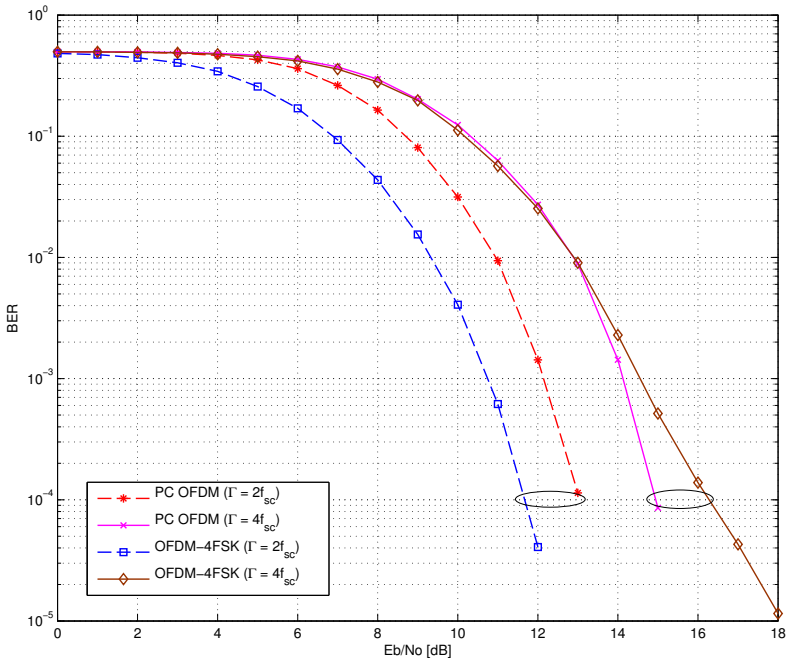

Figure 6.1: DQPSK-based schemes at varying Γ

Figure 6.2 shows the performance of QPSK-OFDM, OFDM-MFSK and PC OFDM at a narrowband disturber bandwidth of $4f_{sc}$, narrowband noise probability of $P_{nbi} = \frac{1}{256}$, and an increased impulse noise probability of $P_{imp} = \frac{1}{64}$. The only change from the previous result at $4f_{sc}$ is the increase in impulse noise probability from $\frac{1}{256}$ to $\frac{1}{64}$. From the result, quadrupling the impulse noise probability deteriorates the performance of PC OFDM by 4 dB and that of OFDM-MFSK by 5 dB at the annotated point corresponding to 10^{-3} BER. This translates to a 1 dB PC OFDM gain over OFDM-MFSK. It can be drawn that the presented scheme provides improved performance to that of OFDM-MFSK in the presence of impulse noise.

On the other hand, Figure 6.3 presents the results obtained when the impulse noise probability is kept low at $\frac{1}{256}$ and the impulse noise probability is

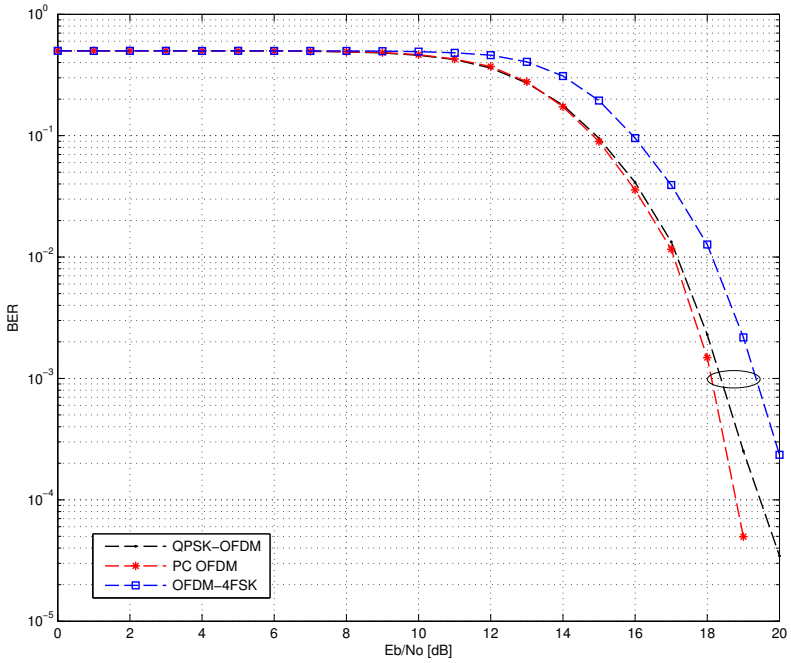

Figure 6.2: DQPSK-based schemes at $4f_{sc}$, $P_{nbi} = \frac{1}{256}$, $P_{imp} = \frac{1}{64}$

increased to $\frac{1}{64}$ at the same frequency disturber bandwidth of $4f_{sc}$. The observation is that the performance of PC OFDM is reduced by 4 dB once again, while OFDM-MFSK becomes impractical to use, with a BER performance becoming asymptotic at 7×10^{-2}. Another conclusion that can be drawn is that while the performance of PC OFDM is drops in similar behaviour to changes in either narrowband interference or impulse noise changes, OFDM-MFSK is more vulnerable to frequency disturbances than impulse noise.

6.1.2 DBPSK and 2FSK-based OFDM Schemes

DBPSK is a very robust modulation scheme compared to other M-ary PSK modulation schemes. This is due to its two distinct phases which makes demodulation relatively easier. Because of the stability of BPSK, it is difficult to improve the BER performance of OFDM when BPSK is used to modulate the subcarriers as compared to larger constellation M-ary PSK schemes.

As already established in the assessment of QPSK, OFDM-MFSK does not perform well in bursty conditions, the same behaviour is replicated when DBPSK is used as a subcarrier modulation as can be seen in Figure 6.4. The reason the scheme does not perform well in a noise bandwidth of $2f_{sc}$ is because

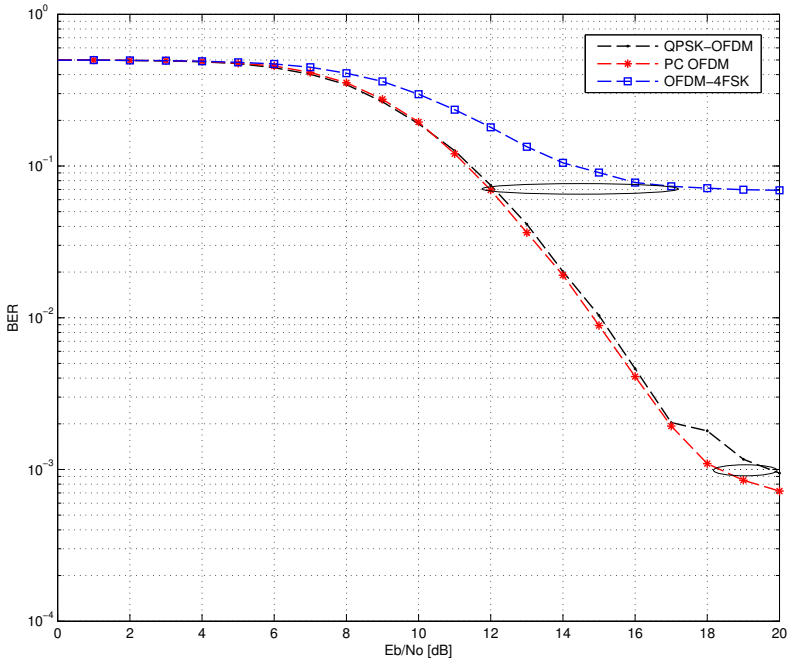

Figure 6.3: DQPSK-based schemes at $4f_{sc}$, $P_{nbi} = \frac{1}{1/64}$, $P_{imp} = \frac{1}{256}$

OFDM-2FSK used in this scenario has only two subcarriers per group, and in the presence of a frequency disturber either both subcarriers lose information or two consecutive subcarrier groups may lose information. The poorer performance when the noise bandwidth of $4f_{sc}$ is applied is caused by that the scheme may lose information in two or three subcarrier groups, resulting to a possibility of up to three bits lost. BPSK-OFDM and PC OFDM suffer a performance drop of 2.5 dB while OFDM-2FSk has a 3.5 dB drop in performance at 10^{-4} BER, translating to a 1 dB deficit compared to the PSK-based scheme. It can also be observed that the performance of the M-ary based schemes, namely BPSK-OFDM and PC OFDM are very similar because of the robustness of BPSK.

6.2 CFO Impact

6.2.1 General Case

Before the performance of the presented scheme under CFO is studied, it is necessary to investigate the performance of OFDM under CFO. The performance can then be used to determine whether the impact of CFO in the scheme is significant enough to bring about a need to develop a better scheme than

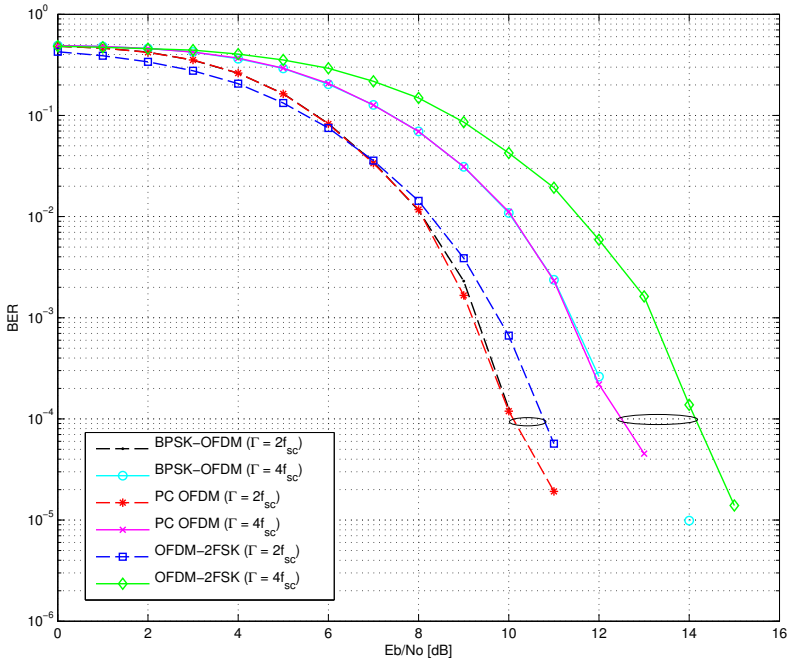

Figure 6.4: OFDM-2FSK and DBPSK-based Schemes at varying noise bandwidth

OFDM to tackle the problem. The two main OFDM subcarrier modulation schemes used in power-line communication are DBPSK and DQPSK. The performance of these under CFO is investigated and a third modulation scheme with a higher data rate is introduced in the study. This differentially encoded 8-PSK. This scheme is referred to as 8-DPSK in the rest of the dissertation. The motivation behind the inclusion of 8-DPSK is the fact that it has a higher data rate than DQPSK and its behaviour to CFO is investigated as a feasibility study.

DBPSK is more robust than both DQPSK and 8-DPSK because of the superior spatial proximity and angular separation of the constellation points. But 8-DPSK has a superior data rate. Because the aim of a communication architecture is to send as much information as possible with as least errors as possible, it is desirable to improve data rate while incurring minimal drop in the error-rate performance. Even though 8-DPSK may boast the best data rate, it has the worst BER performance and is the most sensitive to carrier frequency offsets. Due to the highly antagonistic properties of the modulation schemes with respect to data rate and bit error rate, there is an emphasis on DQPSK as it provides good stability between the data and error rate.

Because CFO is the focus in this section, noise probability is kept low so that the impact of noise does not affect the study of how CFO impacts the system. Figures 6.5, 6.6 and 6.7 show the BER performances of OFDM under different CFO values when DBPSK, DQPSK and 8-DPSK are used to modulate the OFDM subcarriers respectively. It can be observed that the performance deteriorates significantly as the CFO increases and the impact is accentuated from one scheme to the next as the M value of the M-ary PSK scheme increases. While there is only a 1.9 dB E_b/N_0 difference at 10^{-3} BER between a CFO of 0.00 to 0.12 when DBPSK is used as the subcarrier modulating scheme (see Figure 6.5), the difference increases to 9.5 dB for DQPSK (Figure 6.6) and it quickly becomes too big for 8-DPSK between a CFO of 0.00 and only 0.04 (Figure 6.7), which is only a third of the CFO range used in DBPSK and DQPSK. Therefore for an increase in the data rate, there is a steep trade-off in sensitivity to frequency offsets and hence inter-carrier interference.

While the M = 2 permutation sequence coded OFDM scheme has been mainly used with DBPSK, it has also been used with DQPSK to Figure 6.8 shows the BER performance curves of 2-permutation sequence coded, DQPSK subcarrier-modulated OFDM in the presence of varying CFO levels. The E_b/N_0 values at minimum and maximum CFO at 10^{-3} BER are 9.1 dB and 16.0 dB, giving a performance degradation of 6.9 dB. In the same CFO range, OFDM's E_b/N_0 values at minimum and maximum CFO at 10^{-3} BER are 9.5 dB and 19.0 dB, corresponding to a performance drop of 9.5 dB.

The bit error rate performance of M = 4 PC OFDM modulated using DQPSK is presented in Figure 6.9. Using the same assessment, E_b/N_0 values at minimum and maximum CFO at 10^{-3} BER are 9.4 dB and 14.4 dB, yielding a performance drop of 5 dB. This is a smaller drop compared to M = 2 PC OFDM, improving on the scheme by 1.9 dB and improving on OFDM by 4.5 dB. The conclusion is that increasing the spacing between transmitting subcarriers improves the ability to combat CFO.

While these results give a general case understanding on the impact of CFO in OFDM systems, they do not offer specific insight to the PLC case because the CFO values used are exaggerated to give a general case perspective. Also, the noise level for both narrowband noise and impulse noise is kept low so that the

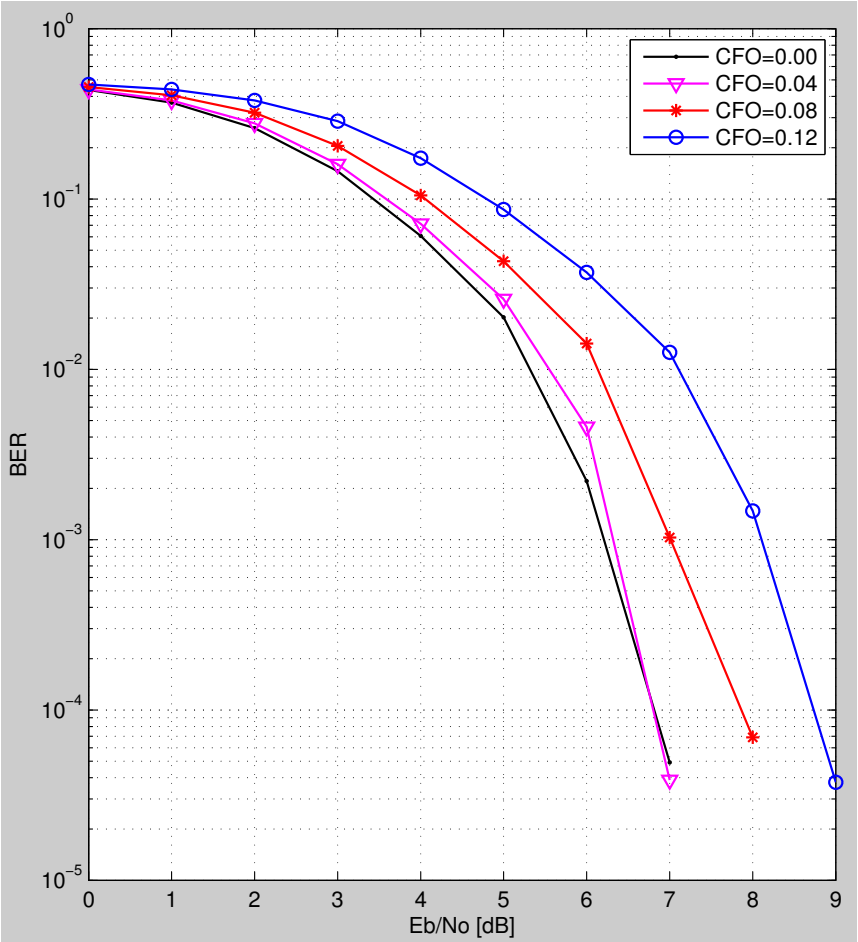

Figure 6.5: Performance of DBPSK modulated ODFM

CFO impact dominates. More simulations were carried out that are specific to power-line communication and these are presented next.

6.2.2 PLC case

Carrier frequency offsets are a problem in high speed communication systems because they alter the phase of symbols, hence affecting decoding. The impact of these frequency offsets also has an impact on inter carrier interference resulting from the loss of orthogonality of subcarriers. This affects the sampling points and as a result not only is the wrong phase obtained, but also the amplitude is affected. However, in power-line communication where the sender position does not change with respect to the receiver, the Doppler effect is not a problem. As a result, the carrier frequency offsets are smaller because they are limited to the mismatch between the oscillator sampling frequencies at the sender and receiver.

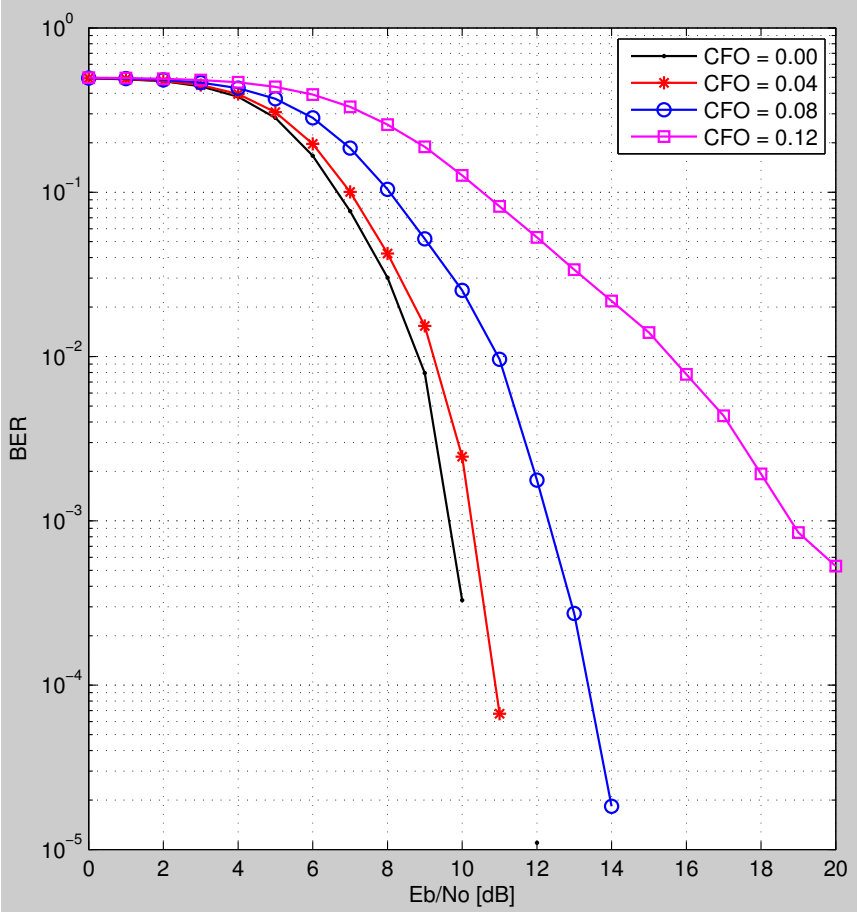

Figure 6.6: Performance of DQPSK modulated ODFM

In Figure 6.10 the different schemes are compared in the absence of carrier frequency offset and at a CFO of 0.1 (10 % f_{sc}) and $4f_{sc}$ frequency disturber bandwidth and a noise probability of $\frac{1}{256}$ for both narrowband interference and impulse noise. The result shows a performance degradation of 3.6 dB in QPSK-OFDM, 3.5 dB in PC OFDM and 0.1 dB for OFDM-MFSK. The outcome shows the prowess of OFDM-MFSK in combating carrier frequency offsets. The strength exhibited by the scheme is attributed to the fact that it sends a one in a specific position of a subcarrier group to convey information instead of sending QPSK symbol as done in both QPSK-OFDM and PC OFDM. As already shown mathematically in Section 3.4.2, a carrier frequency offset introduces a phase offset, which affects the phase of the QPSK symbols. By eliminating this susceptibility, OFDM-MFSK performs well in the presence of carrier frequency offsets.

Figure 6.11 is the same figure as the previous one without OFDM-MFSK to show more clearly the comparison between PC OFDM and OFDM in the

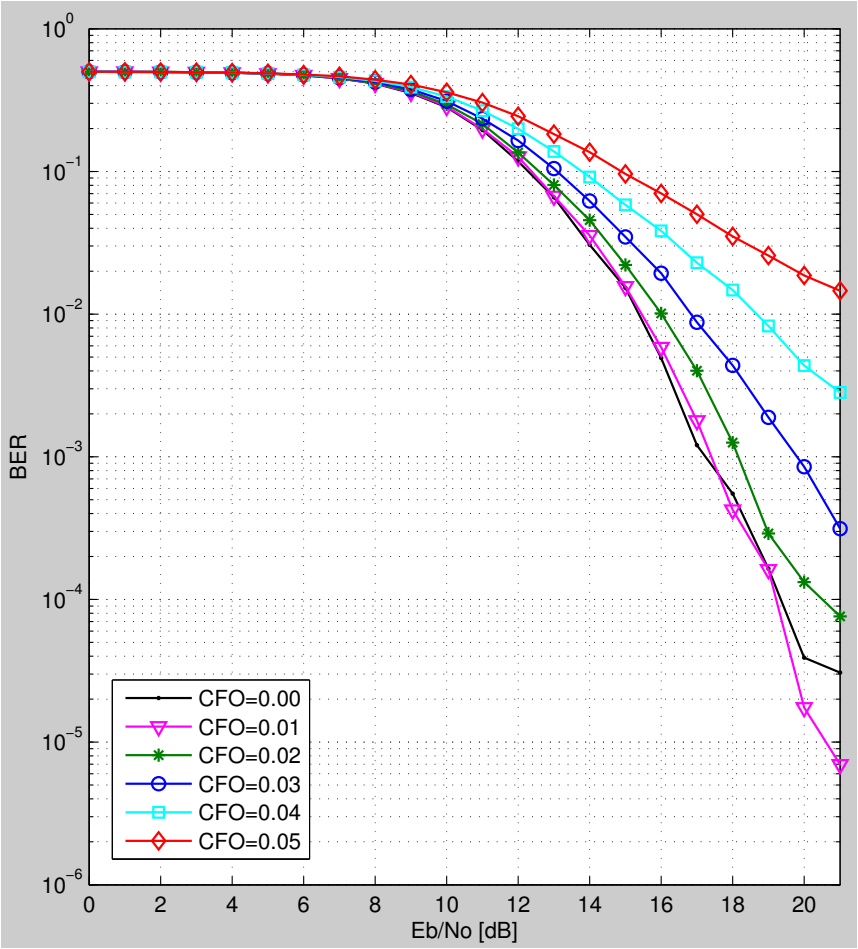

Figure 6.7: Performance of 8-DPSK modulated ODFM

presence of CFO. PC OFDM has a 0.1 dB gain compared to QPSK-OFDM which is attributed to the subcarrier spacing preventing the inter-subcarrier interference. The modification of the subcarrier phase by the frequency offset considerably affects the decoding because the superposition of subcarrier phases in the OFDM symbol contributes to diminished performance. The 0.1 dB improvement may be attributed to the nulls around each information subcarrier, which rids the most significant phase offset contribution from adjacent subcarriers that are set to zero.

As established in the G3-PLC standard, carrier frequency offsets of 2 % or less are regarded as insignificant in power-line communication, the results presented in Figure 6.12 whereby the CFO is set to 0.02 substantiate the assertion. The performance of all three schemes does not show any drop when compared to Figure 6.10 at zero CFO. Considering that only a maximum of 0.03 % CFO can be experienced in the power-line communication specification for G3-PLC,

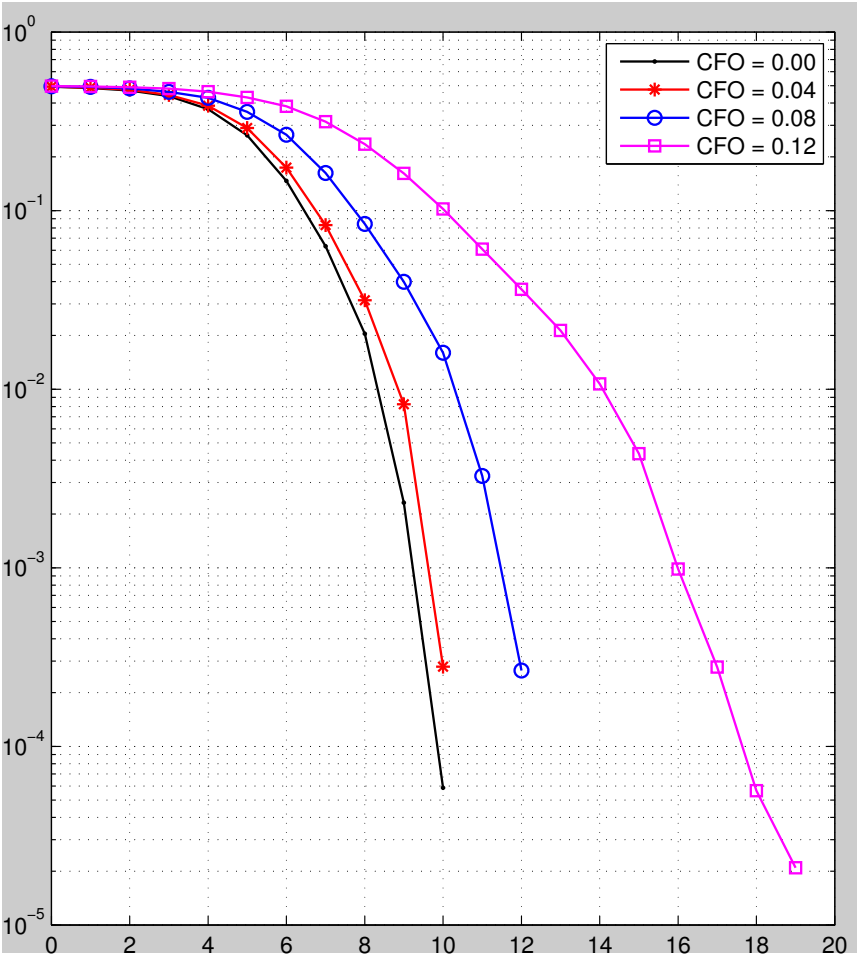

Figure 6.8: $M = 2$ PE DQPSK subcarrier-modulated OFDM

the ability of to combat carrier frequency offsets is not paramount. As a result, even though OFDM-MFSK is good in combating frequency offsets, the ability to combat noise takes precedence.

6.3 Chapter Summary

In this chapter, carrier frequency offsets are shown to be an impairment in OFDM that degrade the performance of OFDM, depending on the sampling and subcarrier frequencies. The bit error rate performance of the different OFDM-based modulation schemes in the presence of frequency offsets is then presented to substantiate the assertion, with a focus on the deviation from zero CFO performance. It is found that DBPSK is the most resistant phase shift keying modulation scheme to frequency offsets when used as the modulation scheme in OFDM subcarriers. The immunity towards the frequency impairment decreases with an increase in the number of constellation points in the

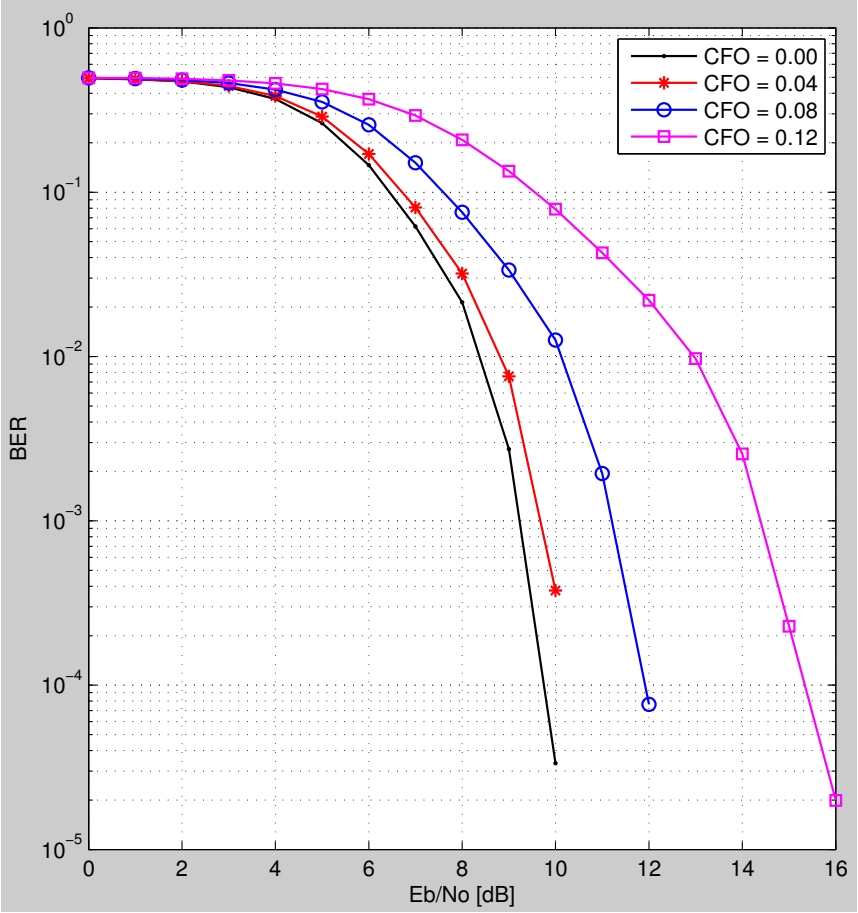

Figure 6.9: $M = 4$ PE OFDM with DQPSK modulated subcarriers

subcarrier modulation scheme I-Q diagram because of the reduced spatial and angular separation of the symbols.

Permutation sequence encoding is shown to be a more bandwidth efficient OFDM-based modulation scheme while achieving better BER performance than OFDM-MFSK when the narrowband noise bandwidth spans from four subcarrier frequencies and higher, or when the narrowband noise probability is increased. MFSK-OFDM has been shown to perform better than PC OFDM for smaller narrowband disturber bandwidths and in the presence of carrier frequency offsets.

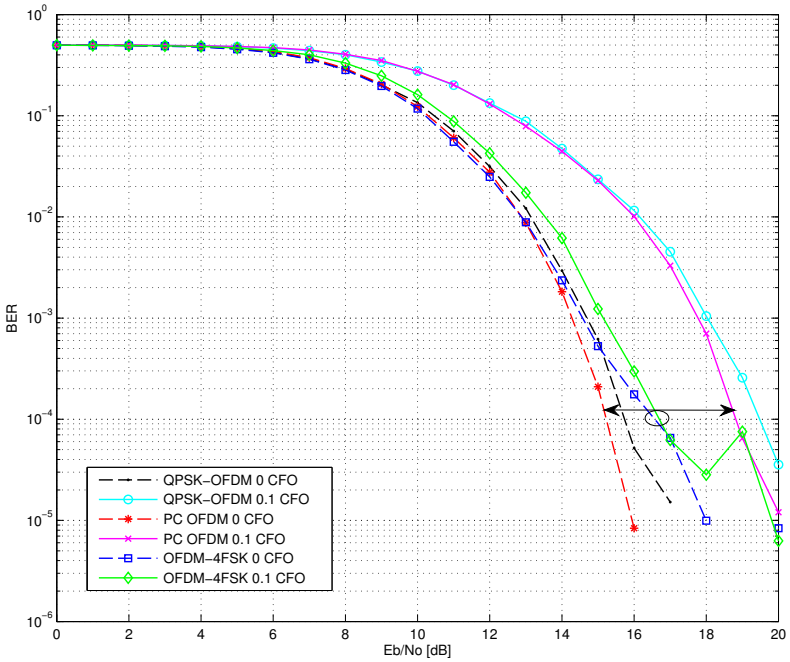

Figure 6.10: OFDM-4FSK and DQPSK-based schemes at varying CFO

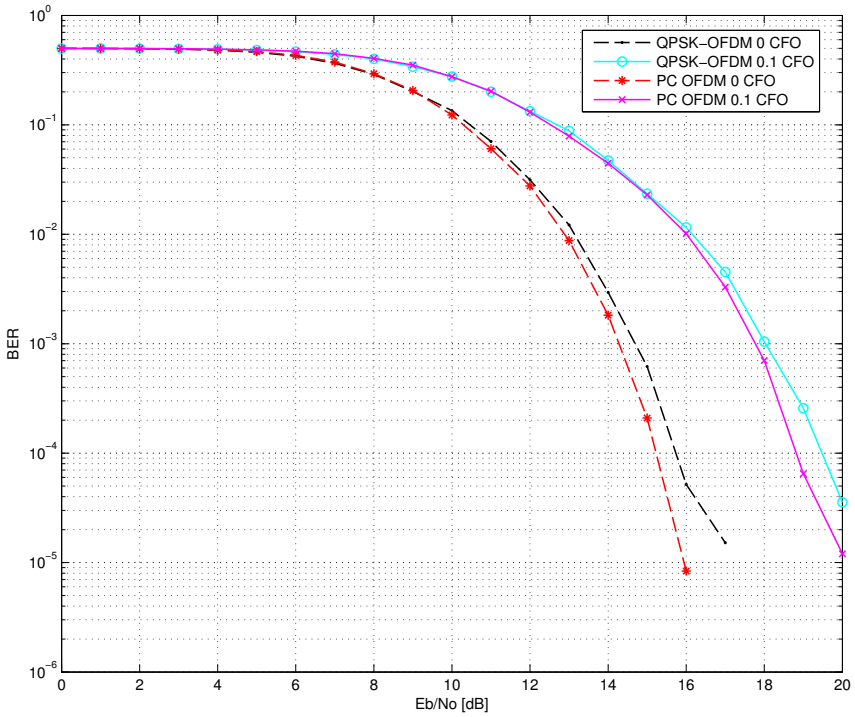

Figure 6.11: OFDM-4FSK and DQPSK-based schemes at varying CFO

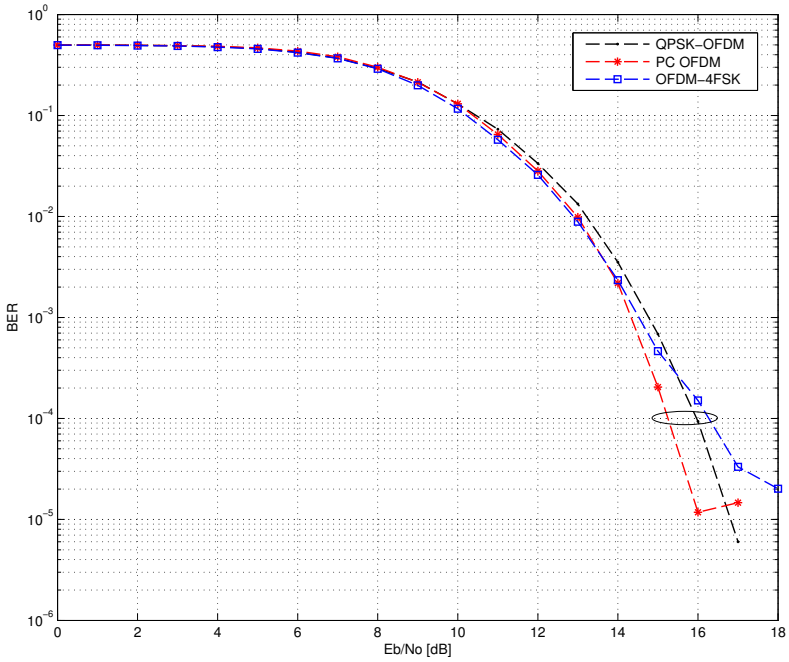

Figure 6.12: OFDM-4FSK and DQPSK-based schemes at a of CFO 0.02

7 CONCLUSION

Another layer of forward error correction can be cascaded to the concatenation of Reed-Solomon codes and Convolutional codes to improve the bit error rate performance and make the system more robust against bit errors from noise. However, it increases the latency and it does contribute towards improving the system's ability to combat carrier frequency offsets. Permutation sequence encoding as a subcarrier spacing coding scheme in OFDM does not add another forward error correction layer but instead mitigates the impact of narrowband disturbances and inter carrier interference by arranging subcarriers to increase frequency diversity.

7.1 Carrier Frequency Offsets Mitigation

Frequency offsets compromise the orthogonality of subcarriers, and the result is that not only do the subcarriers add destructively to each other but also the sampling is not carried out at the peak of the subcarriers. Because permutation sequence encoding ensures that no single symbol-carrying subcarrier is adjacent to another, the nulls introduced between them ensure that even if the communication system experiences frequency offsets, the offsets do not cause inter-carrier interference.

The inter-carrier interference mitigation effectiveness of permutation sequence encoding depends on the sampling frequency. The higher the sampling frequency the higher are the carrier frequency offsets, and subsequently the more effective the scheme is in the system. At much lower sampling frequencies carrier frequency offsets become insignificant and the scheme becomes unnecessary from the perspective of ICI mitigation.

The maximum possible CFO in the power-line communication G3-PLC setup is only 0.33 % of the subcarrier frequency, which is significantly much smaller than the 2 % maximum CFO acceptable as quoted by the G3-PLC standard. Such a small amount of CFO does not considerably affect performance. However, with the requirement of faster data rates in power-line communication

which will inevitably be accomplished by much higher sampling frequencies, the use of PC OFDM will become more useful beyond its noise mitigation ability. Such a requirement will also imply using M-ary PSK systems using a bigger number of bits per symbol that are more sensitive phase and frequency changes.

The immunity of OFDM-MFSK to carrier frequency offsets has been demonstrated by simulated results. While the scheme may not perform well in very noisy conditions and when the noise is bursty, it is well suited in applications where carrier frequency offsets are a major problem such as in high speed trains communications where the Doppler effect and delay spread are significant.

7.2 Bandwidth Considerations

While it is important to consider the BER performance of a scheme to determine whether it is suitable for certain applications, its bandwidth usage is also very important because all physical communication channels are band-limited by constraints of the medium. $M = 2$ PC OFDM uses a total of 126 information subcarriers out of 256 OFDM subcarriers, using a fraction of 0.49 of the total system bandwidth. OFDM-2FSK uses 0.5 of the system bandwidth. In terms of bandwidth considerations, the two schemes use resources equally.

QPSK-based schemes are less stable with respect both noise and frequency offsets compared to BPSK schemes. Therefore noise and frequency offset mitigation becomes more crucial. Frequency diversity becomes necessary, although it comes at a cost to the bandwidth. $M = 4$ PC OFDM takes up 85 information subcarriers out of 256 subcarriers. This corresponds to 0.33 of the total bandwidth. OFDM-4FSK uses 64 subcarriers to carry data, which represents 0.25 of the total system bandwidth. The aim of a communication system is to transmit as much information per unit time as possible and as accurately as possible. In addition, assuming a fixed allocated bandwidth, the aim is to use as much of the bandwidth as possible to transmit information. Using the entire bandwidth but transmitting less information is not resource efficient. Therefore from a bandwidth perspective, PC OFDM is more resource efficient than OFDM-MFSK. MFSK-based systems are more efficient in combating CFO given they avoid sending modulated symbols but use tones instead. However the major drawback of the scheme is that they become inefficient at large M values from a bandwidth perspective.

7.3 Noise Mitigation

Narrowband noise is a major issue in power-line communication. An interesting finding of the study is that the impact of the variation in narrowband noise bandwidth does not give an expected constant change in bit error rate performance in OFDM-MFSK as it does for OFDM and PC OFDM. In low narrowband disturbance bandwidth, OFDM-MFDK outperforms both QPSK-OFDM and PC OFDM, but its performance is significantly reduced in high noise bandwidth and also when the noise probability is increased. Therefore OFDM-MFSK is suitable for low bandwidth narrowband noise systems. However, the major trade-off that needs to be made is bandwidth. In contrast, PC OFDM provides better usage of bandwidth and performs better at higher narrowband noise bandwidths. In other words, it is preferable in systems with harsher narrowband noise conditions as it gives a better BER performance.

7.4 Comparison with Similar Work

Wetz et al. developed with a scheme combining MFSK and OFDM that is named OFDM-MFSK. They showed that their scheme performed well in the presence of carrier frequency offsets, and they identified that the scheme is suitable for use for communication in high speed modes of transport such as high speed trains. Most of the presented research does comparisons with this scheme on narrowband noise, impulse noise and carrier frequency offsets. The presented scheme performs better than the scheme developed by Wetz et al. in the presence of high narrowband and impulse noise. However, it does not better the work of Wetz et al. with respect to carrier frequency offset mitigation. The main difference between the presented scheme and that of Wetz et al. is that they used MFSK to modulate OFDM while this research uses MPSK.

Another similar work is that of Papilaya et al. who presented a modified OFDM-MFSK by sending QPSK symbols rather than sending ones as done in OFDM. They also developed a modified QPSK-OFDM scheme whereby selected subcarriers are used to send information by sending the real and imaginary parts of a QPSK symbol separately in such a way as to maximise the Euclidean distance between carriers. The modified QPSK-OFDM scheme yielded no net loss in SNR requirements and demonstrated superior bit error rate performance in the presence of frequency disturbances and frequency selective fading noise, although the resultant data rate is half that of conventional

QPSK-OFDM.

7.5 Research Contribution

The core of the research is developing an OFDM-based modulation scheme that improves the performance of OFDM in the presence of narrowband noise and carrier frequency offsets. The aim is to improve on the qualities of OFDM-MFSK with respect to bandwidth usage without weakening its performance. The research therefore contributes a new scheme that fares well in bit error rate performance than OFDM and OFDM-MFSK in a channel with significant noise bandwidth, while providing improved system bandwidth usage over OFDM-MFSK. The scheme is adaptable for use with both BPSK and QPSK although it is more suitable for the latter, given the robustness of the former.

The main contribution of the scheme therefore is in improving the BER performance of OFDM in the presence of narrowband noise and carrier frequency offsets while offering improved bandwidth usage when compared to OFDM-MFSK. The advantage presented by the scheme is that it offers the use of M-ary PSK instead of M-ary FSK, which is useful in increasing the data rate without incurring a bandwidth trade-off.

7.6 Future Work

Implementing PC OFDM in a software defined radio and carrying out tests to measure the throughput and spectral efficiency of the scheme in comparison to OFDM and MFSK-OFDM would make a good study. By transmitting actual data over a channel and the download speed measured when each of the schemes is used could provide practical results on the data rate performance of each scheme, and this is a consideration for future work.

Additional future work would involve using permutation codes' minimum distance property to decode information sent using the presented scheme and compare it to permutation sequence decoding. Ultimately, the assessment of the data rate between the two schemes would help investigate the latency each method introduces to the system. This could be useful to studying the overhead incurred by computation used by various decoding algorithms.

Based on the current work, another aspect of future work would be to implement the scheme by sending ones in information subcarriers like in OFDM-

MFSK, instead of QPSK symbols. Decoding can be accomplished by using the permutation codes used in the sequence encoding. The possible improvement of this approach is the performance of the scheme in the presence of carrier frequency offsets. The reason attributed to the superior performance of OFDM-MFSK is that since it does not rely on phases to decode, it is immune to frequency offsets.

7.7 Conclusion

In conclusion, permutation sequence encoding has been shown to be a frequency-domain scheme that combats carrier frequency offsets, narrowband noise and impulse noise in power-line communication systems. The scheme ensures that the presence of frequency offsets does not cause inter-carrier interference between OFDM subcarriers even though orthogonality may be lost. By providing frequency diversity in OFDM, the scheme also improves the performance of OFDM in the presence of narrowband noise.

Permutation sequence encoded OFDM provides a unique solution in that it prevents errors from occurring rather than correcting them by not only nullifying inter-carrier interference but also by providing frequency diversity. The scheme has an application in the frequency domain on symbols rather than typical forward error correction schemes that are applied on binary data. Moreover, it does not require highly computational decoding operations and instead it uses a simple look up table method to decode information because the positions of OFDM subcarriers carrying information are known. A disadvantage of the scheme is that although it improves the performance of OFDM, it does not improve the performance of OFDM-MFSK in combating carrier frequency offsets.

Bibliography

[1] M. Hilbert and P. Lopez. "The World's Technological Capacity to Store, Communicate and Compute Information." *Science*, vol. 332, no. 6025, pp. 60–65, 2011.

[2] H. Hransica, A. Haidine, and R. Lehnert. *Broadband Poweline Communications Netork Design*. John Wiley & Sons, Ltd, 2004.

[3] B. Capehart and L. Capehart. *Web Based Enterprise Energy and Building Automation Systems*. U.S.A: Library of Congress Cataloging-in-Publication Data, first ed., 2007.

[4] T. A. Papadopoulos, C. G. Kaloudas, A. I. Chrysochos, and G. K. Papagiannis. "Application of Narrowband Power-Line Communication in Medium-Voltage Smart Distribution Grids." *IEEE Transactions on Power Delivery*, vol. 28, no. 2, pp. 981–988, Apr. 2003.

[5] J. Anatory and N. Theethayi. *Broadband Communication Systems Theory and Applications*. WIT Press, first ed., 1984.

[6] K. Dostert. "Telecommunications over the Power Distribution Grid - Possibilities and Limitations Proc." *International Symposium on power Line Comms*, pp. 294–296, 1997.

[7] R. Broadridgen. "Power-line modems and networks." *4th International Conference on Metering Applications and Tariffs for Electricity Supply IEE Conference*, pp. 294–296, 1984.

[8] "IEEE P1901 draft standard for broadband over power line networks: Medium access control and physical layer specifications." *IEEE P1901 working group*, Jul. 2009.

[9] "PRIME Technology white paper: PHY, MAC and convergence layers." Jul. 2008.

[10] T. C. Chuah. "On Reed-Solomon for Data Communications Over Power-Line Channels." *IEEE Transactions on Power Delivery*, vol. 24, no. 2, pp. 614–620, Apr. 2009.

[11] L. Cheng and H. C. Ferreira. "Time-Diversity Permutation coding Scheme for Narrow-Band Power-Line Channels." *2012 IEEE International Symposium on Power Line Communication and its Applications*, pp. 120–125, 2012.

[12] T. Guzel, E. Ustunel, H. Celebi, H. Delic, and K. Mihcak. "Noise Modelling and OFDM Receiver Design in Power-Line Communication." *IEEE Transactions on Power Delivery*, vol. 26, no. 4, pp. 2735–2742, Oct. 2011.

[13] H. Meng, Y. Guan, and S. Chen. "Modelling and Analysis of Noise Effects on Broadband Power-Line Communications." *IEEE Transactions on Power Delivery*, vol. 20, no. 2, pp. 630–637, Nov. 2005.

[14] M. H. L. Chan and R. W. Donaldson. "Amplitude, width, and interarrival distributions for noise impulses on intrabuilding power line communication networks." *IEEE Transactions on Electromagnetics and Compatibility*, vol. 31, no. 3, pp. 320–323, Aug. 1989.

[15] K. Dostert. *Powerline Communications*. Prentice-Hall, 2001.

[16] M. Zimmerman and K. Dostert. "Analysis and modeling of impulsive noise in borad-band powerline cmmunications." *IEEE Transactions on Electromagnetics and Compatibility*, vol. 44, no. 1, pp. 249–258, Feb. 2002.

[17] E. Biglieri. "Coding and modulation for a horrible channel." *IEEE Communication Magazine*, vol. 41, no. 5, pp. 92–98, May 2003.

[18] G. D. Forney. "Concatenated Codes." *MIT Press*, 1966.

[19] K. Razazian, M. Umari, and A. Kamalizad. "Error Correction Mechanism in the New G3-PLC Specification for Powerline Communication." *IEEE International Symposium on Power Line Communications and Its Applications*, pp. 50–55, Mar. 2010.

[20] F. Daneshgaran, M. Laddomada, and M. Mondin. "Interleaver Design for Serially Concatenated Convolutional Codes: Theory and Application." *IEEE Transactions on Information Theory*, vol. 50, no. 6, pp. 1177–1188, Jun. 2004.

[21] M. Cao, K. Subramanian, and V. K. Dubey. "Optimal interleaver design for concatenated coding in DSL systems." *Electronic Letters*, vol. 35, pp. 1630–1631, Sep. 1999.

[22] "G3-PLC physical layer specification." *Electrical Reseau Distribution France*, Aug. 2009.

[23] C. E. Shannon. "A mathematical theory of communication." *Bell Sys. Tech. J.*, vol. 27, pp. 379–423 and 623–656, 1948.

[24] D. J. Costello and D. G. Forney. "Channel Coding: The Road to Channel Capacity." *Proceedings of the IEEE*, vol. 95, no. 6, pp. 1150–1177, jun 2007.

[25] T. K. Moon. *Error Correction Coding: Mathematical Methods and Algorithms*. John Wiley & Sons, 2005.

[26] R. Hamming. "Error detecting and error correcting codes." *Bell Systems Technical Journal*, vol. 29, pp. 41–56, 1950.

[27] R. A. Carrasco and M. Johnston. *Non-Binary Error Correction Coding for Wireless Communication and Data Storage*. John Wiley & Sons, 2008.

[28] E. Prange. *Cyclic error-correcting codes in two symbols*. Cambridge, MA, Tech: Air Force Cambridge Tes. Center, sep 1957.

[29] I. S. Reed and G. Solomon. "Polynomial Codes over Certain Fields." *Journal of the Society for Industrial and Applied Mathematics*, vol. 8, pp. 300–304, Jun. 1960.

[30] D. G. Forney. "Burst error-correcting codes for the classic bursty channel." *IEEE Trans. Commun. Technol.*, vol. COM-19, pp. 772–781, oct 1971.

[31] S. Lin and D. J. Costello. *Error Control Coding: Fundamentals and Applications*. U.S.A: Pearson Prentice Hall, second ed., 2004.

[32] P. Elias. "Coding for Noisy Channels." *IRE Conv. Rec.*, vol. 4, pp. 37–47, 1955.

[33] J. M. Wozencraft and B. Reiffen. "Sequential Decoding." *MIT Press*, 1961.

[34] J. L. Massey. "Threshold Decoding." *MIT Press*, 1963.

[35] A. J. Viterbi. "Error Bounds for Convolutional Codes an Asymptotically Optnimum Algorithm." *IEEE Transaction on Information Theory*, vol. 13, pp. 260–269, Apr. 1967.

[36] L. R. Bahl, J. Cocke, F. Jelinek, and J. Raviv. "Optimal Decoding for Linear Codes for Minimal Symbol Error Rate." *IEEE Transaction on Information Theory*, vol. 20, pp. 284–287, Mar. 1974.

[37] G. Ungerboeck and I. Csajka. "On Improving Data-Link Performance by Increasing the Channel Alphabet and Introducing Sequence Coding." *IEEE International Symposium on Information Theory (ISIT 1976) Book of Abstracts*, p. 53, Jun. 1976.

[38] F. J. Williams. "Permutation decoding of systematic codes." *Bell System Technical Journal*, vol. 43, pp. 485–505, 1964.

[39] L. Cheng, G. Swart, and H. C. Ferreira. "Adaptive Rateless Permutation Coding Scheme for OFDM-based PLC." *IEEE International Symposium on Power Line Communications and its Applications*, 2013.

[40] A. J. H. Vinck. "Coded modulation for powerline communications." *Int. J. Elec. Commun.*, vol. 54, no. 6, pp. 45–49, 2000.

[41] G. Ungerboeck. "Channel coding with multilevel/phase signals." *IEEE Transactions on Information Theory*, vol. IT-28, no. 1, pp. 55–67, Jan 1982.

[42] M. Biagi, E. Baccarelli, N. Cordeschi, V. Polli, and T. Partiarca. "Physical-layer Goodput Maximization for Power Line Communications." *IEEE Wireless Days Proceedings of the 2nd IFIP Conference on Wireless Days*, pp. 1–5, Sep 2009.

[43] J. G. Proakis and M. Salehi. *Communication Systems Engineering*. New Jersey: Prentice Hall, second ed., 2001.

[44] S. H. Muller and J. B. Huber. "OFDM with Reduced Peak to Average Power Ratio by Optimum Combination of Partial Transmit Sequencies." *IEE Electronic Letters*, vol. 33, no. 5, pp. 368–369, feb 1997.

[45] A. E. Jones, T. A. Wilkinson, and S. K. Barton. "Block coding scheme for reduction of peak to mean envelope power ratio of multicarrier transmission schemes." *Electronic Letters*, vol. 30, no. 25, pp. 2098–2099, 1994.

[46] X. Li and J. A. Ritcey. "M-sequencies for OFDM PAPR reduction and error correction." *Electronic Letters*, vol. 33, pp. 545–546, 1997.

[47] P. V. Eetvelt and G. W. amd M. Tomlinson. "Peak to Average Power Reduction for OFDM Schemes by Selective Scrambling." aug 1996.

[48] M. Pauli and H. P. Kuchenbecker. "On the reduction of the out of band radiation of OFDM signals." *IEEE conference proceedings*, vol. 3, pp. 1304–1308, 1998.

[49] R. V. Nee and A. Wild. "Reducing the Peak to Average Power Ratio of OFDM." *IEEE conference proceedings*, pp. 2072–2076, 1998.

[50] R. O'Neil and L. B. Lopez. "Envelope Variations and Spectral Splatter in Clipped Multicarrier Signals." *IEE Conference proceedings PMIRC*, pp. 71–76, 1995.

[51] X. Li and L. J. Cimini. "Effects of Clipping and Filtering on the Performance of OFDM." *Communication Letters*, vol. 2, no. 5, pp. 131–133, may 1998.

[52] D. Wulich and L. Goldfeld. "Reduction of peak factor in orthogonal multicarrier modulation by amplitude limiting and coding." *IEEE Transactions on Communications*, vol. 47, no. 1, pp. 18–21, jan 1999.

[53] K. Xu, W. Ma, L. Wu, W. Xie, D. Zhang, and Y. Xu. "Carrier Frequency Offset Estimation Approach for Multicarrier Transmission on Hexagonal Time-Frequency Lattice." *arXive*, Jan 2013.

[54] V. Taranalli. "Carrier Frequency Offset in Sngle Carrier and OFDM Systems.", Apr. 2012. URL `http://veeresht.info/blog/cfo/`.

[55] J. Ahn and H. S. Lee. "Frequency domain equalization of OFDM signal over frequency non selective Rayleigh fading channels." *Electronic Letters*, vol. 29, no. 16, pp. 1476–1477, 1993.

[56] R. Li and G. Stette. "Time limited orthogonal multicarrier modulation schemes." *IEEE transactions on communications*, vol. 43, pp. 1269–1272, 1995.

[57] Y. Zhao and S. G. Haggman. "Sensitivity to Doppler Shift and Carrier Frequency Errors in OFDM Systems - The Consequences and Solutions." *IEEE conference proceedings VTC*, pp. 2474–2478, 1996.

[58] B. Chen and H. Wang. "Blind Estimation of OFDM Carrier Frequency Offset via Oversampling." *IEEE Transactions on Signal Processing*, vol. 52, no. 7, pp. 2047–2057, Jul 2004.

[59] H. Zhou, A. Malipatil, and Y. Huang. "Maximum-Likelihood Carrier Frequency Offset Estimation for OFDM Systems in Fading Channels." *Wireless Communications and Networking Conference*, pp. 1461–1464, Apr 2006.

[60] J. Lee, H. Lou, D. Toumpakaris, and J. Cioffi. "SNR Analysis of OFDM Systems in the Presence of Carrier Frequency Offset for Fading Channels." *IEEE Transactions on Wireless Communications*, vol. 5, no. 12, pp. 3360–3364, Dec 2006.

[61] Y. Wang and T. Ottosson. "Cell Search in W-CDMS." *IEEE Journal on Selected Areas in Communications*, vol. 18, no. 8, pp. 1470–1482, Aug 2000.

[62] O. G. Hooijen. "On the Channel Capacity of the Residential Power Circuit used as a Digital Communications Medium." *IEEE Communication Letters*, vol. 2, no. 10, pp. 267–298, oct 1998.

[63] M. Wetz, I. Perisa, W. G. Teich, and J. Lindnera. "OFDM-MFSK with Differentially Encoded Phases for Robust Transmission over Fast Fading Channels." In *11th Int. OFDM-Workshop*. Hamburg, Germany, aug 2006.

[64] V. Papilaya, T. Shongwe, and A. J. Vinck. "Selected Subcarriers QPSK-OFDM Transmission Schemes to Combat Frequency Disturbances." In *Proc. IEEE International Symposium on Power Line Communication and its Applications*, pp. 200–20. Beijing, China, mar 2012.

[65] E. R. Berlekamp. *Algrebraic Coding Theory*. New York: McGraw-Hill, 1968.